

**LIGHT-EMITTING DIODES AND PHOTODIODES IN THE  
DEEP ULTRA-VIOLET RANGE FOR ABSORPTION  
PHOTOMETRY IN LIQUID CHROMATOGRAPHY,  
CAPILLARY ELECTROPHORESIS AND GAS SENSING**

**Inauguraldissertation**

zur

Erlangung der Würde eines Doktors der Philosophie

vorgelegt der

Philosophisch-Naturwissenschaftlichen Fakultät

der Universität Basel

von

Duy Anh BUI

aus

Vietnam

Basel, 2016

**Genehmigt von der Philosophisch-Naturwissenschaftlichen Fakultät auf Antrag von**

**Prof. Dr. Peter C. Hauser**

**und**

**Prof. Dr. Jörg Huwyler**

**Basel, den 21.06.2016**

**Prof. Dr. Jörg Schibler**

**Dekan**

## **Acknowledgements**

The completion of this doctoral thesis was achieved with the valuable help of many people to whom I am always grateful.

First of all, I would like to express my sincere thanks to my supervisor Prof. Dr. Peter C. Hauser for giving me a chance to study and do research in his group. He has instructed me in various analytical techniques, electronics and systems development that played a significant role in my PhD accomplishment. His great supervision, suggestions and corrections were extremely crucial and helpful to my research progress. I also would like to thank the co-author Benjamin Bomastyk for his assistance and contribution to the instrumentation.

Secondly, I would like to send my thankfulness to all the members of Prof. Hauser's research group for their cooperative working environment as well as fruitful suggestions and assistance, including: Dr. Thanh Duc Mai, Dr. Jorge Saiz, Joel Koenka, Ralf Dumler, Thi Thanh Thuy Pham, Benjamin Bomastyk, Mario Lovrić, Dr. Marko Stojkovic, Dr. Hong Heng See and Neha Shastry. Special thanks to my colleague Joel Koenka for his kind help in the programming essential to my experiments. I would like to appreciate Mrs. Beatrice Erismann for her valuable assistance in the administration work during my doctoral study at the University of Basel. Especially, I would like to acknowledge Mr. Andres Koller from the workshop for his great contribution to the mechanical assembly of instruments. Many thanks to Mr. Markus Hauri for his kind help in ordering the consumables.

Thirdly, I would like to express my deep gratitude to Prof. Hung Viet Pham for his support and recommendation giving me an opportunity to come to Switzerland for my further study. I also would like to acknowledge the valuable financial supports from Swiss Federal Commission for Scholarship for Foreign Students (FCS) and the Commission for Scholarships for young professionals from developing countries of Canton Basel-Stadt.

Finally, the sincere thank of mine is given to my family for their great encouragement and support giving me the strength and motivation to finish my doctoral study. Above all, I would like to express my deepest and warmest gratitude to my wife Cam Lien Nguyen Phuoc for her eternal happiness and companionship she has brought to me.

## Summary

This dissertation concerns the utilization of light-emitting diodes (LEDs) and photodiodes (PDs) in the deep ultra-violet range (below 300 nm) as radiation sources and light detectors, respectively used as alternatives to conventional discharge lamps with a monochromator and photomultiplier tubes for absorption photometry in high-performance liquid chromatography (HPLC), capillary electrophoresis (CE) and gas sensing.

The performance of LEDs serving as light detectors in analytical photometry was investigated and compared with that of standard silicon PDs in three different measuring configurations. The light intensity was measured as the current generated from diodes in the current follower mode with an operational amplifier and in a conventional setup with the reference signal. Measured in the voltage follower mode, the radiation intensity correlates to the voltage across diodes by the irradiation. Another method for the light measurement was carried out in which the discharge time for the junction capacitance of diodes by a photocurrent was recorded. LEDs as detectors were generally found to be adequate for the analytical work but PDs offered higher sensitivity and linearity as well as provided stable readings with faster settling times.

An absorbance detector for a miniaturized HPLC setup based on 255 and 280 nm LEDs and PDs selective for the deep ultra-violet (UV) range was constructed for the use of a narrow column HPLC. It was designed to use a 250  $\mu\text{m}$  inner diameter (i.d) quartz tubing for the absorbance measurement and to optimize the light throughput with a flexible arrangement of an LED, a tubing and a signal photodiode. This optical cell allows measurements of absorbance units by emulating the Lambert-Beer's law with a log-ratio amplifier-based circuitry and a beam splitter for the reference signal. The performance of this photometric device in the quantification for HPLC separations employing a column of 1 mm i.d in both isocratic and gradient elution was promising in terms of linearity, baseline noise and reproducibility.

High-intensity deep UV-LEDs as radiation sources were then employed for the development of an absorbance detector for CE in which PDs for the deep UV range playing a role of light detectors displace a previously used photomultiplier tube. The design of this optical cell is more challenging than that for a narrow column HPLC due to the higher efficiency in the light focus onto a narrow detection window of a capillary (50  $\mu\text{m}$  wide) with the minimum of

stray light and the mechanical stability to minimize the baseline noise is required. This optical detector was employed successfully for the direct as well as indirect detection in CE separations at examined wavelengths of 255 and 280 nm. The quantitative data of all measurements including correlation coefficients of calibration curves, reproducibility for peak areas and the separation efficiency were satisfactory. Notably, the level of baseline noise was found to be comparable with that of more complex and costly UV-visible detectors currently used in commercial CE instruments.

The potential of a deep UV-LED as a radiation source for absorption spectroscopy was further investigated for the detection of benzene, toluene, ethylbenzene and the xylenes compounds in the gas phase at 260 nm. In the first part of this work, its performance in the acoustic waves excitation was preliminarily investigated with some different measuring systems for the detection of the toluene vapor. It was found that the intensity of a deep UV-LED was insufficient to produce detectable acoustic signals. This was followed by the construction of an absorbance detector for the determination of these target compounds based on the combination of a deep UV-LED and PDs. This optical device was designed to use optical fibers for the light coupling from the LED to a measuring cell and a reference PD, that allows removing a beam splitter previously required for detectors of a narrow column HPLC and CE. Its performance with regard to linearity and reproducibility was sufficient. Detection limits of about 1 ppm were determined.

## Table of Contents

<b>1. Introduction .....</b>	<b>5</b>
1.1. High Performance Liquid Chromatography (HPLC).....	5
1.1.1. A brief history of the development of HPLC.....	5
1.1.2. Basic principles of HPLC.....	6
1.1.3. Detection in HPLC .....	13
1.1.4. HPLC instrumentation.....	16
1.2. Capillary electrophoresis (CE).....	17
1.2.1. Brief history of the development of CE .....	17
1.2.2. Basic principles of CE.....	18
1.2.3. Detection in CE .....	24
1.2.4. Capillary electrophoresis setup .....	26
1.3. Ultraviolet-visible absorption spectroscopy.....	27
1.3.1. Brief history of UV/Vis absorption spectroscopy .....	27
1.3.2. Basic principles of UV/Vis absorption spectroscopy.....	28
1.4. Light-emitting diodes for absorption spectroscopy.....	31
1.4.1. Brief development history of LEDs .....	31
1.4.2. Working principles of LEDs .....	32
1.4.3. Applications of LEDs for absorption spectroscopy .....	34
1.5. Research objectives .....	35
<b>2. Results and discussion.....</b>	<b>37</b>
2.1. Comparative study of light-emitting diodes and standard silicon photodiodes in photometric measurements.....	37
2.2. Development of a deep UV-LED based absorbance detector for narrow column high-performance liquid chromatography.....	38
2.3. Development of a deep UV-LED based absorbance detector for capillary electrophoresis .....	40
2.4. Development of deep UV-LED based absorption spectroscopic detectors for benzene, toluene, ethylbenzene and the xylenes compounds.....	43
<b>3. References .....</b>	<b>92</b>
<b>4. Curriculum Vitae .....</b>	<b>98</b>
<b>5. List of publications and posters .....</b>	<b>100</b>
5.1. Publications .....	100
5.2. Posters .....	101

## List of Figures

- Figure 1-1. Retention time of an analyte in the chromatogram
- Figure 1-2. Van-Deemter plot
- Figure 1-3. The overview of a HPLC instrument
- Figure 1-4. Electroosmotic flow in a capillary
- Figure 1-5. Laminar flow in HPLC and flat flow of EOF in CE
- Figure 1-6. The overall arrangement of a CE setup
- Figure 1-7. Electron transitions in the UV/Vis spectroscopy
- Figure 1-8. Inner working diagram of an LED
- Figure 1-9. A light-emitting diode in a common package
- Figure 2-1. The photo of a deep UV-LED based absorbance detector for narrow-column HPLC
- Figure 2-2. The photo of a mechanical assembly of a deep UV-LED based absorbance detector for CE
- Figure 2-3. Photoacoustic measuring configurations of the toluene vapor detection
- Figure 2-4. The experimental setup of the photoacoustic spectroscopy measurement
- Figure 2-5. The mechanical arrangement of an absorbance detector for BTEX compounds

# **1. Introduction**

## **1.1. High Performance Liquid Chromatography (HPLC)**

### **1.1.1. A brief history of the development of HPLC**

High-performance liquid chromatography or high pressure liquid chromatography is the separation technique based on the column chromatography under high pressure conditions in which a mixture of components in a mobile phase is introduced into a column filled with an absorbent material (stationary phase). It is the most widely used chromatographic method for separation, identification, quantification and purification of compounds in research and industrial production of biochemistry, medicine, pharmacy, food and environment. The term “chromatography” was first introduced by Mikhail Tswett in 1903, a Russian botanist who used the column packed with calcium carbonate to separate different plant pigments into a series of colored bands [1]. The principle of the partition chromatography was developed by Martin and Synge in 1943 with the application of a silica gel-containing column and a moving organic solvent for the separation [2]. Consden and his co-workers subsequently reported the paper chromatography technique for the separation of amino acids based on a filter paper as a stationary phase in 1944 [3]. Piel was the first to report an application of the high pressure to drive a mobile phase through microparticulate beds by centrifugal forces or a pump operated at several thousand psi. These approaches allowed fast separations of spinach pigments in only a few minutes [4]. In 1967, the first commercial HPLC instrument (known as the ALC-100 system) coupled with UV and refractive index (RI) detectors was introduced by Waters Associates [5]. Since then the liquid chromatography (LC) has been developed in terms of the separation method, instrumentation and column technology for the higher efficiency, selectivity and sensitivity.

Majors introduced a narrow bore column (2 mm i.d) packed with 5 - 10  $\mu\text{m}$  silica gel particles by the use of the high pressure, balanced-density slurry techniques in 1971. It was found that the smaller particle size column helped increase the efficiency [6]. Small reported an ion chromatography system for the separation and quantification of cations or anions in which the additional column packed with an anion exchange resin in the hydroxide form was used to suppress or neutralize the background without any significant effects on target species in the effluent. This allowed a successful employment of a conductivity detector for the LC system [7]. The new method of reversed-phase LC has been widely used from the commercialization



of the chemical bonded silicone phase (Si-O-Si-C) in the 1970s [8]. Opposite to the normal phase, this separation mode was based on a polar mobile phase (water - organic solvents like methanol or acetonitrile) and a non-polar stationary phase (octylsilane, octadecylsilane), that helped improve the separation between very similar compounds. Being the most popularly used method in HPLC by far, reversed-phase chromatography has been developed rapidly with the introduction of thousands of reversed-phase columns in the period of 1970 - 2010.

The introduction of a diode array detector by Hewlett-Packard in 1979 facilitated the quantification of analytes by ultraviolet-visible (UV/Vis) absorption spectroscopy. During the 1980s, the availability of computers for automation and simulation programs has provided the convenience in the operation and optimization of separations. The LC instrumentation has been continuously developed over the 1990s for the improvement of reproducibility and high precision. In 2004, the first ultra-high performance liquid chromatography system (UHPLC) introduced by Waters Corporation with the pressure limit up to 15.000 psi allowed the separation with 2  $\mu\text{m}$  particles [9]. It was investigated that small particles (less than 2.5  $\mu\text{m}$ ) offered a significant improvement in efficiency at an increased linear velocity of the eluent. Other benefits are the faster separation, consumable savings, the higher sensitivity with a UV/Vis photometric detection and an ease of use with the mass spectrometry. In the near future, micro-bore columns with advanced particles will be continuously developed to satisfy the need for higher speed and efficiency of separations. The hardware will be innovated following the trend of portability (compactness and low-power consumption) along with the multiple detectors as a standard as well as the robotic automation for the loading and handle of hazardous samples. HPLC undoubtedly has been one of the most important and powerful separation techniques for analytical sciences with a variety of applications in biochemical, pharmaceutical, environmental and clinical analyses.

### **1.1.2. Basic principles of HPLC**

High-performance liquid chromatography is an innovation from the column chromatography. It is the separation technique based on the difference in equilibrium distribution of components between two phases under dynamic conditions: one is the liquid moving through a column in one direction referred as the mobile phase and the other is the stationary phase. HPLC separations generally can be conducted based on three primary characteristics of an analyte including polarity, electrical charge and molecular size which were also called partition

chromatography, ion exchange chromatography and size exclusion chromatography, respectively.

#### *1.1.2.1. Modes of HPLC*

##### ***Partition chromatography***

This chromatographic mode is performed based on the difference in the polarity of the compounds. It was estimated that approximately 80-90% of HPLC separations have been performed in this mode. In polarity based chromatographic separation, molecules that are similar in polarity to that of a stationary phase have a strong attraction to its particles. Those whose polarity is similar to a mobile phase will be attracted to it and elute faster. The term “normal phase chromatography” is used if a stationary phase is more polar than a mobile phase. As the stationary phase has a higher affinity to the polar compounds, those which are least polar elute first followed by the weakly polar and the polar compounds eventually. In this mode, the common stationary phases are bare silica [-Si-OH] or silica-based organic materials to which the functional groups of amino, cyano...are bound such as aminopropylsilyl [-Si-(CH<sub>3</sub>)<sub>2</sub>-NH<sub>2</sub>] and cyanopropylsilyl [-Si-(CH<sub>3</sub>)<sub>2</sub>-CN]. Mobile phases are non-polar organic solvents like hexane, heptane, isooctane, etc., with a small amount of methanol, ethanol, isopropanol for the polarity modification. Normal phase chromatography is useful for the separation of high polar compounds whose molecular mass are not relatively high.

Opposite to the normal phase separation is the reverse-phase chromatography with the application of a non-polar stationary phase and a polar mobile phase. Nowadays, octadecylsilyl [-Si-(CH<sub>2</sub>)<sub>17</sub>CH<sub>3</sub>] - C18 bonded silica is the most popular material for a stationary phase as it strongly interacts with non-polar compounds by its long side chains. Water miscible with polar organic solvents as methanol, acetonitrile or tetrahydrofuran is commonly used as mobile phases. The higher concentration of an organic solvent in a mobile phase, the higher elution strength it has, leading to the decrease in a retention time. In this mode, highly polar solutes elute first because of their weak interaction with a stationary phase resulting in the fastest movement in a polar mobile phase. Reverse-phase chromatography is more popular than normal-phase chromatography as it covers a wide range of applications, improves the reproducibility and helps save the running cost with the less costly water-based eluent. It roughly accounts for 75% of all HPLC separations. It is especially useful for the separation of non-polar compounds with long carbon chains. There are two elution modes in reverse-phase

LC: one is the isocratic elution in which the composition of an eluent is constant during the analysis time and the other is the gradient elution with an elevation of the organic solvent. In the later mode, columns needed to be re-equilibrated with at least 10 column volumes of an original mobile phase before initiating the next run to ensure the repeatability of retention. The main reason for the use of gradient elution is to improve the selectivity of separations with complex samples (more than 10 components) in a short time and the peak resolution of late-eluting compounds resulting in an increase in sensitivity [10]. However, there are some limitations of gradient elution in terms of higher complexity of instrumentation as well as the longer time of each run with the addition of re-equilibration procedure compared to an isocratic method.

### ***Ion exchange chromatography***

This separation technique is based on the difference in affinity of ionic molecules to reversely charged resin functional groups of the stationary surface. Cation exchange chromatography with a negatively charged ion exchange resin is used to separate positively charged ions. Reversely, the mode involving the separation of negatively charged molecules is referred as anion exchange chromatography with a positively charged ion exchange resin. The aqueous mobile phase and the stationary phase composed of a polymer matrix with charged functional groups are often used for this method. Ion exchange chromatography has been a widely used method for the quantification and purification of proteins, amino acids and nucleotides.

The strong resin functional groups like quaternary amine for the anion exchange and sulfonic acid for the cation exchange are normally used for the binding and separation of weak ions. Conversely, strong ions are retained and separated with the use of weak resin functional groups like amine and carboxylic acid. Ionic molecules of interest bound to a stationary surface will elute a column in one of two ways: displacing those with counterions in a mobile phase that have a stronger attraction to the stationary phase or changing the mobile phase pH to neutralize molecules resulting in their loss of attraction. The selectivity of separations can be controlled through varying mobile phase pH as it causes a change in the ionic strength of molecules.

### ***Size exclusion chromatography***

Size-based chromatography relies on the different exclusion of sample molecules from the pores of packing material as they flow through a column. In 1959, Porath and Flodin reported the gel filtration method for the size-based separation of peptides and proteins with the use of a synthesized dextran gel whose hydrophilic chains were cross-linked with epichlorohydrin [11,

12]. This material was then commercialized under the trademark of Sephadex, a synthesized porous sphere material that has been used for the standard separation of proteins [13]. The process using an aqueous mobile phase combining with hydrophilic materials of a stationary phase was termed gel filtration chromatography (GFC) to separate polysaccharides and proteins. The other process is called gel permeation chromatography (GPC) for separations of synthetic oligomers and polymers relying on the non-aqueous mobile phase and hydrophobic packing materials.

In size exclusion chromatography, the larger molecules the sooner they elute from a column as in one hand, they don't penetrate into pores of materials as the small ones do. On the other hand, the number of the pores that small molecules have to move out of is much higher resulting in their slow travel through a column.

#### *1.1.2.2. Factors of Chromatography*

##### ***Partition coefficient***

The equilibrium of an analyte (X) between two phases (mobile phase and stationary phase) is described as:



The equilibrium constant,  $K$ , is called partition coefficient and defined as follow:

$$K = \frac{C_s}{C_m} \quad (2)$$

where  $C_s$ : molar concentration of an analyte in a stationary phase

$C_m$ : molar concentration of an analyte in a mobile phase

Partition coefficient in chromatography is dependent on the characteristics of analytes, the mobile phase as well as the stationary phase.

### ***Retention time, capacity factor and selectivity factor***

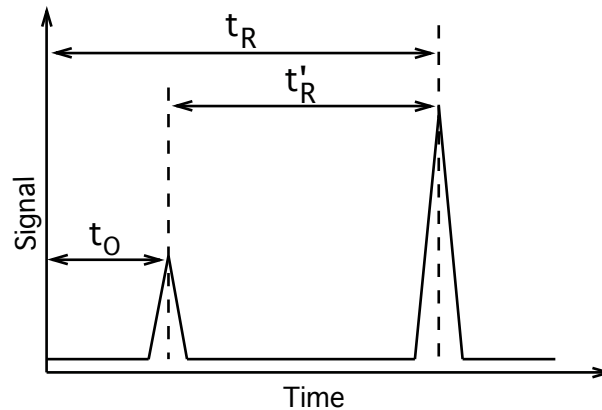


Figure 1-1. Retention time of an analyte in the chromatogram

The time between the injection of an analyte into a column and its elution at the end of a column with a peak reaching the detector is called retention time ( $t_R$ ) as demonstrated in figure 1-1. Each analyte in the mixture has its own retention time based on how it interacts with a stationary phase, given as:

$$t_R = t'_R + t_0 \quad (3)$$

where  $t'_R$ : the time an analyte retained in a column

$t_0$ : the time for a mobile phase travel through a column or so-called dead time.

The term of retention factor or so-called capacity factor ( $k$ ) is used to demonstrate the migration rate of an analyte in a column, given as:

$$k = \frac{t'_R}{t_0} \quad (4)$$

The higher the retention factor, the longer an analyte is retained in a column. The ideal value of this factor is between two to five. However, this value obtained in the separation of a complex sample with various components is acceptable in the wide range ( $2 < k < 20$ ).

The relative difference in retention of two analytes is termed the selectivity factor, described as:

$$\alpha = \frac{k_2}{k_1} \quad (5)$$

Two components will be separated if the first one is less retained in the column whereas the second one is more retained, hence the selectivity factor must be greater than 1 ( $\alpha > 1$ ).

### ***Band broadening and efficiency factor***

In chromatography, the column efficiency is determined either by the number of theoretical plates of a column ( $N$ ) or the plate height ( $H$ ). The higher number of plates or the smaller of plate height, the greater efficiency of the column, given in the following equation:

$$H = \frac{L}{N} \quad (6)$$

where  $L$ : the length of a column

The number of plates can be experimentally calculated from the chromatographic peak as follow:

$$N = 5.54 \left( \frac{t_R}{w_{1/2}} \right)^2 \quad (7)$$

where  $t_R$ : the retention time  
 $w_{1/2}$ : peak width at half-height (in units of time)

When the solute are injected into a column, some molecules pass through it quickly because of their inclusion in the eluent whereas others travel slowly due to their strong interaction with a stationary phase. This affects the band shape of chromatographic peaks. In chromatography, the bands of separated solutes are ideally as narrow as possible. The high-efficiency column makes it possible to obtain narrow and sharp peaks in a chromatogram. It is, therefore, essential to minimize the band broadening. According to the Van Deemter equation, the column efficiency characterized by a plate height relates to three main factors that contribute to the band broadening:

$$H = A + \frac{B}{u} + Cu \quad (8)$$

where  $H$ : the plate height (cm)  
 $u$ : the linear velocity of mobile phase (cm/s)  
 $A$ : Eddy diffusion parameter  
 $B$ : Longitudinal diffusion coefficient  
 $C$ : Resistance to mass-transfer coefficient

From equation (8), it can be deduced that the lower values of these factors contributing to the band broadening, the lower resulting value of the plate height. As a result, these factors need to be minimized in order to improve the separation efficiency.

*Eddy diffusion (A):* Solute molecules will randomly travel through a column on different paths. Some taking shorter paths will elute earlier than those traveling longer ways. This causes the broadening of the band. A column well packed with small-size particles should be used to minimize this diffusion.

*Longitudinal diffusion (B/u):* The concentration of analytes is higher in the center of the band than that at its edges. Naturally, molecules in the center will migrate to the edges, leading to the diffusion or the band broadening. Increasing the velocity of mobile phase helps decrease this diffusion as the shorter time an analyte travels through a column, the fewer molecules spread out.

*Resistance to mass transfer (Cu):* Molecules retained strongly by a stationary phase are left behind if the mobile phase velocity is high flowing over them without transferring them. This makes the band of an analyte broadened. This effect becomes greater in case the eluent velocity increases.

It can be concluded from the Van Deemter equation that, the velocity of a mobile phase is the most important parameter that must be optimized in order to minimize the longitudinal diffusion and the resistance to mass transfer to obtain the minimum value of the plate height. The optimum velocity and plate height are described in the Van Deemter plot below:

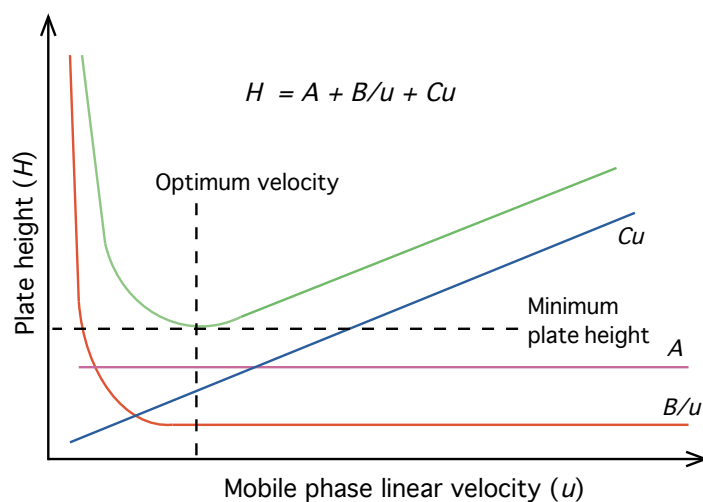


Figure 1-2. Van-Deemter plot

### ***Resolution factor***

The term of resolution ( $R$ ) used to describe how well components are separated is expressed in the combination of three factors including selectivity ( $\alpha$ ), number of theoretical plates ( $N$ ) and retention factor ( $k$ ), as shown in an equation below:

$$R = \frac{\sqrt{N}}{4} \left( \frac{\alpha - 1}{\alpha} \right) \left( \frac{1 + k}{k} \right) \quad (9)$$

In order to obtain a high-resolution, the three factors should be increased. The number of theoretical plates will be increased by reducing the particle size of a stationary phase rather than using a longer column as it maximizes the band broadening due to an increase in the retention time. The selectivity and retention factors can be experimentally manipulated by two methods: one involves the alteration of the composition and pH value of a mobile phase, the other is a change in the composition of a stationary phase.

#### **1.1.3. Detection in HPLC**

Quantification of compounds after chromatographic separations is conducted based on two approaches: Selective property detections measure the typical property of compounds like UV/Vis absorbance detection and fluorescence detection. Bulk property detections are used for measuring a change in the property typical to the eluting solvent and compounds as a whole. What type of the detection technique is the best choice depends on the characteristics of solutes and analytical purposes.

##### *1.1.3.1. UV/Vis absorbance detection*

UV/Vis absorbance detection is based on the property of many compounds that absorb the light in the UV/Vis region. It has been the most popular and commonly used detection technique in HPLC as it is highly responsive to a variety of interest organic compounds and easy to handle. The conventional single wavelength detectors have been gradually replaced by diode-array detectors (DADs) for the detection of a sample in several wavelengths simultaneously in order to get more information of the sample composition. DADs, therefore, provide qualitative information of the sample together with a quantitative analysis that single wavelength detectors cannot offer. The detection with DADs also enables to determine the highest sensitivity wavelength of an analyte in case there is no information on its molar absorptivity at different



wavelengths. The other major advantage of DADs is the peak purity analysis by examining a spectral homogeneity across the peak at several wavelengths. DADs have been employed for such many applications as: peptide mapping [14], toxicological drug screening [15, 16], identification and quantification of pesticides [17], quantification of fermentation inhibitors in the production of fuel ethanol [18].

#### *1.1.3.2. Fluorescence detection*

This technique is highly selective for fluorescent species that absorb the excitation radiation at specific wavelengths and instantly emit the light at longer wavelengths. It was investigated that fluorescence detection has been so far the most sensitive optical-based detection method whose sensitivity is one to three orders of magnitude higher compared to the UV/Vis absorbance detection. This method significantly depends on the determination of excitation and fluorescent emission wavelengths of the specific component in a sample. With advantages of high selectivity and sensitivity, fluorescence detection is useful for analyzing food and pharmaceutical products as well as the toxicological and environmental monitoring. It, however, has disadvantages of poor versatility with roughly 10% of fluorescent organic compounds and variation in fluorescence intensity caused by ambient temperature fluctuations.

#### *1.1.3.3. Refractive index detection*

Refractive index (RI) is a bulk property detection measuring the changes in the overall refractive index of a mobile phase induced by eluting components. The selectivity of this technique is poor as any component from an eluent that differs in the refractive index can be detected. The drawbacks this technique are low sensitivity, temperature dependence and incompatibility with a gradient elution that changes the refractive index of a mobile phase. They are useful for the detection of non-ionic components that are neither fluorescent species nor absorbing compounds in the UV/Vis range. RI detection has been often used for quantification of sugar [19, 20] and proteins in size exclusion chromatography [21].

#### *1.1.3.4. Electrochemical detection*

This detection technique is used to determine analytes that can be oxidized or reduced on the electrode surface. The output signals of a detector in terms of electric currents generated from oxidation and reduction reactions will be detected. Electrochemical detection is a highly selective technique as a voltage required for oxidation or reduction reactions depends upon the

voltammetric property of a solute. The major limitation of this method is its sensitiveness to the changes in the composition and flow-rate of a mobile phase. There are two types of electrochemical detectors: one is called a dynamic detector involving oxidation and reduction reactions of solutes, the other is termed an equilibrium detector which measures variations in the conductance of an eluent induced by components. A typical application of this detection is the quantification of biogenic compounds like dopamine and its metabolites [22], catecholamine [23].

#### *1.1.3.5. Evaporative light scattering detection (ELSD)*

This technique involves the three steps of nebulization, evaporation and detection. Nebulization is the transformation of an eluent from a chromatographic column to an aerosol of the fine spray. Followed by the evaporation in which only a mobile phase is evaporated in a hot drift tube and target components are left behind and then introduced into the optical head for the detection. A high-intensity radiation beam illuminating components is scattered and its photons are detected by a photomultiplier tube [24]. ELSD is regarded as a universal method as it can detect any non-volatile analytes or semi-volatile substances that are less volatile than a mobile phase. Setting the temperature of a hot drift tube should be taken into account when analyzing semi-volatile compounds in order to avoid their thermal decomposition resulting in poor signals. The sensitivity for low molecular components, however, is slightly poor due to the dependence of detection on their molecular size property [25]. This detection technique is useful for analyses of various non-absorbent compounds, for example carbohydrates [26, 27], lipids [28, 29] and polymers [30, 31].

#### *1.1.3.6. Mass spectrometry detection*

A state of the art detection method, mass spectrometry, which is capable of providing quantitative and qualitative results of components in a complicated mixture along with an extremely high sensitivity and reproducibility is by far the most powerful detection technique for pharmaceutical, chemical, clinical and toxicological analyses. This technique involves the thermal ionization of compounds to generate ions that subsequently separated and detected based on their mass to charge ratios ( $m/z$ ). Electrospray ionization (ESI) is among the most popular ionization techniques in which a liquid phase is transformed to charged droplets by an electric field. The solvent evaporates when passing a dry nitrogen combining with heat, decreasing the size of droplets. As a result, the charge density on the surface of droplets

increases and the residual charge of droplets is transferred to compounds to form gas-phase ions [32]. Various mass analyzers have been developed and commercialized with differences in mass range, resolution, scan-rate and detection limits to satisfy a wide range of analytical applications [33]. Mass spectrometry in combination with HPLC has been the standard analytical method facilitating the identification and quantification of proteins, small-molecule biomarkers, pharmacology screening analyses and the determination of pesticides and toxins [34-36].

#### 1.1.4. HPLC instrumentation

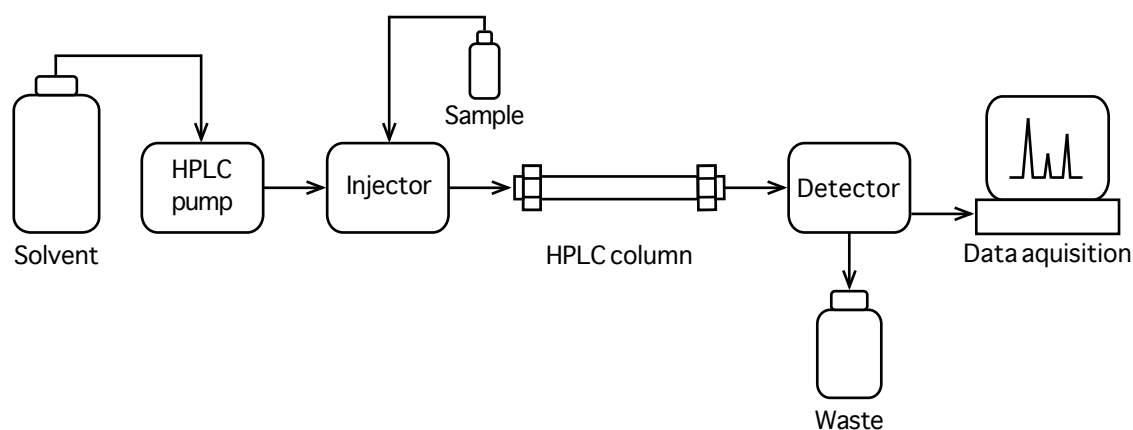


Figure 1-3. The overview of a HPLC instrument

A typical HPLC system is shown in figure 1-3 consisting of a pump for solvent delivery, a sample injector, a separation column, a detector and a data acquisition system. A thermostat for temperature conditioning of the column and a pre-column for protecting the column from impurities are often equipped with standard HPLC instruments. A degassed mobile phase is pumped through the column with a traditional pump (pressure limit up to 6000 psi) and a sample solution is introduced into the column with a manual or an auto-injector. The column in which a separation of analytes occurs is packed with chemically bonded silica-based particles. The particle size from 3 to 5  $\mu\text{m}$  has been normally used. Note that, the use of smaller particles (1.7 to 2.7  $\mu\text{m}$ ) for higher efficiency should be considered as a higher-pressure pump is required. A standard UV/Vis absorbance detector or a diode array detector is positioned at the outlet of a column for the detection. Alternative detectors can be employed depending upon analytes and analytical purposes. Output signals from a detector are recorded and processed for the exhibition of chromatographic peaks as results.

## **1.2. Capillary electrophoresis (CE)**

### **1.2.1. Brief history of the development of CE**

Electrophoresis is a separation technique on the basis of differential migration of charged species through an electrolyte solution under the influence of an applied electric field. The history of electrophoresis dates back to important experiments of Kohlrausch in 1897 from which equations of the ionic migration were formulated [37]. Tiselius was the first to work on electrophoresis and won the Nobel Prize in 1948 for his development of “moving boundary electrophoresis” described as a new method for the investigation of physico-chemical properties of proteins [38]. For the first time, his experiments were carried out in a quartz U-shaped tube employed as an electrophoretic cell and the protein boundaries were observed with an optical detection in the UV range. Later on, a rectangular cross-section cell was used in combination with an efficient cooling in order to reduce the thermal convection caused by an electrical heating. This unexpected effect leads to the band broadening and hence decreases the separation efficiency. Later on, a variety of supporting media has been developed to counteract the convection to improve zone electrophoresis. Durrum in 1950 reported the use of filter papers for the separations of amino acids, peptides and proteins in mixtures into zones [39]. The pioneering employment of starch gels as supporting media for the successful separation of serum proteins by Smithies in 1955 initiated the application of gels in zone electrophoresis of proteins [40]. Polyacrylamide prepared in acid or alkaline buffer solutions was first used as stabilizing media in zone electrophoresis by Raymond in 1959 [41]. The polyacrylamide-based gel (PAG) with its features of high stability and transparency when it has been formed was well suited for electrophoresis. Shapiro in 1966 performed the separation and identification of polypeptide chains of a disulfide-linked protein with electrophoresis in the polyacrylamide gel with the presence of sodium dodecyl sulfate (SDS) [42]. Electrophoretic separation in PAG with SDS so far has been the most widely used tool for determining the molecular weight and size of polypeptides and proteins.

The use of stabilizing media as anti-convection agents in electrophoresis, however, has major disadvantages of poor reproducibility and low sensitivity in some cases presumably due to undesirable adsorptive interactions of analytes and supporting media. Hjertén in 1967 proposed an alternative approach to a reduction of the convection effect. In this work, he developed an automated apparatus to rotate a 0.3 mm quartz capillary tube coated with methylcellulose for the electroosmosis elimination along its longitudinal axis [43]. His

method was called free zone electrophoresis. Following the feasible anti-convection solution investigated by Hjertén, in late 1970s Mikkers reported an electrophoresis separation cell formed by a 200  $\mu\text{m}$  i.d PTFE capillary tubing [44]. A new era for CE was opened up with the introduction of a 75  $\mu\text{m}$  i.d fused silica capillary for separations in combination with the application of high voltages up to 30 kV and an on-line fluorescence detection for the determination of ionic species and amino acids by Jorgensen and Lukasc in 1981 [45]. The employment of narrow tubings helped reduce zone broadening as it allowed an efficient dissipation of the heat generated by the use of high voltages. Since the early 1980s, the use of fused silica capillaries in micrometer (20 - 100  $\mu\text{m}$  i.d) as separation channels for zone electrophoresis has been widespread. Terabe in 1984 reported an electrokinetic separation of neutral compounds with a micellar solution in open tubular capillaries [46]. In 1988, the first commercial CE instrument was introduced by Brownlee and coworkers [47]. It featured on-column UV/Vis absorbance and fluorescence detectors, an automated injection as well as a computerized data acquisition for fast and high-resolution separations. Along with the commercial availability of powerful and higher automation CE instruments during the past decades, many efforts have been dedicated to the development and construction of miniaturized devices in which all steps of injection, separation and detection are performed in micro-channels (Lab-on-chip concept). CE with advantages of high speed and resolution, low cost and ease of operation has been a useful separation technique for numerous applications in pharmaceutical, biological, clinical and environmental analyses.

### **1.2.2. Basic principles of CE**

Capillary electrophoresis is the separation technique of ions in narrow-bore capillaries (20 - 100  $\mu\text{m}$  i.d) performed by the application of high voltages. When introduced to an electric field, ions with different masses and charges will move differently within a homogeneous solution in terms of directions and velocities. That is the separation principle of CE. In capillary zone electrophoresis (CZE), the migration of charged species is affected by two fundamental processes. One is their electrophoretic migration in an electric field and the other is called the electroosmosis caused by the surface charge of the internal capillary wall when a high voltage is applied.

### 1.2.2.1. Electrophoretic migration

The separation in CZE under an electric field is principally based on the difference in migration of ionic solutes or electrophoretic velocities ( $v$ ) that are given by:

$$v = \mu_e E \quad (10)$$

where  $\mu_e$  is the electrophoretic mobility of an ion

$E$  is the electric field strength calculated by dividing the applied voltage by the total length of a capillary

A molecule with charge  $q$  experiences two forces. The first is an electric force given by:

$$F_e = qE \quad (11)$$

The second is a frictional force caused by viscosity on a spherical molecule moving through a viscous buffer, expressed by Stocks' law:

$$F_f = 6\pi\eta r v \quad (12)$$

where  $q$  is the charge of an ion

$\eta$  is the viscosity of the solution

$r$  is the ion radius

$v$  is the ion velocity

When a steady state is obtained, these forces balance each other and have opposite directions that can be expressed by:

$$qE = 6\pi\eta r v \quad (13)$$

Electrophoretic mobility can be determined by substituting equation (13) into equation (10) as:

$$\mu_e = \frac{q}{6\pi\eta r} \quad (14)$$

It can be deduced from equation (14) that, large and slightly charged ions have low mobilities, inversely small and highly charged ions possess high mobilities.

### 1.2.2.2. Electroosmosis

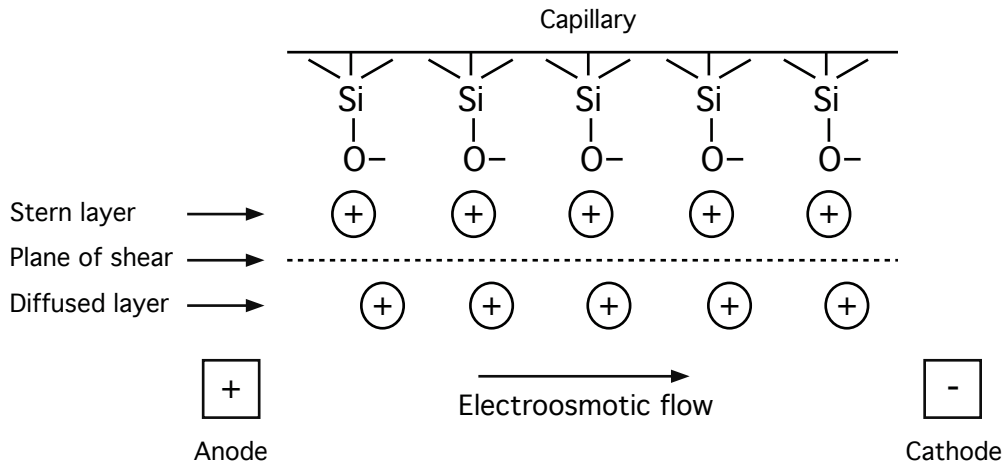


Figure 1-4. Electroosmotic flow in a capillary

The other primary process involved in CE separation is the electroosmosis originating at the internal capillary wall. Once fused silica capillaries contact with buffer solutions at pH values above two, its surface silanol groups (Si-OH) are ionized to silanoate (Si-O<sup>-</sup>) forming a negatively charged surface as shown in figure 1-4. Positively charged ions (counter-ions) existing in the buffer electrostatically interact with these negatively charged silanoate groups resulting in the formation of an electrical double layer. It was found that the counter-ions are bound to the capillary wall in two layers. One is the fixed layer, so-called Stern layer, on which cations are firmly held and the other is the outer layer termed the diffused layer. When a high potential is applied, cations in a diffused layer to which they are loosely bound are attracted to the cathode (negative electrode). As these cations are solvated, their migration towards a cathode drags a bulk of buffer solution with them, generating a flow of liquid known as the electroosmotic flow (EOF). The linear velocity and mobility of EOF are given by the following equations:

$$v_{EOF} = \frac{\epsilon \zeta}{\eta} E \quad (15)$$

$$\mu_{EOF} = \frac{\epsilon \zeta}{\eta} \quad (16)$$

where  $\epsilon$  is the dielectric constant of a buffer solution  
 $\zeta$  is the zeta potential of a capillary wall  
 $\eta$  is the viscosity of a buffer solution

Because of the presence of EOF, the overall mobility of an ion that is termed apparent mobility ( $\mu_a$ ) is an aggregate of its electrophoretic mobility and electroosmotic mobility expressed by:

$$\mu_a = \mu_e + \mu_{EOF} \quad (17)$$

As the mobility of EOF is higher than that of most solutes at the neutral and alkaline buffer pH, all species regardless of charge are swept in one direction from an anode (positive electrode) to a cathode (negative electrode) if the capillary wall is negatively charged. This facilitates the simultaneous determination of cations and anions in a single run. For the optimization of separations in CZE, the EOF can be controlled or modified by altering experimental conditions including the temperature, the buffer concentration, a buffer pH, organic solvents and buffer additives. Adjusting the buffer pH affects the dissociation of the silanol groups, therefore, affecting the EOF. At a high pH value of an electrolyte solution, the deprotonation of those is accelerated leading to an increase in the EOF. The buffer concentration has an effect on EOF through altering the zeta potential. An increase in concentration will reduce the EOF as it inversely relates to the square root of the electrolyte concentration. An addition of organic solvents to a buffer solution changes its viscosity and zeta potential resulting in the modification of EOF. The use of additives including methyl cellulose, polyacrylamide and quaternary amines is found to be significantly effective in some certain operation modes of CE in which the suppression of EOF is required.

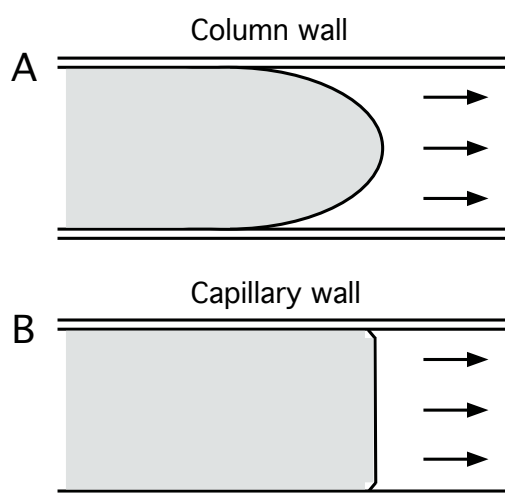


Figure 1-5. Laminar flow in HPLC (A) and Flat flow of EOF in CE (B)

In contrast to the laminar flow with a parabolic profile in pressure-driven systems, the EOF electrically driven through a capillary has a flat flow velocity profile as demonstrated in figure



1- 5. This can be explained by the uniform distribution of the EOF driving force along a channel leading to its uniform flow velocity within the entire length of a tubing. The unique feature of a flat flow velocity is a major advantage of CE since the dispersion of analytes zone (band broadening) is significantly reduced providing a high separation efficiency.

#### *1.2.2.3. Modes of CE*

Capillary electrophoresis consists of diverse techniques based on different physical-chemical characteristics and operative principles. Those commonly performed are capillary zone electrophoresis (CZE), capillary gel electrophoresis (CGE), micellar electrokinetic capillary chromatography (MEKC), capillary isoelectric focusing (CIEF) and capillary isotachopheresis (CITP).

#### ***Capillary zone electrophoresis (CZE)***

CZE is the most frequently used technique in which the separation of analytes is carried out in an open capillary filled with a homogeneous electrolyte solution under the application of high voltages. This mode, also termed free solution CE, is based on the electrophoretic mobilities of charged solutes and an electroosmosis phenomenon. In principle, the separation in CZE is governed by a buffer pH as it affects the migration of ions and the EOF mobility. At a high buffer pH, both cations and anions can be separated in a single run because anions whose mobilities are significantly lower than that of EOF are swept towards the cathode. At low pH where EOF is insubstantial, it is impossible to determine cations and anions in a single separation. In this case, anion measurement is facilitated by reversing the polarity of electrodes in which they migrate to the anode and pass a detector with the same direction of the EOF. This electro-based separation technique is not applicable to neutral species as they migrate at the velocity of EOF and are not separated from each other.

#### ***Capillary gel electrophoresis (CGE)***

Originated from the traditional gel electrophoresis, the separation mechanism of CGE is based on the difference in size of components as they are traveling through the pores of gels filled in 50 - 100  $\mu\text{m}$  i.d capillaries. In practice, the EOF is suppressed in order to minimize an extrusion of the gel from a capillary. Non-crosslinked polymers and linear polyacrylamide are presently popular as sieving media as they overcome the disadvantages of traditional crosslinked gels. Size separation in gel-filled capillaries offers the high-efficiency and

reproducibility that makes it by far one of the most suitable methods for proteins characterization and DNA fragmentation analyses.

### ***Micellar electrokinetic capillary chromatography (MEKC)***

MEKC has the principles of reverse-phase LC and CZE in which micelles added to the buffer solution to interact with analytes play a role of a stationary phase and an aqueous buffer acts as a chromatographic mobile phase. The separation mechanism of this technique relies on the individual partitioning equilibrium of different solutes between the hydrophobic tail of micelles and an electrolyte solution. This method allows the simultaneous separation of ions and neutral species. Hydrophobic components with their stronger interactions to micelles have lower velocities than those of more polar molecules. Sodium dodecyl sulfate (SDS) is the most popular anionic surfactant used in MEKC. This technique is relevant to separate a wide range of small nonionic compounds as well as peptides and proteins.

### ***Capillary isoelectric focusing (CIEF)***

Isoelectric focusing is performed in a pH gradient between two electrodes and its separation principle is based on the individual isoelectric points (pI) of molecules where they stop migrating. A pH gradient is generated by adding ampholytes, so-called zwitterionic compounds, to an electrolyte solution. Ionic molecules under application of a voltage migrate toward the reversely charged electrodes till they reach pH regions where their net charges are zero and thus focusing. As a result, different focusing zones are created along a channel and then subsequently shifted toward the detector by applying a pressure flow. The separations of proteins and peptides are typical applications of this mode.

### ***Capillary isotachopheresis (CITP)***

CITP features the separation of components based on their mobilities in the zone between a leading and a terminating electrolyte solutions when an electric field is applied. A leading electrolyte has the highest mobility of all ions existing in system whereas a terminating solution possesses the lowest mobility. In this method, the different solutes migrate at the same speed forming individual zones before a terminating electrolyte and after a leading one. CITP is employed for the pre-concentration before the separation and sample purification.

### 1.2.3. Detection in CE

In short, the most widely used methods for detection in HPLC have been adapted for the quantification in CE where narrow capillaries are used for the separation. These include UV/Vis absorbance, fluorescence, electrochemical detection and mass spectrometry detection.

#### 1.2.3.1. UV/Vis absorbance detection

This on-column method has been so far most commonly employed for CE as many analysts absorbing radiation in the UV/Vis range can be directly detected. Moreover, the instrumentation is available from HPLC. To quantify non UV-absorbing species in the indirect mode, an UV probe is often introduced to the background electrolyte. The presence of this ionic UV absorbent, however, decreases the amount of light coming to the detector resulting in a reduction in the measurement sensitivity. The major drawback of UV/Vis absorbance is the poor detection limit ( $10^{-6}$  -  $10^{-5}$  M) due to a short optical path-length that is theoretically equal to the inner diameter of a capillary in the detection zone. Some promising approaches have been carried out to improve the sensitivity by increasing the path-length through modification of capillary geometries at detection window [48-50] and a multi-reflection cell [51].

#### 1.2.3.2. Fluorescence detection

Among those detection methods mentioned above, fluorescence by far has been the most sensitive approach in which the detection limits of femtomole ( $10^{-13}$  M) could be achieved with a laser excitation source [52]. A laser induced fluorescence detector has been commonly used in most CE applications as it provides high-intensity incident light easily focused to a relatively narrow detection zone of a capillary. The major disadvantage of this detection technique is that many analytes of interest do not possess the native fluorescence. Two alternative approaches can be employed for detecting non-native fluorescent species: one is an indirect measurement by the use of fluorophores in buffer solutions; the other is the chemical derivatization of species prior to the detection. Detection limits of micromole range ( $10^{-6}$  M) obtained with an indirect fluorescence technique are significantly poorer compared to those of direct measurements. This makes indirect detections rarely used in CE while derivatization fluorescence techniques have been popularly used in pharmaceutical and forensic analyses. CE in combination with the native fluorescence detection has been employed for determining proteins and peptides [53, 54], drugs and their metabolites [55, 56], and single cells [57, 58].

### *1.2.3.3. Electrochemical detection*

Potentiometric detection (PD) is based on the measurement of voltages between a working electrode and a reference electrode. The working electrode acting as a selective sensor for a specific ion is produced from a crystalline, liquid or glass membrane. The potential difference between two electrodes is generated at the working electrode as a result of the ion migration through a semipermeable membrane, which can be given by the Nernst equation. In PD, signals do not go up with the electrode size. This feature is beneficial to the miniaturization. Some applications of CE-PD include measurements of inorganic and organic anions [59, 60], alkali and alkaline earth cations [61].

Amperometric detection (AD) relies on measuring a current produced by the oxidation or reduction of an analyte at the working electrode surface under the application of a fixed potential. This current is directly related to the concentration of a solute. Though AD features high selectivity and sensitivity, it has a major disadvantage in which the absorption of intermediate products from a redox reaction of a solute onto the electrode surface influences the working electrode activity. AD is well suited for the determination of electroactive species, for instance catecholamines [62, 63], amino acids [64, 65] and carbohydrates [66].

Conductivity detection determines analytes of interest based on measuring the conductivity of a solution in the gap between two electrodes. Conductivity detectors consist of two electrodes placed side by side around a capillary across which an AC potential at high frequency is applied. On the surface of an electrode, there is a double layer of electrons established that behaves like two plates of an electronic capacitor. The equivalent circuitry of a conductivity detector, therefore, consists of two capacitors that are connected by a resistor formed by the solution in the gap between those. When an analyte travels through this gap, the conductivity of solution changes. According to the Ohm's law in which the current relates to the conductivity, there is a current resulting from the difference in conductance between the solute and the background electrolyte that will be measured as an output signal. In the course of measurement, AC voltage is applied instead of DC potential so as to avoid electrolysis reactions on electrode surfaces. Conductivity detection can be performed in two approaches: one is based on the galvanic contact between electrodes and an electrolyte solution; the other is carried out in contactless mode. Various applications of the conductivity detection for CE in diverse disciplines are described in publications [67-71].

#### 1.2.3.4. Mass spectrometry

Mass spectrometry (MS) provides not only a highly sensitive detection but also structural information of compounds. CE-MS has become a powerful tool for the separation and identification of biomolecules [72-74]. Electrospray ionization (ESI) is the most commonly used interfacing technique to couple CE with MS as its mild ionization facilitates the direct transfer of solutes from CE to MS. This coupling, however, poses a major problem regarding the acceleration of a liquid flow coming from capillary in the nL/min range to higher values (200  $\mu\text{L}/\text{min}$ ) to form a stable spray. Three different ESI interfaces have been developed to overcome this hurdle including sheath-flow, sheathless and liquid-junction interfaces. Further details on the principles and formation of those electrospray-based interfaces can be found in a publication [75]. The combination of CE with MS has been employed for a wide range of applications in various disciplines of biological, environmental, pharmaceutical and drugs, food and forensic analyses [76-80].

#### 1.2.4. Capillary electrophoresis setup

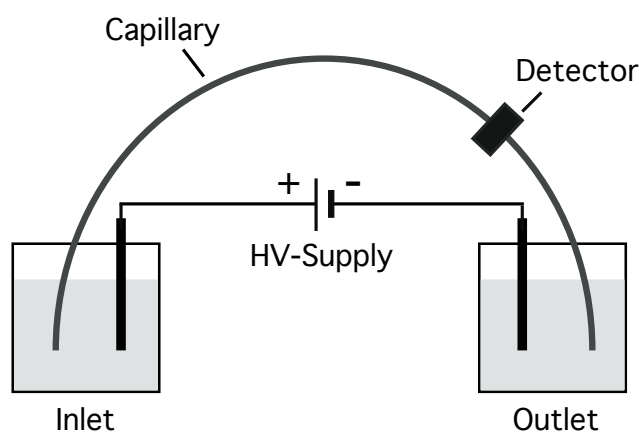


Figure 1-6. The overall arrangement of a CE setup

As shown in figure 1-6, a typical capillary electrophoresis system comprises a fused silica capillary for separation, a high voltage power supply of 20-30 kV, two electrodes, two buffer vials, a detector and data acquisition system. Based on analytical purposes, this basic configuration of CE can be upgraded for the better performance with such advanced components as: an auto-sampler, a temperature conditioner and multi-detectors. Two electrodes normally made from platinum connected with a power supply and two ends of a capillary are submerged in vials containing an electrolyte solution. A detector can be arranged

either on-column or off-column at the outlet of a capillary for detecting separated components. Output signals of a detector recorded and processed by the data acquisition system are plotted versus time in an electropherogram.

In short, the sample can be introduced into a capillary in two methods: Hydrodynamic injection is performed either by the pressure injection in which a pressure is applied at the injection end or vacuum is used at the exit side of a capillary to force analytes into a column. In siphoning injection, analytes are dragged to the outlet by gravity if the inlet of a capillary is lifted up. Electrokinetic injection is accomplished by the application of an electric field in which solutes move into a channel by both the electrophoretic migration and the dragging effect of an EOF.

### **1.3. Ultraviolet-visible absorption spectroscopy**

#### **1.3.1. Brief history of UV/Vis absorption spectroscopy**

UV/Vis spectroscopy is one of the most commonly used detection techniques in analytical sciences based on the absorbance measurement of radiation at specific wavelengths in the region of 190 - 1000 nm. This versatile analytical technique is useful for the quantification of various compounds in liquid, gas and solid samples in many applications of environmental, biological, pharmaceutical, clinical and material analyses.

The early history of UV/Vis spectroscopy dates back to the theory about the light and colors of Newton in 1672 in which the white light was separated into its component colors as it passed through a prism [81]. Kirchhoff in 1860 introduced a theory of emission and absorption with the discovery that a good radiation emitter at a certain wavelength also absorbs the light at the same wavelength [82]. A milestone in the development of spectroscopy was set by Bohr in 1913 with his famous paper "On the constitution of atoms and molecules" based on the quantum theory previously proposed by Planck and Einstein. He demonstrated that electrons either absorb or emit energy during their transitions from one state of the constant energy to another state. The amount of this energy was found to be absolutely equal to the energy difference between two states [83]. Emission and absorption spectroscopy in the visible range was used as a convenient tool to study electronic transitions and identify elements. The potential of absorption photometry to the analytical chemistry was marked by August Beer who was the first to investigate the proportional relationship between

the absorption of radiation and concentrations of an analyte in the sample [84]. One of the first spectrophotometers was developed in the 1930's based on fundamentals of the spectroscopy and a photo-detector, that employed a prism or a grating to isolate a particular wavelength for absorption measurements [85]. In this instrument, the concentration of an analyte was determined relying upon the Lambert-Beer's law, a combination of two laws in which the absorbance is proportionally related to the molar absorptivity coefficient ( $\epsilon$ ), the thickness of sample through which the light passes or so-called the path-length ( $l$ ) and the concentration of an absorbing analyte ( $C$ ). In 1947, the first commercial UV/Vis spectrometer, the Carry 11, was released by Varian [86]. The first commercial availability of a diode-array spectrophotometer in the 1970s allowed a simultaneous scan of the whole spectrum of wavelengths in seconds due to the use of an array of photodiodes [86]. The development of instrumentation for UV/Vis absorption spectroscopy has progressed so far in order to achieve the improvement focusing the portability, ease of use and specific applications of life science and material analyses.

### 1.3.2. Basic principles of UV/Vis absorption spectroscopy

#### 1.3.2.1. The origin of the light absorption

Ultraviolet and visible light constituents a small proportion of an electromagnetic spectrum in the range of wavelengths from 400 to 700 nm that can be seen by the human eyes. The deep ultraviolet region with its wavelengths from 200 to 390 nm is invisible to typical human eyes. Electromagnetic spectrum comprises other radiation forms ranging from very short wavelengths (gamma, X-rays) to extremely long wavelengths (microwave, radio).

According to the quantum theory, the radiation is considered as a stream of photons. The energy carried by a photon at a certain wavelength is given by the following equation:

$$E = h\nu \quad (18)$$

where  $h$  is the Planck's constant ( $6.63 \times 10^{-34}$  Js)  
 $\nu$  is the frequency (Hz)

It was already known that radiation behaves as a wave whose frequency relates to wavelength ( $\lambda$ ) by an equation:

$$c = \nu\lambda \quad (19)$$

where  $c$  is the velocity of light ( $3 \times 10^8 \text{ ms}^{-1}$ )

From equations (18) and (19), we have:

$$E = h \frac{c}{\lambda} \quad (20)$$

It can be deduced from equation (20) that in the UV/Vis range, short wavelengths of UV region has the higher energy than the visible light at longer wavelengths.

A molecule of any substances exists in some defined energy states and the energy level of each state is considered as the sum of its electrons' energy. The change of energy level occurs when a molecule absorbs or emits energy in the form of photons. When a radiation of high-energy photons is absorbed by the sample, the valence electrons of molecules are excited to transit from their normal states (ground states) to higher energy states (excited states). This process is called an electronic transition. Valence electrons are categorized in three types of electron orbitals including non-bonding orbitals ( $n$ ), single bonding orbitals ( $\sigma$ ) and double or triple bonding orbitals ( $\pi$ ). When a radiation of the exact frequency is absorbed, a transition arises from one of these bonding orbitals to an anti-bonding orbital ( $\pi^*$  or  $\sigma^*$ ) as shown in figure 1-7. The absorption bands arisen from the  $\pi$  to  $\pi^*$  and  $n$  to  $\pi^*$  transitions (red color) are important to the UV/Vis spectroscopy as they are associated with the absorption of radiation in the region of 200 - 800 nm. The higher transitions (blue color) require more energy resulting from the absorption of the deep UV light of wavelengths less than 200 nm.

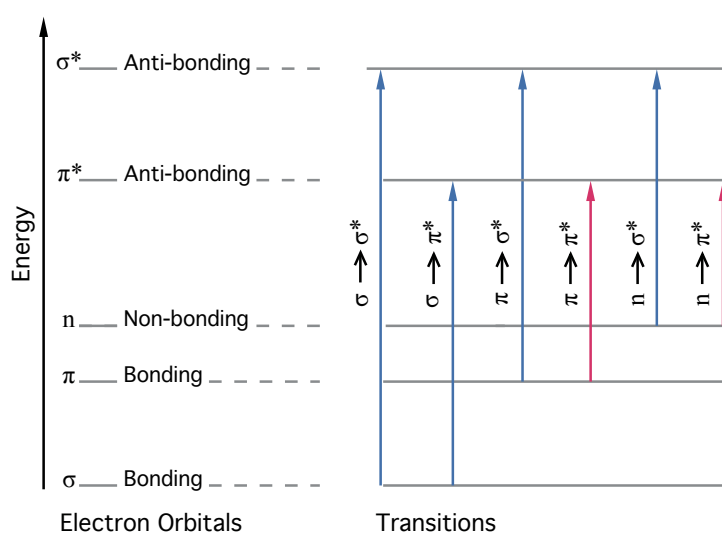


Figure 1-7. Electron transitions in the UV/Vis spectroscopy



Table 1. Chromophores and maximum absorption wavelengths

Chromophores	Formular	Example compound	$\lambda_{\max}$ (nm)
Nitrile	RC=N	Acetonitrile	< 160
Acetylene	RC $\equiv$ CR	Acetylene	173
Ethylene	RHC=CHR	Ethylene	193
Carboxyl	RCOOH	Acetic acid	204
Amide	RCONH <sub>2</sub>	Acetamide	208
Ketone	RR'C=O	Acetone	271
Nitro	RNO <sub>2</sub>	Nitromethane	271
Carbonyl	RHC=O	Acetaldehyde	293

A variety of organic compounds exhibit absorption spectra in the UV/Vis region due to the presence of functional groups containing a  $\pi$  bond that are called chromophores. Some of chromophores and their maximum absorption wavelengths ( $\lambda_{\max}$ ) are shown in table 1. A multiple chromophores are formed if a simple chromophoric group is conjugated with another that shows a more intense absorption band at a longer wavelength than that of the single chromophore.

#### 1.3.2.2. Lambert - Beer's law

Lambert's law states that the amount of light absorbed or absorbance ( $A$ ) is defined as a logarithmic function of incident light intensity ( $I_0$ ) and transmitted light intensity ( $I$ ) given as:

$$A = \log \frac{I_0}{I} \quad (21)$$

According to Beer's law, the light absorption is proportional to the concentration of an absorbing compound ( $C$ ), molar absorptivity coefficient ( $\epsilon$ ) and the optical path-length ( $l$ ), specified as:

$$A = \epsilon l C \quad (22)$$

Combining the two equations of (21) and (22), the Lambert - Beer's law is derived as:

$$A = \log \frac{I_0}{I} = \epsilon l C \quad (23)$$

The Lambert - Beer's law is only true for the radiation of a single wavelength that is termed a monochromatic light and applicable to the measurement of absorbing species whose physical and chemical properties do not change with the concentration.

## **1.4. Light-emitting diodes for absorption spectroscopy**

### **1.4.1. Brief development history of LEDs**

Light-emitting diode (LED) is a two-terminal radiation source based on an electroluminescent effect in an inorganic material that occurs when an electric current passes through it. The phenomenon of electroluminescence was discovered by Round in 1907 while he attempted to construct a rectifying solid-state detector. He reported that a yellowish light was produced when a potential was applied between two points on a carborundum crystal [87]. Oleg Losev, a Russian talented scientist, was the first to report the light emission from a zinc oxide and silicon carbide diode in the mid 1920s. He is believed to have discovered a semiconductor LED [88]. Losev comprehensively investigated the current-voltage characteristics of an LED and proposed a well-known formula to calculate the voltage drop on the diode contact,  $V$ , as a function of the light emission frequency,  $\nu$ , the electronic charge,  $e$ , and Planck's constant,  $h$ , that is  $\nu = eV/h$ . The infrared radiation generated from gallium arsenide (GaAs) and other semiconductor alloys of gallium antimonide (GaSb), Indium phosphide (InP) and silicon germanium (SiGe) at room temperature and 77 Kelvin was recognized by Braunstein in 1955 [89]. In 1961, Biard and Pittman observed the near infrared radiation emitted from GaAs when exposed to an electric current. Not long afterward, the first commercial *p-n* junctions infrared LED (the SNX-100) was launched by Texas Instruments in 1962 that employed the pure GaAs crystal as an illumination substrate for the light emission at 890 nm [90]. Holonyak in 1962 was the first to develop a visible (red) LED based on Ga(As<sub>1-x</sub>P<sub>x</sub>) *p-n* junctions whose peak emission wavelength at 710 nm was sharply demonstrated [91]. The wavelength output of visible LED was subsequently moved down to the yellow spectrum by Craford in the early 1970s [92]. Another milestone in the LED development was marked by Nakamura with his invention of a high-intensity blue LED in 1994 [93]. This indium gallium nitride (InGaN)-based blue LED featured the peak wavelength at 450 nm. The availability of a high-output blue LED promptly led to the development of the first white LED in 1996. White light is generated either by a mixture of LED substrates of different colors (red, green and blue) or a combination of blue and yellow lights resulted from the fluorescent phosphor layer that appears white to human eyes. Nakamura and his coworkers were awarded the Noble

prize in 2014 for their great invention that facilitated the creation of the bright and efficient white light in a new way. Near ultraviolet devices emitting at 390 nm were commercially released in early 2000s. The progression of aluminum gallium nitride substrates for illumination (AlGaN and AlGaInN) made the deep UV-LEDs with emission wavelengths down to 230 nm available recently [94, 95].

LEDs with their advantages of high-efficiency, long lifetime, low-heat generation, low-cost and compact size are beneficial to industrial production and scientific research. The most prominent application of visible LEDs is the indicators and display on electronic circuits and instruments and notably for the illumination in which they have been replacing the incandescent light sources. Near infrared (IR) LEDs have been widely used for the remote control and fiber optic telecommunications while UV-LEDs have been commonly employed for UV curing, banknote and security, disinfection and sensing purposes.

#### **1.4.2. Working principles of LEDs**

The light generation of an LED results from an electroluminescence in the p-n junction diode under the application of an electric field. When an electric field is applied, free electrons in the n-region and electron holes in the p-region are driven to the active layer at which the recombination occurs as illustrated in figure 1-8. Free electrons are of conduction band whose energy level is higher than that of valence band of which electron holes exist. The recombination of electrons and holes at the active layer releases an energy in the form of photons or heat. In the radiative recombination, a photon with energy equal to the band-gap energy is produced. In the course of a non-radiative recombination, the electron energy is transformed into the vibrational energy of lattices atoms known as phonons, which results in heat in devices [26]. The dissipate energy for silicon and germanium semiconductors is predominantly in the form of heat whereas the dissipate energy in gallium phosphide (GaP) and gallium arsenide phosphide (GaAsP) is an emission of photons. The non-radiative recombination is an unwanted process reducing the light emission efficiency and thus it must be minimized.

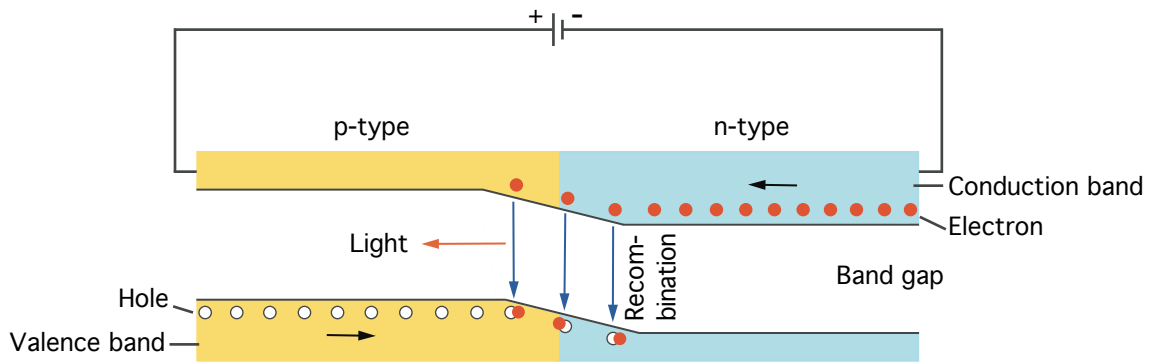


Figure 1-8. Inner working diagram of an LED

As shown in figure 1-9 is a sketch of an LED in the most common package. The light emits from a semi-conducting material that is contained in a reflective cup on top of one connecting lead. A thin wire connected the other lead contacts material layers from the top. The whole assembly is encapsulated in an epoxy resin. Different types of package are available including a surface mounted high-power LED and a miniature version for multiple applications. For low power LEDs in the standard package, the heat sink is not as crucial as high power LEDs due to their low power consumption. This standard package features the dome for a light dispersion. However, the wide beam is not usually beneficial to analytical purposes in which the highly focused beam is required. In these cases, an LED in the standard package equipped with ball lens at the dome for radiation focusing has been employed.

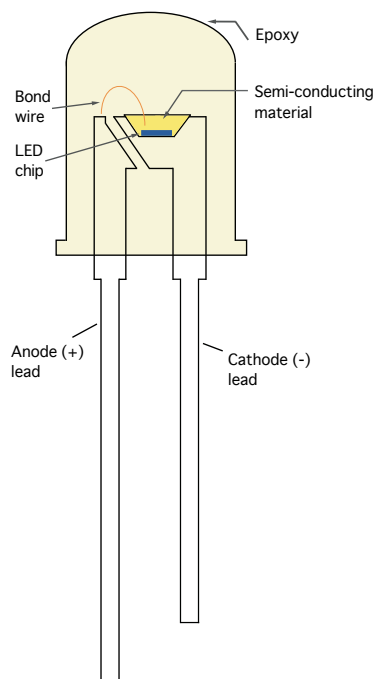


Figure 1-9. A light-emitting diode in a common package

### **1.4.3. Applications of LEDs for absorption photometry**

The development of LEDs covering the wide region from IR to deep UV along with the improvement of intensity and reducibility made them potential alternatives to discharge lamps as radiation sources for photometric instruments especially for portable devices due to their low power consumption. Notably, a narrow emission band of typically 20 nm in width allows removing a costly monochromator that is indispensable to tungsten-halogen or deuterium lamps. To date in the field of analytical sciences, LEDs have been mostly applied for absorbance measurements. The first LED-based detector using a red LED was reported by Flaschka in 1971 [96]. Hauser was among the first to report the use of a blue LED for absorption photometry after its invention in 1991 [97]. Infrared LEDs have become ideal light sources for the detection of gas molecules such as carbon dioxide (CO<sub>2</sub>) [98, 99], methane (CH<sub>4</sub>) [100-102], and carbon monoxide (CO) [99]. The commercial availability of UV-LEDs and the recent release of deep UV-LEDs have extended applications of LEDs as the majority of organic species absorb in these ranges rather than the near-UV and visible regions. LEDs as radiation sources for absorbance photometer have been reviewed repeatedly. Dasgupta was the first to review absorption spectroscopy based on LEDs [103, 104]. O'Toole and Diamond wrote the review of absorbance optical sensors and sensing devices with the use of LEDs in 2008 [105]. There have been some reports focusing on the LED-based absorbance detection in CE [106, 107] and LC [108-110]. The LED-based absorption photometry was found to be the simple, low-cost and sensitive detection technique whose applications cover various fields of research including chemical, biological, pharmaceutical and clinical analyses.

## 1.5. Research objectives

The objective of this dissertation was to develop absorbance detectors employing deep UV-LEDs as radiation sources for absorption spectroscopy and evaluate their performance in the quantification of some model compounds in the applications with narrow column high-performance liquid chromatography and capillary electrophoresis as well as aromatic hydrocarbons in the gas phase. Some photometric devices were designed and constructed for different analytical purposes:

- (1) ***Comparative study of light-emitting diodes and standard silicon photodiodes in photometric measurements.*** Reverse biased LEDs are known to serve as photodetectors. Some LED-based devices for photometric measurements employing one LED for the emission and the other of the same type for the detection have been reported. To our knowledge, the practical reasons for the substitution of LEDs for conventional silicon photodiodes in those devices has not been given. The first project, hence, investigated the performance of LEDs as light detectors and standard silicon photodiodes in measuring the light intensity. Emission spectra of LEDs and sensitivity spectra of the same LEDs used as detectors were examined. Some different measuring configurations were constructed to measure photocurrents in the photocurrent mode, voltages across the diode by irradiation in the photovoltaic mode and the time to discharge a diode junction capacitance in the discharge time mode.
- (2) ***Development of a deep UV-LED based absorbance detector for narrow column high-performance liquid chromatography.*** To date, absorption photometry in the deep UV range has been the most common detection method for HPLC as most organic molecules exhibit strong absorption bands in this region. Deep UV-LEDs have been commercialized in recent years and subsequently employed as light sources for absorbance measurements for a standard HPLC instrument previously reported by our group. The deep UV-LED based detector for a standard HPLC, however, is not useful for applications in which a limited amount of analytes is available or a saving in high-purity organic solvents is desirable. In this work, an absorbance detector for narrow column HPLC (1mm i.d) relying on deep UV-LEDs, photodiodes and a 250  $\mu\text{m}$  quartz tubing for a detection cell was designed and constructed. This purpose-made optical detector was used for the determination of model compounds at 255 and 280 nm separated in both an isocratic and a gradient elution.

(3) ***Development of a deep UV-LED based absorbance detector for capillary electrophoresis.*** The commercial availability of deep UV-LEDs made them potential radiation sources for absorption photometry in CE even though the design and assembly of a detection cell for CE are more challenging than for HPLC due to the detection window is down to 75  $\mu\text{m}$  or even smaller. We furthered our work on developing the absorbance detector for CE based on high-intensity deep UV-LEDs and photodiodes selective for the examined wavelengths. The performance of this photometric device was evaluated in both direct absorbance quantification and indirect measurement with standard compounds at common wavelengths of 255 and 280 nm. This optical device can be substituted for the more complex and costly UV/Vis detector of commercial CE instruments, making it possible to construct simple and inexpensive CE systems. It is also found to be suitable for on-site measurements with the portable battery-powered instruments.

(4) ***Development of a deep UV-LED based absorption spectroscopic detectors for benzene, toluene, ethylbenzene and the xylenes compounds (BTEX compounds).*** Absorption spectroscopy has been one of the commonly used detection methods for gases. LEDs with advantages of small size, lightweight and low-power consumption are extremely useful for portable devices where the compactness and operation by batteries are required. Infrared LEDs were employed as light sources for the detection of methane and carbon dioxide many years ago. It was of our interest to further explore the potential of a deep UV-LED for absorption spectroscopy in the gas phase. Photoacoustic spectroscopy (PAS) is among the most sensitive absorption spectroscopic techniques for trace gases monitoring of which detection limits could be down to ppb range. In PAS, laser light has been conventionally employed as an excitation source due to its extremely high output. In this contribution, the possibility of a 260 nm LED as an alternative to a conventional laser source for acoustic signals excitation was preliminarily tested for the detection of the toluene vapor. This exploration was fulfilled with the construction and evaluation of an absorbance detector for BTEX compounds relying on a high-intensity 260 nm deep UV-LED, PDs and optical fibres for the light transmission.

## 2. Results and discussion

The majority of results presented in this dissertation were published in or submitted to scientific journals in the field of analytical chemistry. This chapter, therefore, consists of a brief summary of research projects together with reprints of three publications and one manuscript in press. The first section (chapter 2.1) is to investigate the capability of the light-emitting diodes acting as detection devices in comparison with that of standard silicon photodiodes. Two following sections (chapters 2.2 and 2.3) present the development of absorbance detectors based on deep UV-LEDs and photodiodes for a narrow column high-performance liquid chromatography and capillary electrophoresis. In chapter 2.4, the utilization of a deep UV-LED as a radiation source for the gas sensing based on photoacoustic spectroscopy and absorption photometry is demonstrated. At the end, a review concerning fundamental characteristics of LEDs as well as their practical uses for analytical sciences and one publication related to the work in chapters 2.2 and 2.3 are included in the appendix.

### 2.1. Comparative study of light-emitting diodes and standard silicon photodiodes in photometric measurements

The advent of semiconductor devices has facilitated the construction of low-cost and ease of use photometric measuring systems based on the combination of LED and PD (LED-PD). Some research groups reported the satisfactory analytical use of simple optical measuring systems relying on a pair of LEDs, one is for the emitter and the other is for the detector, so called PEDD (paired emitter-detector diodes) [105]. The only advantage of these LED-LED arrangements compared to LED-PD systems that has been stated is a cost saving rather than the practical uses. In this work, visible LEDs (5 mm, clear epoxy dome-shaped) and two types of conventional silicon PD (1 mm<sup>2</sup> active area) were selected to evaluate their performance in current and voltage measuring modes. Recorded in the current follower configuration with the use of an operational amplifier, photocurrents generated by PDs were found to be 5 to 40 times higher than those produced by LED as detectors. In a further test when paired with a yellow LED-emitter ( $\lambda_{\text{max}} = 595 \text{ nm}$ ), the same yellow one as a detector was a worse photo-detector than a red-orange LED whose sensitivity spectrum ( $\lambda_{\text{max}} = 594 \text{ nm}$ ) best matches to the emission spectrum. This difference is largely due to the discrepancy between the emission spectrum and the responsivity range of a yellow LED ( $\lambda_{\text{max}} = 534 \text{ nm}$ ). The magnitude of the photocurrent or an incident light intensity was also measured through recording the time it



takes to discharge the junction capacitance of diodes from 5 V to 1.7 V with a simple microcontroller-based measuring system. The shorter the discharge time, the higher level of the light intensity. It was also found that, discharge times for the LED were about 5 - 10 times longer than those of a photodiode. Note that, these measurements were carried out based on the best spectral match of the LED-LED system. The LED-detector exhibited poorer reproducibility than the PD especially at high levels of the light intensity.

Another approach to measuring the light intensity was applied that is called a photovoltaic mode. In this method, the voltage developed across a diode by an irradiation, without load was recorded with the use of either a high-impedance operational amplifier in a voltage follower configuration ( $10^{13} \Omega$  of input impedance) or with a multi-meter that has a relatively low input impedance of 10 M $\Omega$ . The potential output of a diode is, thus, proportional to an amount of the light intensity. We found that, the response of the LED was not linear with the logarithmic light intensity in both measuring options whilst linear curves were obtained with the PD. Noticeably, the readings for the LED differed several hundred millivolts for a change of radiation intensity of about one order of magnitude while the variation was about 64 mV per decade for a PD that is close to the theoretical expectancy. Stable readings for the LED as a detector were obtained in 1-2 minutes, relatively slower compared to those appearing within seconds for the PD.

Importantly, the peaks of sensitivity spectra of LEDs were 40 - 60 nm shifted relative to their peaks of emission spectra. This demonstrates that the overlap region between the emission spectrum and sensitivity spectrum is very small if two LEDs of the same type are paired. It can be deduced that LEDs used as light detectors with its major advantage of spectral sensitivity is not relevant to the analytical photometry when paired with an emitter of the same type.

## **2.2. Development of a deep UV-LED based absorbance detector for narrow column high-performance liquid chromatography**

An absorbance detector based on deep UV-LEDs for a HPLC setup that employed a standard separation column (4.6 mm i.d) successfully reported by our group exhibited the feasibility of LEDs as ideal alternatives to conventional thermal light sources [110]. In HPLC, the reduction in sample volumes and amount of high-purity organic solvents is crucial to applications in clinical and pharmaceutical analyses. This certainly can be obtained with the

use of a narrower column for chromatographic separations. Downscaling the column requires a smaller detection cell. For this purpose, a fused silica tubing of 250  $\mu\text{m}$  i.d was employed for a flow-through cell, relevant to the use of a 1 mm i.d separation column. Precisely produced in the workshop, all mechanical components together with an electronic circuitry were placed on a baseplate as demonstrated in figure 2-1. The entire assembly was contained in a metal case to restrict interferences of the ambient light and external vibrations. This cell allowed a signal PD to receive the maximum transmitted light intensity as the placements of an LED and a signal PD could be adjusted both vertically and horizontally when mounted on positioning stages. A holder of the LED also enabled its forward and backward movement to get the focal point at the center of the detection window. To prevent the stray light reaching a signal photodiode but not contacting the sample, an optical slit (100  $\mu\text{m}$  wide) was fixed in front of the tubing. Similar to the cell for standard HPLC previously reported, a beam splitter and a reference PD were also employed in this work to produce reference signals. With the availability of reference signals and the use of a log-ratio amplifier, this optical device allowed the direct relationship between absorbance values and concentrations of analytes by emulating the Lambert - Beer's law. Its electronic circuitry facilitated the reduction of the high-frequency noise with a low-pass filter and a zero setting of absorbance readings with an offset unit.

In the absorbance measurements of Tryptophan and 4-hydroxybenzoic acid at 280 and 255 nm, respectively, calibration curves up to mM range were obtained with this optical detector demonstrated that an amount of the stray light is negligible. Subsequently, it was then successfully coupled to a miniature HPLC setup for the quantification of strong UV-absorbing compounds at 280 nm namely ascorbic acid, paracetamol, caffeine separated by an isocratic elution and sulfa drugs by a gradient mode. Standard solutions of paracetamol, 4-hydroxybenzoic acid, 2-acetylsalicylic acid and sorbic acid as well as some nucleosides were determined with this photometric device at 255 nm. The wide range of linearity between absorbance responses and concentrations (up to millimole) with good correlation coefficients ( $r > 0.999$ ) was acquired. The baseline noise levels of 80 to 100  $\mu\text{AU}$  (peak to peak over 60 s) were determined in these measurements with the application of a low-pass filter at 1 Hz cut-off frequency. In the gradient elution, the baselines were found to be not as flat as those of the other mode, with the drifts approximately amounting 0.17 and 0.46 mAU over the separation times at 280 and 255 nm, respectively. This unwanted characteristic is inevitable and mainly due to refractive index changes of a mobile phase. Detection limits of all compounds were in

the low  $\mu\text{M}$  range and the reproducibility for peak areas was found to be satisfactory (RSD < 1%).

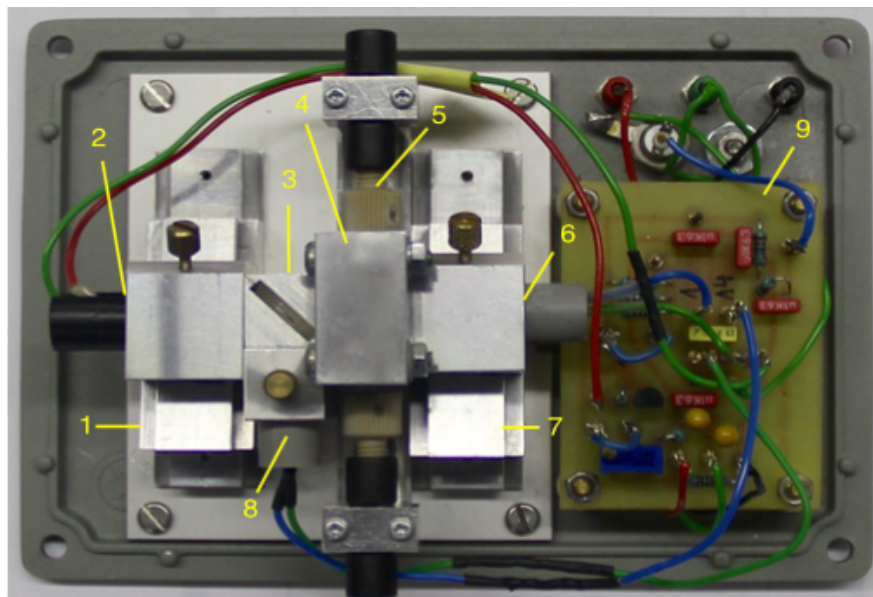


Figure 2-1. The photo of a deep UV-LED based absorbance detector for narrow-column HPLC. (1) a positioning stage for the UV-LED; (2) an UV-LED with its holder; (3) a beam splitter with its holder; (4) a holder of a fused-silica tubing and an optical slit; (5) a fused-silica tubing; (6) a signal PD with its holder; (7) a positioning stage for the signal PD; (8) a reference PD; (9) an electronic circuitry

My participation in this project was to conduct all the measurements to evaluate the fundamental characteristics of this detector and its performance when coupled to a HPLC setup. Bomastyk, the co-worker of this project, contributed to the design of this optical device and optimization for maximum outputs of the signal photodiode.

### **2.3. Development of a deep UV-LED based absorbance detector for capillary electrophoresis**

In commercial CE instruments, an UV/Vis absorbance detector is probably the most complex and costly component. Deep UV-LEDs successfully employed as the radiation sources for HPLC are able to substitute for conventional deuterium and tungsten lamps in combination with a monochromator for wavelength selection. The application of LEDs makes it possible to construct simple, inexpensive, miniaturized and especially low-energy consumption detectors. Due to the relatively small detection window that is theoretically equivalent to the

inner diameter of a capillary, the light focusing onto a narrow aperture and the avoidance of stray light are crucial to obtain a good sensitivity and linearity. A high precision of the mechanical construction and assembly was required to minimize the baseline noise resulted from fluctuations. In this cell, high-intensity UV-LEDs driven at 100 mA and PDs selective for emission bands were used. Regarding the design, some modifications were established compared to the earlier arrangement for narrow-column HPLC. The first change concerns the improvement of light focusing onto the detection window together with the minimization of stray light. A 4 mm fused-silica ball lens was fixed in front of the channel in a circular support to improve the focus. This support attached to the capillary holder by means of a thread that enabled to optimize the distance between the lens and a capillary. A 50  $\mu\text{m}$  in width optical slit was mounted in front of a standard 50  $\mu\text{m}$  i.d capillary while a 100  $\mu\text{m}$  slit was fixed in case a bubble capillary was used. The second improvement relates to the adjustment of the LED and the signal PD placements in 3 axes. This could be achieved with positioning stages and holders based on T-shaped grooves and their matting counterparts that were tightly fixed by screws as shown in figure 2-2. An electronic circuitry also featured a log-ratio amplifier for the emulation of Lambert - Beer's law to produce output signals equal to absorbance values, an offset facility to zero absorbance of the baseline and a low-pass filter for removing high-frequency noises.

The performance of this optical detector in terms of such fundamental characteristics as linearity, baseline noise and detection limits in measuring the absorbance of 4-hydroxybenzoic acid and L-tyrosine at 255 and 280 nm, respectively was found to be promising. Calibration curves up to 1 mM with good correlation coefficients ( $r > 0.999$ ) and detection limits of the low  $\mu\text{M}$  range were obtained for both systems. Determined as peak to peak fluctuations over 60 second and with the application of a low-pass filter at 2Hz cut-off frequency combining with an analog output filter of the circuitry itself, the baseline noise values were approximately 50  $\mu\text{AU}$ . These values were better with that of previously reported CE detectors based on a UV-LED and a photomultiplier tube [109]. When determined as standard deviations, they of about 7.6  $\mu\text{AU}$  were not as good as the lowest values of 4.4  $\mu\text{AU}$  for the chromatographic detector based on a UV-LED that has a relatively longer path-length (150  $\mu\text{m}$ ) [111]. Following the preliminary test was a further investigation in the quantification for CE. Mixture solutions of four aromatic compounds namely sulfanilic acid, 4-nitrobenzoic acid, 4-hydroxybenzoic acid and 4-aminobenzoic acid were separated and quantified at 255 nm. Notably, when an extended capillary was employed, the improvement

of sensitivity by a factor of 3 was obtained corresponding to the theoretical increase in an optical path-length. A further application at this wavelength was the indirect detection of four carboxylic acids including acetic acid, propionic acid, butyric acid and caproic acid by displacing benzoate as an UV-absorbing anion in the electrolyte solution. Performed at 280 nm were two detections: one comprised of vanillic acid, L-tyrosine and DL-tryptophan and the other served for the separation of three sulfonamides compounds. The quantitative parameters were found to be satisfactory with the achievement of good linearity over 3 orders of magnitude, reproducibility for peak areas, detection limits as low as  $\mu\text{M}$  and high separation efficiency in terms of theoretical plates number (29500 - 179700). Measured in detection for CE, the noise levels of approximately 50  $\mu\text{AU}$  were comparable with that of more expensive and complex UV/Vis detectors equipped with modern commercial CE instruments of Agilent and PrinCE manufactures (models of Agilent 7100 and PrinCE-C700).

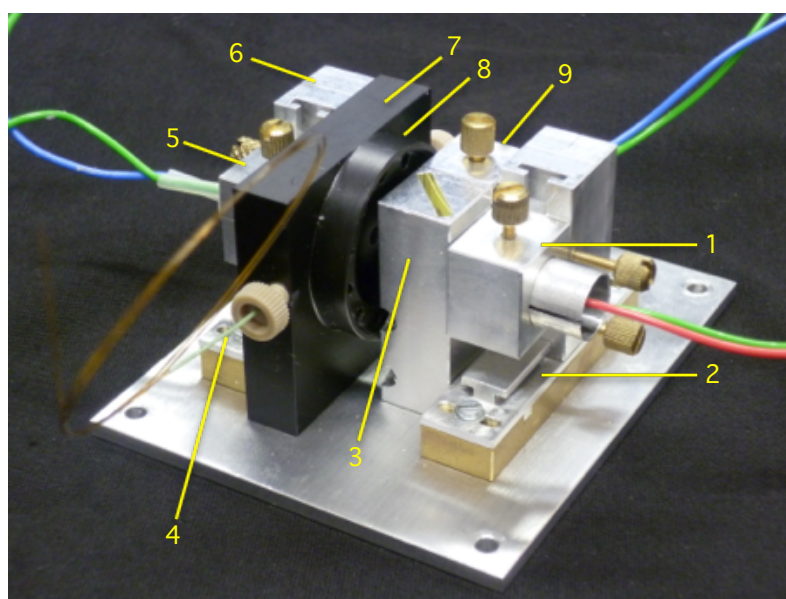


Figure 2-2. The photo of a mechanical assembly of a deep UV-LED based absorbance detector for CE. (1) an UV-LED with its holder; (2) a positioning stage for an UV-LED; (3) a beam splitter with its holder; (4) a capillary; (5) a signal PD with its holder; (6) a positioning stage for the signal PD; (7) a holder of a capillary and an optical slit; (8) a support on which a ball lens is mounted; (9) a reference PD

## **2.4. Development of deep UV-LED based absorption spectroscopic detectors for benzene, toluene, ethylbenzene and the xylenes compounds**

BTEX compounds that comprise of benzene and its derivatives namely toluene, ethylbenzene and the xylenes have become a great concern to people as they can cause long-term adverse health effects and diseases, especially cancer associated with an exposure to benzene. An exposure may occur ubiquitously due to their presence in the exhaust of vehicles as well as their widespread use as solvents and additives in the industrial production. Known as the strong absorbing species in the UV region, these aromatic hydrocarbons can be directly determined by absorption photometry in the region of 255 - 275 nm [112]. Deep UV-LEDs commercially released in recent years were successfully employed as light sources for photometric detectors for ozone (O<sub>3</sub>) and sulfur dioxide (SO<sub>2</sub>) at 255 and 280 nm, respectively reported by Degner, Kalnajs and Aoyagi [113-116]. Their good performance in terms of sensitivity (detection limits are about 100 ppb) exhibited the potential of deep UV-LEDs based absorption spectroscopy to determine BTEX compounds.

### *2.4.1. Application of a deep UV-LED as an excitation source for photoacoustic spectroscopy*

Photoacoustic spectroscopy (PAS) also relies on the absorption of an electromagnetic radiation by analytes. This spectroscopic technique, however, allows the direct measurement of an absorbed energy in the form of a pressure wave/sound wave rather than the absorbance indirectly derived from the transmittance in UV/Vis spectroscopy. Not only has PAS been successfully deployed for the gas sensing but also analyses of condensed matter. A variety of analytical applications in the fields of air and water quality monitoring, industrial and agricultural processes and medical diagnostics were described in review papers [117, 118]. This detection method facilitated the availability of portable devices for on-site monitoring of smoke, toxic gases and hydrocarbons.

Once an analyte absorbs the radiation at a specific wavelength, its molecules will be excited to a higher energy state. Their subsequent transition to the ground state of lower energy level emits energy either through the release of photons or heat in the non-radiative process. The thermal energy produced in the later process causes the expansion that sequentially leads to an increase in pressure. If a light source is modulated, a periodic generation of heat in the sample will occur resulting in pressure fluctuations or sound waves. These waves, regarded as photoacoustic (PA) signals, have the same frequency as the modulated light and can be detected by a sensitive microphone. Tuning the modulation frequency to one of the resonance

frequencies of the cell will increase the magnitude of signals. In the resonant condition, the signal can be amplified by the quality factor of the resonance (Q-factor) in the range of 100 - 1000. This factor is significantly dependent on the size and geometry of the cell. Several microphone-based PAS cells with different geometries were constructed and evaluated in terms of sensitivity for the gas detection [119].

The commercially available quartz tuning fork (QTF) which has been used as a sharply resonant acoustic transducer is a great alternative to a microphone as it enables the detection of weak PA signals and the miniaturization of the PAS cell. The QTF with a resonant frequency of about 32768 Hz has been mostly used in photoacoustic spectroscopy. In a quartz tuning fork-based PAS, so-called quartz-enhanced photoacoustic spectroscopy (QEPAS), a measuring cell has been usually equipped with an acoustic resonator (AR) to amplify signals. The size and geometry of an AR as well as the position and characteristics of the piezoelectric material of QTF are crucial factors to the amplification. To detect PA signals with QTF, two configurations of QEPAS were introduced. On-beam QEPAS with the passage of a light beam through the gap between two prongs of a QTF features a QTF placed in between two resonator tubes. In the off-beam QEPAS, a QTF is separated from the light beam which is placed alongside the AR tube and adjacent to a small aperture on the resonator to detect sound waves inside. The later configuration overcomes a drawback of the former in which the light beam and the inner diameter of tubes are limited to the relatively small gap between QTF's arms (300  $\mu\text{m}$ ).

In PAS, laser light sources have been conventionally used due to their excellent beam quality. The commercial release of low-cost LEDs with an increasing intensity makes them ideal alternatives to lasers. However, there have been a very few LEDs-based PAS instruments reported so far. Böttger was the first to introduce the off-beam QEPAS using a 280 nm LED as a radiation source for the detection of ozone in 2013. A detection limit of about 1.27 ppmv was reported [120].

In this work, three different PAS configurations were in-house constructed to examine the capability of a deep UV-LED in acoustic waves generation for detecting vapors of BTEX compounds as given in figure 2-3. It was found from the BTEX species' absorption spectra that the emission wavelength of 260 nm exhibits a good compromise for determining those. A 260 nm LED, thus, was chosen as the light source for all measurements. A microphone was used in the first measuring system for the detection of sonic outputs. This was mounted on an aluminum tube (6 cm long, 8 mm i.d) in between the LED at one end and the photodiode at

the other end. The second arrangement employed a QTF as the sensor of acoustic signals that was placed in a plexiglas box (5x5x7 cm) used as the photoacoustic cell. The radiation beam from the LED transmitted via an optical fibre (300  $\mu\text{m}$  i.d) passed through the gap between two prongs of a QTF (0.3 mm). The distance between an optical fibre and a QTF was 2 mm. In the last configuration, a QTF was fixed alongside the photoacoustic cell made from an aluminum tube (3 cm long, 2 mm i.d). This tube also acted as a resonator of the QEPAS detector. A 0.3 mm aperture of the resonator was simply created by a drill hole. The gap between a QTF and the aperture was about 0.5 mm. A bundle of optical fibres (20 fibres, 1.9 mm outer diameter) was used for the light coupling from the LED to the tube.

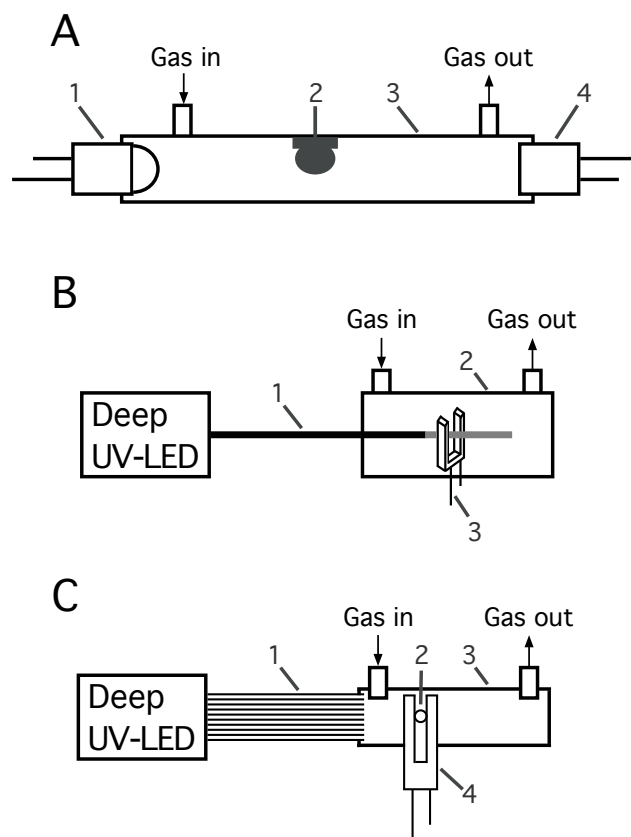


Figure 2-3: Photoacoustic measuring configurations of the toluene vapor detection

(A)-1: an UV-LED; 2: a microphone; 3: a photoacoustic cell; 4: a photodiode

(B)-1: an optical fibre; 2: a photoacoustic cell; 3: a quartz tuning fork

(C)-1: a bundle of optical fibres; 2: an aperture; 3: a resonator tube;

4: a quartz tuning fork.

Demonstrated in figure 2-4 is the experimental setup of the PAS measurements. A 260 nm LED was modulated at expected frequencies by a function generator (Model: AFG1022,



Tektronix, USA). An LED was driven at the maximum peak current of 60 mA. Signals detected by a microphone and a QTF were recorded by a lock-in amplifier combining preamplifier circuitries in which feedback resistors of 220 k $\Omega$  and 10 M $\Omega$  were employed for the former and later, respectively. The time constant of 100 ms and a band-pass filter were set at a lock-in amplifier (Model: 5210, Princeton Applied Research, USA). A function generator was also used as a reference source for a lock-in amplifier. The data acquisition was performed by an e-corder acquisition system (Model: ED401, EDAQ, Australia) with a Chart software running on a computer. The vapor of a target compound was formed through the vaporization with nitrogen in a dreschel bottle (total internal volume of 200 ml). The introduction of nitrogen to the bottle and the vapor to photoacoustic cells for measurements was performed by mass flower controllers (maximum flow rate of 100 mL/min).

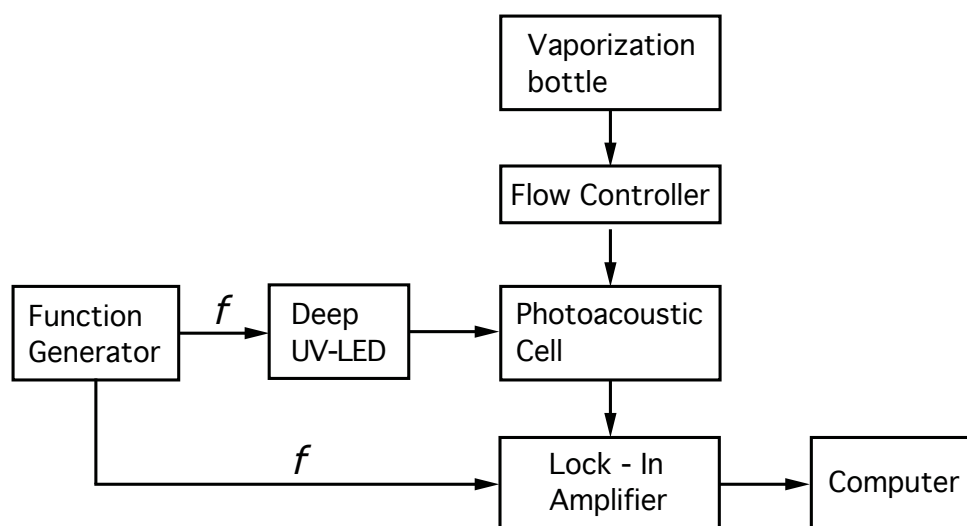


Figure 2-4: The experimental setup of the photoacoustic spectroscopy measurements

Prior to the sample measurements, the sine wave modulation of the UV-LED at different frequencies by a function generator was examined. The UV-LED and a photodiode selective for the emission wavelengths were oppositely mounted on the aluminum tube as shown in the measuring configuration (A), figure 2-3. Signals from a photodiode were read out by the current-follower mode with a 100 k $\Omega$  feedback resistor. Observed by an oscilloscope, the sine wave outputs of a photodiode in the wide range of modulation frequencies up to 50 kHz were obtained. It was proved that the radiation source of the UV-LED could be modulated at desired frequencies. The practical uses of a microphone and a QTF was also tested via their responses to the acoustic outputs of a loudspeaker and an ultrasonic transmitter, respectively.

The performance of these PAS configurations was preliminarily tested for the detection of toluene vapor. It was initiated by measuring the absorption of toluene vapor introduced from the dreschel bottle with configuration (A) to establish an efficient introduction of target vapor to the cell and its absorption at the emission band. The absorbance value produced by a photodiode in a current-follower mode with a 10 M $\Omega$  resistor was 483 mA.U. When a microphone was deployed for the PA signals detection, the modulation frequencies were tuned from 1000 to 5000 Hz with the steps of 25 Hz to obtain its highest output. In the detection with a QTF, the light source was modulated at the range of 32740 Hz - 32800 Hz with the steps of 2 Hz that covers the resonant frequency of a QTF ( $f = 32768$  Hz). It was found that in all measurements with three configurations, there were no variations in PA signals when the toluene vapor was introduced to PA cells. The poor sensitivity of these PAS configurations mainly results from an insufficient radiation intensity of the UV-LED. In spite of efforts to optimize the position of a QTF and the size of a resonator, the outputs were not improved. The fluctuation of background signals of the on-beam QEPAS arrangement was found to be significantly higher than those of the others. This was presumably due to the touch of a light beam onto the prongs of a QTF, which accelerates their mechanical bending.

#### *2.4.2. Development of a deep UV-LED absorption cell for BTEX compounds*

An optical detector was designed and constructed for the absorbance measurements of BTEX compounds which featured the simplicity based on the use of a high-intensity 260 nm LED and PDs selective for an emission band of the LED as given in figure 2-5. Additionally, its direct relationship between absorbance values and concentrations was also required. In this design, a bundle of 20 optical fibres (7 cm long, 1.9 mm i.d) was used for a light coupling from the LED to an aluminium absorption cell (40 cm long, 2 mm i.d) and a reference PD to which only one optical fibre of a bundle was targeted. With the use of an optical fibre, a beam splitter that had been used in earlier designs for narrow-bore HPLC and CE was not necessary. All mechanical holders for the LED, an absorption cell and photodiodes were produced at a very high precision in order to minimize the noises induced by mechanical fluctuations. The whole assembly was placed in a grounded metal case to shield the ambient light and restrict the electromagnetic interference on a circuitry. The effect of temperature variations on measurements was minimized with the attachment of insulating materials inside a case. An electronic circuitry previously used for the detection with CE was employed featuring a log-ratio amplifier for processing photocurrents and generating output voltages corresponding to concentrations, an offset facility for zeroing the baseline and a

low-pass filter for a high-frequency noise removal with a 10 Hz cut-off frequency. An efficient heat-sink system was applied to the LED to maintain its performance when operated at the high current of 100 mA.

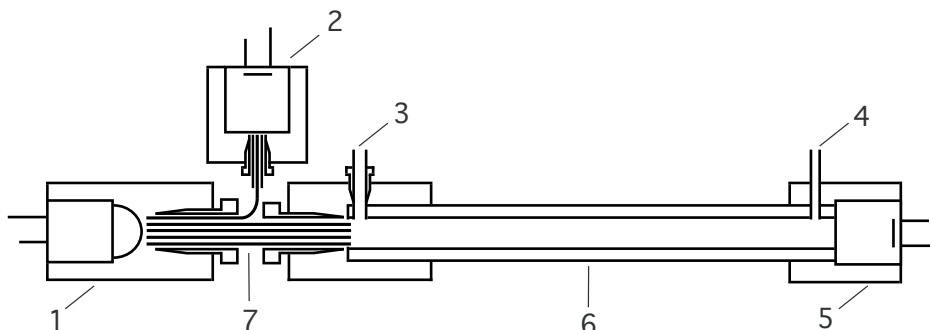


Figure 2-5. The mechanical arrangement of a detector

- (1) an UV-LED;(2) a reference photodiode; (3) gas inlet; (4) gas outlet;  
(5) a signal photodiode;(6) a measuring cell; (7) a bundle of optical fibres

BTEX compounds were vaporized and diluted with nitrogen to obtain the concentrations of vapors in ppb and ppm ranges by the use of mass flow controllers. The calculation of concentration values is in the dependence on the amounts of introduced nitrogen that were precisely determined from the mass difference acquired with a balance arranged underneath the dilution container. Evaluated in absorbance measurements of vapors produced from individual compounds, the performance of this detector was promising. Calibration curves over two orders of magnitude (from 1 to 110 ppm) with good correlation coefficients ( $r > 0.999$ ) and reproducible output signals ( $RSD < 2.5\%$ ) were achieved with all species. The baseline noise values measured as peak to peak fluctuations of about 40  $\mu$ AU are comparable with those of the early-developed detector for CE (50  $\mu$ AU) with the same application of a low-pass filtering. Excluding benzene, the detection limits of the others were below 1 ppm (457 - 658 ppb). It was found that this photometric cell has a better sensitivity than the reported deuterium lamp-based device of which the detection limit for benzene was determined as 13 ppm with the path-length of 30 cm [121]. For the verification, the absorbance of a 60 ppm BTEX standard mixture (10 ppm for each components) was measured. The deviation between the absorbance value for a standard mixture (9.55 mAU) and the sum of expected values for each compound at 10 ppm (9.7 mAU) was found to be less than 2%. Detection limit for the BTEX standard mixture down to 680 ppb could be obtained.

**1<sup>st</sup> project:**

**Absorbance measurements with light-emitting diodes as sources:**

**Silicon photodiodes or light-emitting diodes as detectors?**

*Talanta (2013), 116, 1073-1078*



## Absorbance measurements with light-emitting diodes as sources: Silicon photodiodes or light-emitting diodes as detectors?



Duy Anh Bui, Peter C. Hauser\*

University of Basel, Department of Chemistry, Spitalstrasse 51, 4056 Basel, Switzerland

### ARTICLE INFO

#### Article history:

Received 3 June 2013  
 Received in revised form  
 6 August 2013  
 Accepted 7 August 2013  
 Available online 23 August 2013

#### Keywords:

Light-emitting diode  
 Photodiode  
 Photometry

### ABSTRACT

Light-emitting diodes may also serve as light detectors, and the combination of two of these devices, one serving as light source, the other for detection, has been reported repeatedly for use in analytical photometry. A comparative study of the performance of light-emitting diodes in this role and that of a standard photodiode is reported herein. The spectral sensitivities of the light-emitting diodes were found to be as narrow as their emission bands, but shifted to shorter wavelengths, so that the spectral overlaps between emission and sensitivity of the same devices are very limited. The photocurrents of the light-emitting diodes were found to be about ten times lower than those of the photodiode. In the discharge mode (the time for discharge of the p/n-junction by the photocurrent is measured) as well as the photovoltaic mode, both of which had previously been reported for light-emitting diodes used as detectors in photometric devices, the performance of a light-emitting diode was on a level that is adequate for many analytical purposes, but the photodiode generally gave better precision and the signals showed faster settling times.

© 2013 Elsevier B.V. All rights reserved.

### 1. Introduction

Light-emitting diodes (LEDs) from the near infrared to the UV-range are often employed as radiation sources for photometric detection in analytical chemistry. They are good alternatives to conventional incandescent sources or discharge lamps for optical measurement systems due to their advantages of small size, long lifetime, high stability, low heat production, low power consumption and low cost. As most LEDs emit only over a narrow wavelength range, monochromators are not needed, which allows the construction of very simple devices (see for example [1]). On the other hand, a change in wavelength requires an exchange of the light source, and it is not possible to acquire spectra of samples. A photometric measurement with an LED was first described by Flaschka in 1973 [2]. Since then a multitude of devices have been described in the literature. These include instruments for absorbance measurements in cuvettes (see for example [3–6]), detection in flow-injection analysis [7–9], on-line detection in process analysis [10,11], as well as detection in HPLC [12–14] and capillary electrophoresis [15–19]. Several reviews have appeared [1,20–23]. Commercial products are also available, in particular in the form of portable instruments for carrying out photometric tests in the field.

Photometric measurements are governed by the well known Lambert–Beer law, which relates absorbance,  $A$ , to concentration,  $c$  ( $\epsilon$  is the molar absorptivity coefficient, and  $b$  the optical path-length). The absorbance is obtained from the light intensity before

( $I_0$ ) and after passage ( $I$ ) through the measuring cell. These parameters are usually determined with detectors which give current outputs that are proportional to light intensity, hence  $A$  can also be expressed as a function of the detector currents ( $i_0$  and  $i$ ):

$$A = \epsilon bc = \log \frac{I_0}{I} = \log \frac{i_0}{i} \quad (1)$$

The mathematical transformation needed to obtain the value of  $A$  from the measured parameters is usually carried out by the instrument. As this is a complication, simple devices often give an output value which is proportional to transmittance,  $T$ , which is given by the simpler relationship

$$T = \frac{I}{I_0} = \frac{i}{i_0} \quad (2)$$

However,  $T$  is not proportional to concentration, and non-linear calibration curves are obtained for this parameter. For devices based on LEDs it is usually also not necessary to obtain the reference parameter ( $i_0$  or  $I_0$ ) as this stays fairly constant due to the inherent stability of these light sources. It is thus possible to work with a single detector for light intensity. The measured value may then be an arbitrary parameter (such as a voltage derived from the detector current by an electronic circuitry) and the exact relationship of this signal with the concentration is established by calibration.

Commonly LEDs are paired with silicon photodiodes (PD) as detectors. These devices are as easy to use as the LEDs, have good sensitivity and are frequently employed in modern commercial photometric instruments. Only when extremely low light levels need to be detected the more complex and expensive photomultiplier tubes

\* Corresponding author. Tel.: +41 61 267 1003; fax: +41 61 267 1013.  
 E-mail address: [Peter.Hauser@unibas.ch](mailto:Peter.Hauser@unibas.ch) (P.C. Hauser).

are still required. Photodiodes are readily available in different forms from suppliers of electronic components.

It has also been known that LEDs can function as photodiodes as well [24]. In similarity to their emission performance, their spectral detection sensitivity is restricted to a narrow band. This feature has been made use of for applications in which the wavelength selectivity of detectors is a requirement, i.e. in a sun spectrometer reported in 1992 by Forrest M. Mims [24] and in remote sensing in agronomy (spectral reflectance to study vegetation coverage) [25]. In these instruments, the LEDs are inexpensive substitutes for photodiodes fitted with interference filters to restrict their wavelength sensitivity range. The latter are expensive due to the inclusion of the costly filters. Some fundamental studies concerning the spectral and dynamic behavior of a blue and of a red LED used as detectors were carried out by Miyazaki et al., (1998) [26].

The possibility of the pairing of two LEDs, one of which acts as detector, was mentioned in 1993 by Dasgupta et al., but was discouraged due to the low photocurrents found for the LEDs then available [1]. In the more recent years however, several research groups have reported the successful use of LED pairs for photometric devices for analytical chemistry [27–38]. The term PEDD (for Paired Emitter-Detector Diodes) has frequently been employed for this arrangement. Nevertheless, in these arrangements the wavelength selectivity of the LED used as detector was not required as this is already determined by the LED used as a source. A rationale for the substitution of silicon photodiodes in these devices has not often been given, but cost saving has been stated and it has been suggested that advantageous measuring modes require the use of LEDs.

This report examines the use of LEDs as an alternative for conventional photodiodes in photometric devices based on LEDs as emitters.

## 2. Experimental

### 2.1. Instrumentation

The LEDs (5 mm diameter plastic package, water clear) of different colors were obtained from Everlight (Shulin, New Taipei City, Taiwan) (R1=Part No. 3832SURC/S530A3), (R2=Part No. 3832SURC/S400A6), (R3=Part No. 3832SURC/S530A3), (Y1=Part No. 3832UYC/H2/S400), (G1=Part No. 383SYGC/S530E2/H2), Kingbright (Chungho, New Taipei City, Taiwan) (RO1=Part No. L7113SEC/H) and Avago (San Jose, CA, USA) (R4=Part No. HLMP3750). The silicon photodiodes (SFH 203P) were products of Osram (Regensburg, Germany). The quartz glass cuvettes with an optical pathlength of 1 cm were obtained from Hellma (Model 1001040, Type 100QS, Müllheim, Germany). The spectrometer used to determine the emission spectra of the LEDs (Model S2000, with a spectral bandwidth of 3 nm) was obtained from Ocean Optics (Dunedin, FA, USA). The sensitivity data of the LEDs were acquired by placing them at the exit slit of the monochromator of a laboratory spectrophotometer fitted with a tungsten lamp (Model CE 303 from Cecil Instruments, Cambridge, England, spectral bandwidth= 10 nm). The beam splitter was sourced from Qioptiq Photonics (Part No. G344312000, Munich, Germany). Purpose made devices were employed for positioning and aligning of light sources, beam splitter, cuvettes and detectors according to different experiments and to exclude ambient light. The different measurement configurations employed are shown schematically in Fig. 1. The operational amplifier (Model OPA121) and the logarithmic ratio amplifier (Model LOG102) were products of Texas Instruments (Austin, TX, USA). The microcontroller used was an ATmega328 (Atmel, San Jose, CA, USA) on an Arduino Uno board (RS Components, Wädenswil, Switzerland). A standard multimeter obtained from Fluke (Model 75, Everett, WA, USA) was used to measure voltage signals. The e-corder data-acquisition system (Model ED401) and the Chart software package employed

to measure the noise levels of the signals from the photodiodes and LED-detectors were obtained from EDAQ (Denistone East, New South Wales, Australia). The noise values were determined as the maximum deviations over a period of 30 s, no electronic filtering was applied. The light intensities of the LEDs used as light sources were controlled with a constant current supply built with a linear regulator from National Semiconductor (Model LM317, Santa Clara, CA, USA). The currents were set to 25 mA, except for the measurements concerning the effects of the light intensity. For these the currents were adjusted to different values between approximately 2.5 mA and 25 mA and the relative intensities were determined with the photodiode used in the photocurrent configuration. As can be seen in Fig. 2 for one of the LEDs the dependence of the intensities on current was found to be close to linear.

### 2.2. Reagents

Thymol Blue and sodium hydroxide of analytical grade were products of Siegfried (Zofingen, Switzerland) and Fluka (Buchs, Switzerland) respectively. Deionized water was used for all experiments and was obtained from a NANO-Pure purification system (Barnstead, IA, USA).

## 3. Results and discussion

### 3.1. Spectral considerations

It has been known that the spectral sensitivity of LEDs when used as photodiodes is restricted to a relatively narrow range but only limited quantitative information has been available. Miyazaki et al. measured the sensitivity spectra of a red and a blue LED and compared these with their emission spectra [26]. It was found that in both cases the detection sensitivity was shifted to shorter wavelengths. The emission and sensitivity spectra for 5 LEDs from green to red are shown in Fig. 3A and B respectively. The sensitivity measurements were carried out in the photocurrent (or photoconductive) mode, i.e. the currents produced by the photodiode were measured. The current follower circuit arrangement employed is shown in Fig. 1A. As can be clearly seen, the sensitivity spectra are shifted significantly to shorter wavelengths. For the selection of LEDs

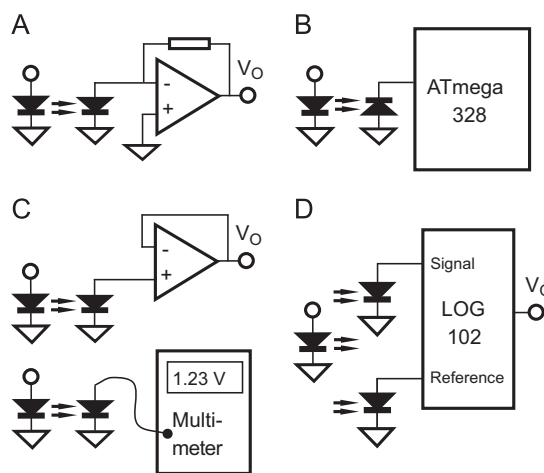


Fig. 1. Measuring configurations used. (A) Photocurrent mode with operational amplifier in the current follower configuration, (B) the capacitance discharge method with microcontroller, (C) photovoltaic mode with two options: high input impedance operational amplifier in the voltage follower configuration or direct connection to a multimeter, and (D) photocurrent mode with log ratio amplifier configuration.

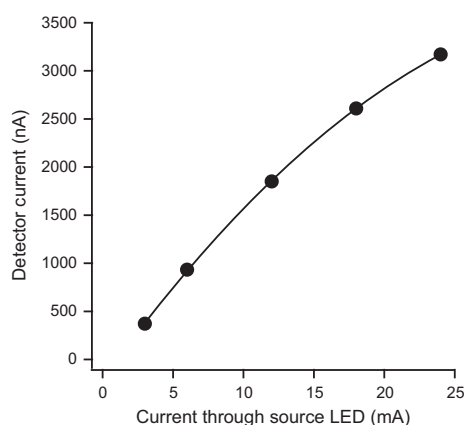


Fig. 2. Photocurrent of the photodiode (SFH203P) in dependence on the forward current of the yellow LED (Y1). Measured with the arrangement of Fig. 1A.

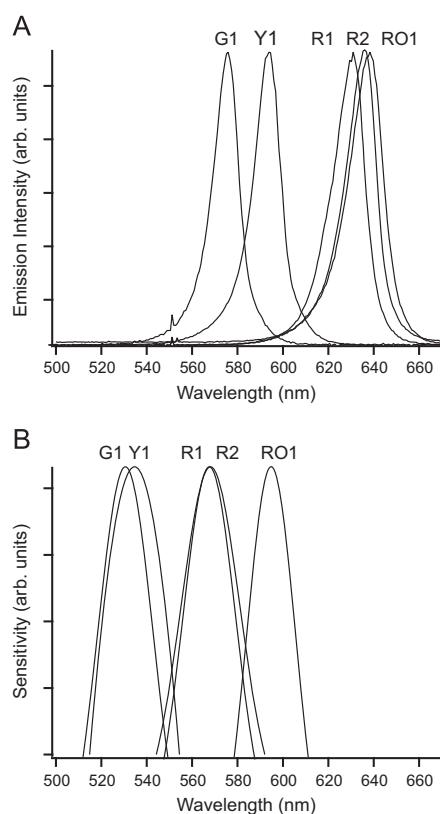


Fig. 3. Emission spectra of the LEDs (A), and sensitivity spectra of the same LEDs used as detector (B).

this shift was between about 40 and 60 nm. The extent of the shift thus varies, for instance the green (G1) and yellow (Y1) LEDs have almost identical sensitivity ranges despite their different emitted colors. Note that while the maxima of the peaks can be expected to be representative, the shapes of the bands of the sensitivity spectra of Fig. 3B should only be taken as a rough indication as they were

affected by the relatively wide spectral bandwidth (10 nm) of the instrument available for these measurements. It was not possible to acquire any sensitivity spectra for blue LEDs, possibly because of the low intensity of this same system at shorter wavelengths, and these were therefore not further considered in this study. The results demonstrate that when the same type of LED is paired, the spectral overlap between emission and sensitivity is very limited.

### 3.2. Current yields for the photodiode and the LED-detectors

A comparison of the sensitivity of the LEDs when used as detectors with that of a standard photodiode was carried out by setting the monochromator of the light source to the wavelength of maximum sensitivity for each LED as determined in the previous section. The LEDs and the photodiode were individually mounted on a positioning stage in front of the exit slit and their geometric positions were optimized for the highest signal. The photocurrents generated by the detectors were again measured with the circuitry of Fig. 1A. As can be seen from Table 1, currents between about 0.5 and 4.5 nA were obtained. These levels are relatively low, but well within the capabilities of inexpensive modern electronic circuitry. The currents obtained for the photodiode, as expected, were higher than for the LEDs, but with a difference by a factor of about 5–40 times for the values between the two devices, the discrepancy was not as large as had been suspected. Note that the photodiode is a standard silicon type with a sensitive area of 1 mm<sup>2</sup>, and is representative for similar models readily available from a range of suppliers. The comparison of the results for the 4 different red LEDs (R1–R4) indicates that there is no relationship between their sensitivity and brightness.

A further test was carried out by matching one of the LEDs as an emitter (Y1) with 3 different detector options: the photodiode, a second LED of the same type, and a different LED (RO1) which has a good match of its sensitivity spectrum to the emission spectrum of the emitter as can be seen from Fig. 3. This experiment was carried out by mounting the two devices on opposite sides of a holder for a standard cuvette of 1 cm pathlength. The positions of the emitter and detectors were again adjusted in each case to obtain the highest output signals which were measured in the photocurrent mode. The measurements were also carried out for different light intensities which were set by adjusting the currents through the LED serving as light source to 2.5 mA, 10 mA and 25 mA. The results are given in Table 2. The currents of the photodiode were again higher by about a factor of 10 compared to the LED with a good spectral match with the emitter. This is in agreement with the results reported in Table 1. The use of the twinned LEDs (same LED types as emitter and detector) led to currents which were about 3–5 times lower than those of the best match LED. The reason for this difference must be the mismatch between the responsivity spectrum ( $\lambda_{\max}=534$  nm) and the emission spectrum ( $\lambda_{\max}=595$  nm) of the yellow LED (Y1) as

Table 1  
Current yields of the LED-detectors and the photodiode placed at the exit slit of the monochromator set to the wavelengths of maximum sensitivity for each LED.

LED	Luminous intensity (mcd)	Peak emission wavelength, $\lambda_{\max}$ (nm)	Wavelength of maximum sensitivity (nm)	Current yield of LEDs (nA)	Current yield of photodiode SFH 203P (nA)
R1	2500	630	568	0.5	20.6
R2	6300	635	570	4.5	20.6
R3	800	639	596	1.8	23.6
R4	125	638	610	1.4	23.5
RO1	10,000	637	594	3.6	22.4
Y1	1000	595	534	2.3	13.4
G1	320	578	530	0.7	13.4

**Table 2**

Current yields and noise levels of two detector LEDs (twinned, Y1, and best spectral match, RO1) and the photodiode (SFH 203P) at different currents supplying the source LED (Y1).

Detector	25 mA			10 mA			2.5 mA		
	Current (nA)	Noise (nA)	S/N	Current (nA)	Noise (nA)	S/N	Current (nA)	Noise (nA)	S/N
Y1	93.6	3.8	24	57.2	2.6	22	11.5	2.0	5.8
RO1	474	2.2	215	223	1.5	149	38.9	1.3	30
SFH 203P	5564	0.8	6950	2516	0.35	7190	441	0.07	6300

illustrated in Fig. 3. The data of this figure leads to the expectation of an even lower current yield for the pairing of two of the yellow LEDs, but note again that the sensitivity spectra shown in Fig. 3 cannot be taken as fully quantitatively representative due to the limitations of the experimental system. Also given in Table 2 are the noise levels associated with these measurements. As can be seen, the absolute noise levels are lowest for the photodiode and highest for the yellow LED with the poor spectral match. Thus for the photodiode and the lowest light intensity (2.5 mA passed through the source LED) the signal-to-noise ratio is still excellent (> 6000) while for the yellow LED as detector this drops to a low 5.8. Note that no electronic noise filtering was applied for these measurements.

### 3.3. Light intensity measurement by the discharge method

PEDD devices have been employed by measuring the discharge time for the incidental junction capacitance of an LED [36,38]. The capacitance is discharged by the photocurrent and thus the rate of discharge is faster for higher levels of irradiation. A plot of the logarithm of the discharge time was reported to be approximately linear with concentration in absorption measurements [36], presumably because the discharge of a capacitor follows a log-function. The method can be implemented with a simple microcontroller without requiring a separate analog-to-digital convertor or analog electronic circuitry. In this work, this mode was evaluated again for the favorable combination of the yellow LED (Y1) as emitter with the red–orange LED (RO1) as detector, as well as the photodiode as detector, again by mounting them on the cuvette holder at a distance of approximately 1 cm. The circuitry is illustrated in Fig. 1B. The reverse biased LED is first charged through the port of the microcontroller which is set to the output mode and turned to a logic HI (5 V). Then the port is switched to the input mode and the time taken for the voltage across the diode to decay to a logic LO level is determined with an internal counter. The discharge times in  $\mu\text{s}$  obtained for the two combinations in dependence of the intensity of the emitting LED are plotted in Fig. 4. Note the different scales for the two devices. The data indicates that both components, the LED as detector as well as the photodiode, may be employed in this mode, but the discharge times are shorter for the photodiode by a factor of about 10. This may be due to the higher current yields for the photodiode, as demonstrated above, but the junction capacitances are not known and can be expected to be different as well. The shapes of the response curves are non-linear with light intensity and different for the two devices. The readings differ by a factor of about 5 between the lowest and highest intensities for the LED while for the photodiode this spans a factor of about 10. A weak point was found to be the reproducibility of the measurements. The resolution of the system is 4  $\mu\text{s}$ , which introduces digitization errors, especially for the shorter measured times, but the fluctuations are generally more pronounced. The relative standard deviations obtained from 5 readings were determined to be between about 2% and 6%. As the measurement is fast, an improvement can be obtained by averaging repeated readings to improve the precision. The standard deviations obtained for averaged readings (1000 individual measurements,

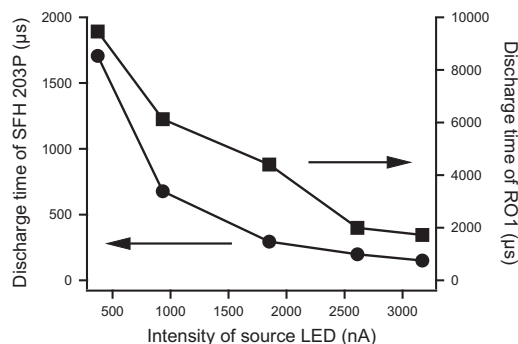


**Fig. 4.** Light intensity measurements using the junction discharge method (see Fig. 1B) for the red–orange LED (RO1) and the photodiode (SFH203 P) for different intensities of the source LED (Y1). These intensities refer to the photocurrents determined with the photodiode using the arrangement of Fig. 1A.

**Table 3**

Discharge times (mean of 1000 readings) and standard deviations for these averaged readings ( $n=5$ ) obtained with the detector LED of best spectral match (RO1) and the photodiode (SFH 203 P) at different currents supplying the source LED (Y1).

Detector	24 mA		12 mA		3 mA	
	Mean discharge time ( $\mu\text{s}$ )	RSD (%)	Mean discharge time ( $\mu\text{s}$ )	RSD (%)	Mean discharge time ( $\mu\text{s}$ )	RSD (%)
RO1	1724.6	3.3	4401.4	2.9	9460.6	0.07
SFH 203P	149.8	0.99	294.4	0.57	1707.0	0.56

which required about 10 s to acquire) for some of the measurements are given in Table 3. The values are generally better, very good for the low light intensities for the LED used as detector, but still around 3–4% for the high intensities. For the photodiode the pattern is more consistent with all values being around 1%. The data demonstrates that photodiodes are at least as suitable for this measurement approach as the LEDs.

### 3.4. Light intensity measurement in the photovoltaic mode

Tymecki and coworkers suggested the use of LEDs as detectors in the photovoltaic mode [32,30]. In this approach the voltage developed across the diode on irradiation, without load, is measured. For a photodiode a logarithmic voltage ( $V$ ) response to photocurrent ( $i$ ), and hence light intensity, is expected [39]

$$V = \frac{kT}{e} \ln\left(\frac{i}{i_0}\right) \quad (3)$$

$k$  is the Boltzman constant,  $T$  the absolute temperature,  $e$  the elementary charge, and  $i_0$  the dark current of the photodiode. The



slope factor at room temperature is approximately 25 mV (or 58 mV for the decadic logarithm). The voltage is thus inversely proportional to absorbance,  $A$ , of Lambert–Beer's law which is also logarithmically dependent on light intensity (see Eq. (2) above). The approach is thus a simple method to obtain signals which are proportional to concentration. The measuring arrangement is illustrated in Fig. 1C. Two options were used in this work. The voltage was either determined via a high input impedance operational amplifier in the voltage follower mode or directly with a standard multimeter. The operational amplifier has a very high input impedance ( $10^{13} \Omega$ ) and a negligible input bias current ( $< 5 \text{ pA}$ ) and thus only draws an insignificant current, comparable to the input of a pH-meter (as used by Tymecki et al. [32,30]), but the multimeter has a standard input impedance of  $10 \text{ M}\Omega$  so that a current in the high nano-ampere range is pulled from the source.

The photovoltaic responses of LED RO1 as detector and the photodiode (using again LED Y1 as emitter) are shown in Fig. 5A and B respectively. As can be seen, the LED as detector showed a much higher sensitivity than the photodiode. Note the different scales for the two plots. For the LED the change in voltage was several hundreds of mV for a change of light intensity of approximately one order of magnitude, but the response function was not linear with the logarithm of light intensity. For the LED as detector the signals were strongly dependent on whether the measurements were carried out by direct connection to the multimeter, or via the high impedance operational amplifier. The multimeter with the relatively low input impedance of  $10 \text{ M}\Omega$  showed a strong loading effect. It was also found that for the readings with the LED as detector it always required about 1–2 min of time to achieve stable voltage signals in both measurements approaches. For the photodiode the response was almost linear with the logarithm of the intensity according to our measurements with a slope close to the theoretically expected (64 and 66 mV per decade for the measurements with the operational amplifier and multimeter respectively). In this case, the readings were almost identical for the two measuring systems. For the photodiode stable readings were established within seconds.

### 3.5. Measurements of dye solutions using the photovoltaic mode

As the photodiode was found to perform very well in the photovoltaic mode using the direct measurement with a multimeter, this promising new configuration was therefore tested for carrying out measurements of dye solutions. For comparison measurements with a conventional set-up using a beam splitter with a reference photodiode were also made. In this case the photocurrents were processed by a log-ratio amplifier in integrated circuit format which gives an output voltage,  $V_o$ , according to the following equation:

$$V_o = \log \frac{i_0}{i} \quad (6)$$

The output voltage therefore directly represents absorbance,  $A$ . The measuring arrangement is shown in Fig. 1D and corresponds to the standard set-up employed in molecular absorption photometry. Solutions of Thymol Blue prepared in 0.1 M sodium hydroxide solutions were tested, and the yellow LED-emitter (Y1) which has a peak at 595 nm was chosen as the light source because of its compatibility with the absorption spectrum of the dye ( $\lambda_{\text{max}} = 592 \text{ nm}$ ). The current driving the LED-emitter was kept constant at 25 mA.

The results obtained for the photodiode in the photovoltaic and the log-ratio modes are shown in Fig. 6A and B respectively. The values for Fig. 6B correspond to mAU (milli-Absorbance units). The plot is almost linear (correlation coefficient,  $r = 0.9997$ ), the very slight curvature is a common feature for LED based absorbance measurements which is due to the not perfect monochromaticity of the light source, which is a violation of the prerequisites for strict

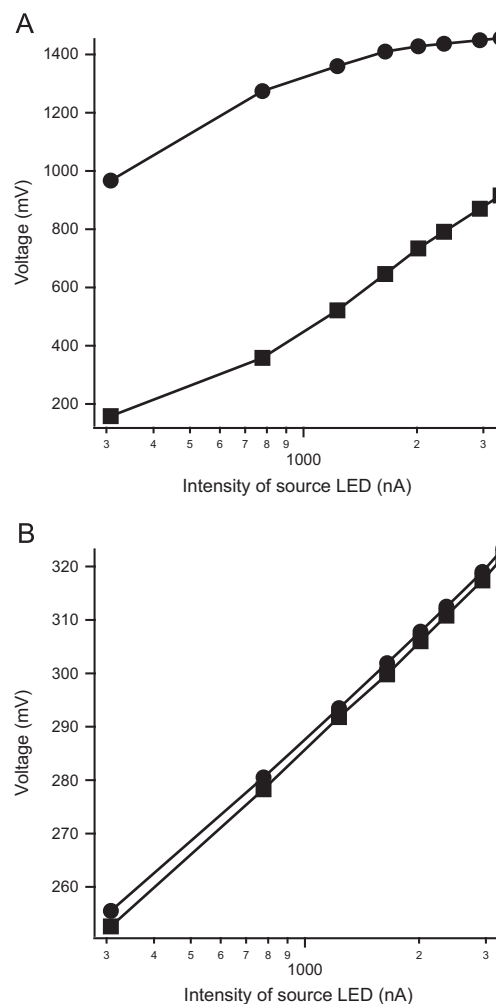
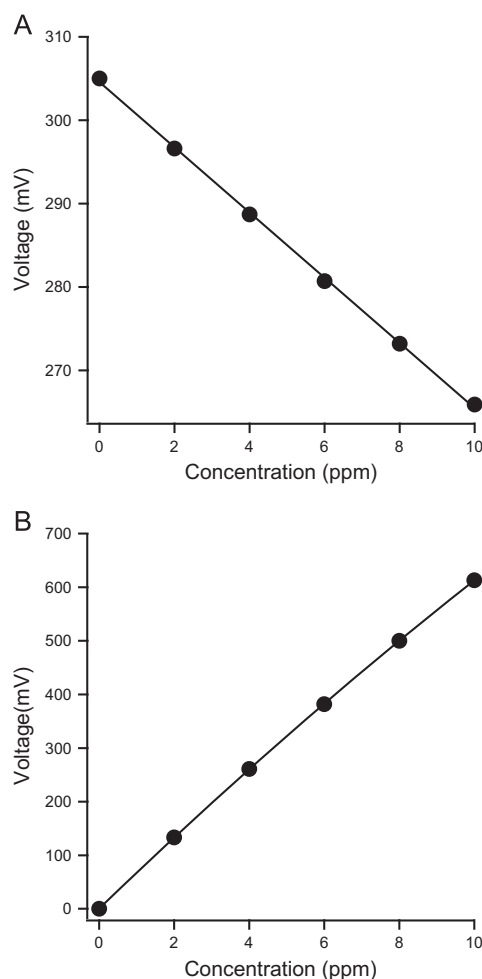


Fig. 5. Responses in the photovoltaic mode (see Fig. 1C) for the red–orange LED (RO1) (A) and the photodiode (SFH203P) (B) using either the high impedance version with the operational amplifier (circles) or the multimeter directly (squares) for different intensities of the source LED (Y1). The intensities refer to the photocurrents determined with the photodiode using the arrangement of Fig. 1A.

adherence to Lambert–Beer's law [40]. The standard deviation for 5 measurements of the solution of 6 ppm ( $n = 5$ ) was determined as 0.12%. The photovoltaic response is also good ( $r = 0.9996$ ), but the slope is negative and the measured voltages do not directly represent absorbance values. The standard deviation for the measurement of the solution of 6 ppm (in terms of concentration) was 0.34%.

## 4. Conclusion

In the direct comparison between the use of LEDs as detectors and a photodiode it was found that, while the LEDs usually gave adequate results, the photodiode generally performed better. First of all, there is no difficulty regarding the spectral match between source and detector when using the latter. The photodiode also tended to give more predictable and reproducible results and stable readings were obtained instantly, while the LEDs settled slowly. This is not surprising,



**Fig. 6.** Measurements of Thymol Blue solutions using the yellow LED (Y1) as emitter. (A) Photodiode (SFH203P) as detector in the photovoltaic mode using the direct measurement with the multimeter. (B) Photodiode (SFH203P) as detector in the log-ratio approach.

given that the latter have been optimized for emission, and hence the underlying physics are different for the two types of components (LEDs are direct bandgap devices, while photodiodes are indirect bandgap devices). For this reason, the reverse is also not possible, *i.e.* photodiodes do not emit light. The results also demonstrate that photodiodes tend to perform better in the special modes which had been suggested for the PEDD transducers (*i.e.* the junction discharge method and the photovoltaic mode). Note that the photodiode employed in these studies is a low cost version, widely available for approximately 1 US\$ from distributors, which is comparable to the cost of LEDs. The use of a photodiode in combination with a log-ratio amplifier remains the best approach as it directly yields absorbance readings. Note that the reference is only necessary for the most demanding applications. The log-ratio amplifiers are now available from distributors for less than US\$ 20 while only a few years ago the cost was significantly higher. If a truly low cost approach to

photometry is sought, a photodiode used directly with an inexpensive multimeter in the photovoltaic mode should give acceptable results. We are not aware of prior reports on this set-up being employed in analytical chemistry. The only advantage of the use of LEDs as detectors is their spectral selectivity, but this is not generally relevant if paired with LEDs as sources.

#### Acknowledgments

The authors would like to express sincere gratitude to the Swiss Federal Commission for Scholarships for Foreign Students (ESKAS) for valuable financial support. Thank you also to Joel Koenka for help with the programming of the Arduino.

#### References

- [1] P.K. Dasgupta, H.S. Bellamy, H.H. Liu, J.L. Lopez, E.L. Loree, K. Morris, K. Petersen, K.A. Mir, *Talanta* 40 (1993) 53.
- [2] H. Flaschka, C. McKeithan, R. Barnes, *Anal. Lett.* 6 (1973) 585.
- [3] Y. Suzuki, T. Aruga, H. Kuwahara, M. Kitamura, T. Kuwabara, S. Kawakubo, M. Iwatsuki, *Anal. Sci.* 20 (2004) 975.
- [4] J.G. Schnable, P.J. Grochowski, L. Wilhelm, C. Harding, M. Kiefer, R.S. Orr, *Field Anal. Chem. Tech.* 2 (1998) 21.
- [5] Y. Shimazaki, F. Fujioka, M. Iwatsuki, *Field Anal. Chem. Tech.* 2 (1998) 173.
- [6] P.C. Hauser, T.W.T. Rupasinghe, *Fresenius J. Anal. Chem.* 357 (1997) 1056.
- [7] B.S. Gentle, P.S. Ellis, P.A. Faber, M.R. Grace, I.D. McKelvie, *Anal. Chim. Acta* 674 (2010) 117.
- [8] H.H. Liu, P.K. Dasgupta, *Anal. Chim. Acta* 289 (1994) 347.
- [9] M. Trojanowicz, J. Szpunar-Lobińska, *Anal. Chim. Acta* 230 (1990) 125.
- [10] P.C. Hauser, T.W.T. Rupasinghe, C.C. Lucas, A. McClure, *Analyst* 120 (1995) 2635.
- [11] J.L. Huang, H.H. Liu, A.M. Tan, J.H. Xu, X.N. Zhao, *Talanta* 39 (1992) 589.
- [12] B. Bomastyk, I. Petrovic, P.C. Hauser, *J. Chromatogr. A* 1218 (2011) 3750.
- [13] S. Wiesufer, A. Boddenberg, A.P. Ligon, G. Dallmann, W.V. Turner, S. Gab, *Environ. Sci. Pollut. Res.* (2002) 41.
- [14] G.J. Schmidt, R.P.W. Scott, *Analyst* 109 (1984) 997.
- [15] L. Kremova, A. Stjernlof, S. Mehlen, P.C. Hauser, S. Abele, B. Paull, M. Macka, *Analyst* 134 (2009) 2394.
- [16] G.A.B. Heras, M.C. Breadmore, C. Johns, J.P. Hutchinson, E.F. Hilder, P. Lopez-Mahia, P.R. Haddad, *Electrophoresis* 29 (2008) 3032.
- [17] M.C. Breadmore, R.D. Henderson, A.R. Fakhari, M. Macka, P.R. Haddad, *Electrophoresis* 28 (2007) 1252.
- [18] M. Macka, C. Johns, P. Doble, P.R. Haddad, K.D. Altria, *LC GC North Am.* 19 (2001) 188.
- [19] P.A.G. Butler, B. Mills, P.C. Hauser, *Analyst* 122 (1997) 949.
- [20] D. Xiao, L. Yan, H.Y. Yuan, S.L. Zhao, X.P. Yang, M.M.F. Choi, *Electrophoresis* 30 (2009) 189.
- [21] M. O'Toole, D. Diamond, *Sensors* 8 (2008) 2453.
- [22] P.K. Dasgupta, I.Y. Eom, K.J. Morris, J.Z. Li, *Anal. Chim. Acta* 500 (2003) 337.
- [23] M. Trojanowicz, P.J. Worsfold, J.R. Clinch, *TrAC—Trends Anal. Chem.* 7 (1988) 301.
- [24] F.M. Mims III, *Appl. Opt.* 31 (1992) 3.
- [25] C. Weber, J.O. Tocho, E.J. Rodríguez, H.A. Acciaresi, *J. Phys. Conf. Ser.* 274 (2011) 1.
- [26] E. Miyazaki, S. Itami, T. Araki, *Rev. Sci. Instrum.* 69 (1998) 4.
- [27] S. Koronkiewicz, S. Kalinowski, *Talanta* 86 (2011) 436.
- [28] E. Mieczkowska, R. Koncki, L. Tymecki, *Anal. Bioanal. Chem.* 399 (2011) 3293.
- [29] M.B. da Silva, C.C. Crispino, B.F. Reis, J. Brazil. Chem. Soc. 21 (2010) 1854.
- [30] L. Tymecki, L. Brodacka, B. Rozum, R. Koncki, *Analyst* 134 (2009) 1333.
- [31] L. Tymecki, R. Koncki, *Anal. Chim. Acta* 639 (2009) 73.
- [32] L. Tymecki, M. Pokrzywnicka, R. Koncki, *Analyst* 133 (2008) 1501.
- [33] M. O'Toole, K.T. Lau, R. Shepherd, C. Slater, D. Diamond, *Anal. Chim. Acta* 597 (2007) 290.
- [34] L. Barron, P.N. Nesterenko, D. Diamond, M. O'Toole, K.T. Lau, B. Paull, *Anal. Chim. Acta* 577 (2006) 32.
- [35] M. O'Toole, K.T. Lau, B. Shazmann, R. Shepherd, P.N. Nesterenko, B. Paull, D. Diamond, *Analyst* 131 (2006) 938.
- [36] K.T. Lau, S. Baldwin, M. O'Toole, R. Shepherd, W.J. Yerazunis, S. Izuo, S. Ueyama, D. Diamond, *Anal. Chim. Acta* 557 (2006) 111.
- [37] M. O'Toole, K.T. Lau, D. Diamond, *Talanta* 66 (2005) 1340.
- [38] K.T. Lau, S. Baldwin, R.L. Shepherd, P.H. Dietz, W.S. Yerzunis, D. Diamond, *Talanta* 63 (2004) 167.
- [39] J. Wilson, J.F.B. Hawkes, *Optoelectronics, An Introduction*, Prentice Hall, London, 1983.
- [40] P.C. Hauser, D.W.L. Chiang, *Talanta* 40 (1993) 1193.

**2<sup>nd</sup> project:**

**Absorbance detector based on a deep UV light-emitting diode  
for narrow-column HPLC**

*Journal of Separation Science (2013), 36, 3152-3157*

Duy Anh Bui<sup>1,2</sup>  
Benjamin Bomastyk<sup>1</sup>  
Peter C. Hauser<sup>1</sup>

<sup>1</sup>Department of Chemistry,  
University of Basel, Basel,  
Switzerland

<sup>2</sup>Centre for Environmental  
Technology and Sustainable  
Development (CETASD), Hanoi  
University of Science, Hanoi,  
Vietnam

Received June 5, 2013

Revised July 12, 2013

Accepted July 12, 2013

## Research Article

# Absorbance detector based on a deep UV light emitting diode for narrow-column HPLC

A detector for miniaturized HPLC based on deep UV emitting diodes and UV photodiodes was constructed. The measurement is accomplished by the transverse passage of the radiation from the light-emitting diode (LED) through fused-silica tubing with an internal diameter of 250  $\mu\text{m}$ . The optical cell allows flexible alignment of the LED, tubing, and photodiode for optimization of the light throughput and has an aperture to block stray light. A beam splitter was employed to direct part of the emitted light to a reference photodiode and the Lambert–Beer law was emulated with a log-ratio amplifier circuitry. The detector was tested with two LEDs with emission bands at 280 and 255 nm and showed noise levels as low as 0.25 and 0.22 mAU, respectively. The photometric device was employed successfully in separations using a column of 1 mm inner diameter in isocratic as well as gradient elution. Good linearities over three orders of magnitude in concentration were achieved, and the precision of the measurements was better than 1% in all cases. Detection down to the low micromolar range was possible.

**Keywords:** Light-emitting diode / Narrow-bore chromatography / UV detection  
DOI 10.1002/jssc.201300598

## 1 Introduction

Light-emitting diodes (LEDs) are compact, have high efficiency, and stability as well as long lifetimes. They also show relatively narrow emission bands. When employed in analytical instrumentation, monochromators or optical filters are therefore generally not necessary, and it is possible to construct simple and inexpensive yet powerful devices by substituting incandescent or discharge lamps and monochromators or filters with LEDs. Their emission bands of typically 30 nm width are well matched to the absorption bands of molecules. Flaschka et al., in 1973, were the first to suggest the use of LEDs as emitters in photometry [1]. Since then, LED-based devices have been developed for many different analytical applications. These include detection in flow injection analysis (see e.g. Ref. [2, 3]), membrane-based optical sensors (see e.g. Ref. [4–6]), detection in CE (see e.g. Ref. [7–10]), and the initiation of polymerization in the fabrication of monolithic columns for chromatography [11]. Different aspects have been reviewed repeatedly [2, 12–15].

The use of LEDs for detectors employed in column chromatography has also been reported. Schmidt and Scott, in 1984, developed a simple 550 nm green LED-based detector coupled to an ion chromatographic setup to determine trace

metals complexed with 4-(2-pyridylazo)resorcinol [16]. A photometric detector for the indirect determination of alcohols in RPLC based on measuring the absorption of methylene blue with a 565 nm LED and a photodiode was described by Berthod et al. in 1990 [17]. In 2006, Diamond and co-workers also reported devices employing green LEDs for the determination of metals complexed by 4-(2-pyridylazo)resorcinol [18] and *o*-cresolphthalein complexone in column chromatography [19]. For HPLC, however, the deep UV range <300 nm is of significant interest because the majority of potential analytes absorb only in this region and thus detectors based on visible LEDs are of limited practical use. LEDs for the short wavelengths <300 nm have only become available in recent years, but two HPLC detectors based on LEDs emitting at 280 and 255 nm have been reported by our group [20, 21]. The detection cells were designed for an HPLC setup employing conventional columns of 4.6 mm id and had a standard optical pathlength of 10 mm. The performance of the optimized second version of the relatively inexpensive device was comparable to a conventional commercial HPLC detector [21]. The use of a 255 nm LED in a detector for CE has also been described [22, 23].

In HPLC, there is a trend of using columns with narrower diameters. The most important reason for this is the increasing use of MS for detection, for which only minute amounts of analytes are required. Also important is the reduction in the amount of consumables (expensive solvents of high purity), waste, and the required sample volumes that goes hand in hand with the reduction of the column diameter. A good introduction to the topic has been given by Saito et al. [24] and recent developments have been summarized by Zotou [25]. On the other hand, with the exception of MS, detection

**Correspondence:** Dr. Peter C. Hauser, Department of Chemistry, University of Basel, Spitalstrasse 51, Basel 4056, Switzerland  
**E-mail:** Peter.Hauser@unibas.ch  
**Fax:** +41-61-267-1013

**Abbreviations:** AU, absorbance unit; LEDs, light-emitting diodes

becomes a challenge on downscaling. The development of special detectors for miniaturized HPLC is therefore of interest. For this reason, the use of contactless conductivity detection has been explored for combination with narrow-bore separation columns [26, 27]. Herein, a deep UV detector based on LEDs for use with 1 mm id columns (micro-LC) is described.

## 2 Materials and methods

### 2.1 Instrumentation

Two UV-LEDs emitting at 255 and 280 nm (UVTOP255TO39BL and UVTOP280TO39BL) were products of Sensor Electronic Technology (Columbia, SC, USA). The photodiodes for the UV range (SG01L-C) were sourced from Sglux Solgel Technologies (Berlin, Germany). The fused-silica tubing (250  $\mu\text{m}$  id/1600  $\mu\text{m}$  od) employed for detection was obtained from Fibertech (Berlin, Germany). The beam splitter (G344312000) was sourced from Qioptiq Photonics (Munich, Germany). The log-ratio amplifier (LOG102) and operational amplifiers (TL072) used for the current measurements were purchased from Texas Instruments (Austin, TX, USA). The micro-HPLC pump/degasser unit (Rheos 2000) was a product of Flux Instruments (Basel, Switzerland) and was fitted with a six-port injection valve (M485) from Upchurch Scientific (Oak Harbor, WA, USA). The column for HPLC separation ( $\text{C}_{18}$ , 3  $\mu\text{m}$ , 150  $\times$  1 mm) was a product of Phenomenex (Torrance, CA, USA). An e-corder ED401 data acquisition system and the chart software package used to digitize the signals were products of EDAQ (Denistone East, Australia).

### 2.2 Reagents

All chemicals were either of analytical or HPLC grade. Methanol and TFA were obtained from J.T. Baker (Deventer, The Netherlands). Acetonitrile was a product of Fisher Scientific (Wohlen, Switzerland). Formic acid, caffeine,  $\text{KH}_2\text{PO}_4$ , 4-hydroxybenzoic acid, and 2-acetylsalicylic acid were purchased from Fluka (Buchs, Switzerland). Ascorbic acid was sourced from Merck (Zug, Switzerland). Phosphoric acid ( $\text{H}_3\text{PO}_4$ ) was obtained from VWR (Dietikon, Switzerland). The other chemicals, namely, DL-tryptophan, paracetamol (acetaminophen), caffeine, sorbic acid, sulfathiazole, sulfamerazine, sulfamethazine, cytidine, uridine, guanosine, adenosine, and xanthosine were products of Sigma-Aldrich (Buchs, Switzerland). Deionized water was obtained from a NANO-Pure water purification system (Barnstead, IA, USA). All solutions were degassed in an ultrasonic bath and filtered through 0.2  $\mu\text{m}$  nylon filters obtained from BGB Analytic (Boeckten, Switzerland). The solutions used to evaluate the linearity of the detector were prepared with deionized water.

## 3 Results and discussion

### 3.1 Design of the detector

According to the Lambert–Beer law, the absorbance value ( $A$ ) is given by  $A = \log(I_0/I)$ , where  $I_0$  and  $I$  are the intensity of the incident light and the transmitted light, respectively. Measured by photodiodes these light intensities ( $I$  and  $I_0$ ) are converted proportionally to electrical currents ( $i_0$  and  $i$ ), hence the absorbance value can also be expressed as  $A = \log(i_0/i)$ . The overall arrangement used to achieve this measurement is sketched in Fig. 1A. The UV-LED was operated with a constant current source in order to minimize variations of intensity. The light from the LED was divided with the aid of a beam splitter; one part was passed perpendicularly through fused-silica tubing, which acted as the optical cell, and then to the signal photodiode, while the other part of the beam was guided to a reference photodiode. Note that special photodiodes suitable for the deep UV range were required. These also contain an optical filter to block longer wavelengths. The reason for this is the occurrence of some additional emission bands in the near UV and even visible range for the deep UV-LEDs [20, 21]. This is thought to be due the presence of weakly fluorescent contaminants in the LED assembly. The currents from the two photodiodes were processed with a log-ratio circuitry, which produces an output voltage ( $V_O$ ) according to  $V_O = \log(i_0/i)$ , where 1 V equals to 1 absorbance unit (AU), and 1 mV = 1 mAU. Details of the circuitry can be found in an earlier publication [21]. It also includes an offset facility to compensate for an imbalance between the intensities of the two signals, i.e. to zero the absorbance reading, as well as an active low-pass filter in order to reduce high-frequency noise.

The mechanical part of the detector was specifically designed and built for use with the narrow-bore chromatographic column. An overview of the mechanical arrangement is given in Fig. 1B. The flow-through cell consisted of fused-silica tubing of 7 cm length with 250  $\mu\text{m}$  id and 1.6 mm od. This was mounted on a black plastic holder, which completely divides the section containing the source LED from the section containing the signal photodiode to avoid stray light reaching the latter. Connections to external tubing were made with appropriate fittings. An optical slit of 100  $\mu\text{m}$  width and 1 mm length was mounted in front of the tubing in order to restrict the light beam to center of the tubing, i.e. the liquid channel, and thus prevent stray light passing sideways through the walls of the tubing. The UV-LED has a built-in ball lens with a focal point approximately 15–20 mm from the LED. This allowed the insertion of the beam splitter in a 45° angle in front of the LED. The disk-shaped splitter has a splitting ratio of 80:20 so that 20% of the light was reflected to the reference photodiode. The UV-LED emitter and the signal photodiode placed at the opposite sides of the detection window were mounted on miniature positioning stages to adjust their placements both vertically and horizontally so that the latter received the maximum transmitted intensity. These positioning stages were based on smooth

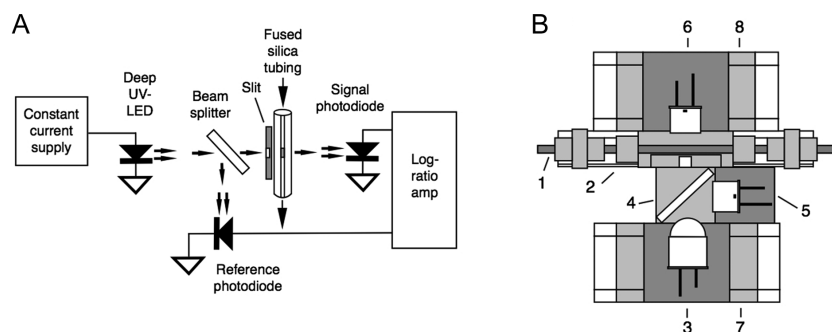


**Figure 1.** Design of the detector. (A) Overview; (B) construction: (1) fused-silica tubing, (2) holder for fused-silica tubing and optical slit, (3) UV-LED, (4) beam splitter with holder, (5) reference photodiode, (6) signal photodiode, (7) positioning stages for UV-LED, (8) positioning stages for signal photodiode.

T-shaped grooves and mating counterparts as well as locking screws and were constructed in our workshop. The holder for the LED also allowed a forward/backward adjustment to account for variations in the focal length between components. The positioning of the reference photodiode is not critical as it receives more light than the signal photodiode, and for this a fixed holder was constructed. All parts had to be made very precisely in order to prevent any mechanical slack and wobble, which would otherwise cause baseline instabilities due to changes in the transmitted light intensity. The entire assembly, including the electronic circuitry, was mounted on a rigid baseplate and despite the relative mechanical complexity could be contained in a metal case of  $137 \times 99 \times 77$  mm to shield it from ambient light.

### 3.2 Noise, detection limits, and linearity performance of the detector

The emitted powers of the deep UV-LEDs are in the microwatt range and therefore very low compared to conventional visible LEDs. In the present setup, the light intensity on the detector photodiode is further reduced compared to previous cell designs [20, 21] due to the aperture restricting the light to the narrow core of the quartz tubing. As at low light levels the precision of signals will deteriorate due to shot noise, it was important to evaluate if this would affect the measurements. The shot noise,  $i_N$ , of a current signal,  $i_S$  (in this case the photocurrent of a photodiode), is given by [28]:

$$i_N = (2 \cdot q \cdot i_S \cdot \Delta f)^{\frac{1}{2}} \quad (1)$$

in which  $q$  is the electron charge and  $\Delta f$  the bandwidth in Hz. The photocurrents for the present cell were determined as 1.3 and 30 nA for the signal and reference photodiode, respectively, when using the 280 nm LED as emitter. For the 255 nm LED, the respective currents were 21 and 460 nA. Note that the currents were lower for the 280 nm LED despite its higher output power ( $300 \mu\text{W}$  as opposed to  $150 \mu\text{W}$ ) due to the wavelength filter built into the photodiodes. The electronic data acquisition system used applied a low-pass filter with a cut-off frequency of 1 Hz. According to Eq. (1),

the shot noise for a signal current of 1 nA is 18 fA, and therefore still negligible.

The fundamental characteristics of the detector were then investigated by measuring the absorbances of standard solutions of tryptophan and 4-hydroxybenzoic acid, which have strong absorption bands at 280 and 255 nm, respectively. The detector was tested on its own, i.e. not as part of an HPLC system, by filling the cell with solutions of the compounds. The measurements were conducted with 1 Hz bandwidth filtering to remove high-frequency noise. Note that the noise level of signals measured with any detector is not only dependent on its intrinsic noise, but also on the applied filter settings. The noise recorded in this mode was determined by reading the maximum fluctuations over a period of 60 s. It was found that the values of noise were typically at 0.25 and 0.22 mAU for the UV-LEDs emitting at 280 and 255 nm, respectively. This performance is comparable with that reported for the 255 nm LED in a cell for CE used with a photomultiplier tube as detector (0.1 mAU [22]) but worse compared to that also obtained for a CE cell with a high intensity green LED and a photodiode-based circuitry similar to that employed here ( $30 \mu\text{AU}$  [10]). Note, however, that the latter values were obtained despite the narrower apertures of the cells for CE. Standard solutions of the two compounds were prepared in a wide range of concentrations, from 0 to 5000  $\mu\text{M}$  for tryptophan and from 0 to 1000  $\mu\text{M}$  for 4-hydroxybenzoic acid. Calibration curves, which were linear up to the highest concentrations measured, were obtained for both systems. Thus, the detector responded strictly according to the Lambert–Beer law indicating the efficient elimination of stray light. The regression equation for the 280 nm LED and 4-hydroxybenzoic acid was determined as  $A = 0.2906 \cdot c - 1.8866$  ( $A$  in milli-absorbance unit and  $c$  in micromolar) with a correlation coefficient ( $r$ ) of 0.99991 (ten concentrations). For the 255 nm LED and tryptophan, the regression equation was determined as  $A = 0.1296 \cdot c - 2.077$  and the correlation coefficient also as 0.99991. Note that the intercepts are somewhat arbitrary as affected by the zero setting of the detector. The highest absorbance readings obtained for the two wavelengths in this experiment were 647 and 289 mAU for the 280 and 255 nm LEDs, respectively. Higher concentrations, and thus higher absorbance values, were not tested as they are not relevant for the envisaged application as a detector in HPLC. The good linearity of the detector indicates that stray light on the signal

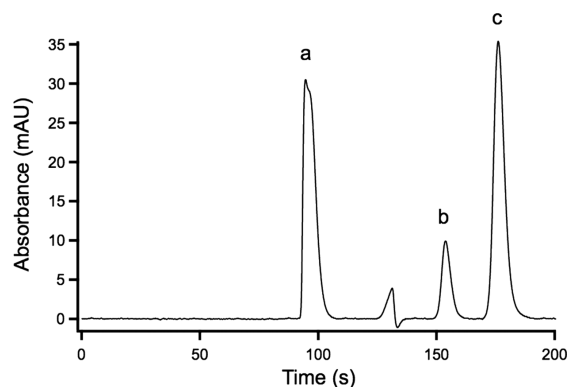


**Figure 2.** Chromatogram of a separation by isocratic elution detected at 280 nm. (A) Ascorbic acid; (B) paracetamol; (C) caffeine (all 1000  $\mu\text{M}$ ); column:  $\text{C}_{18}$ , 3- $\mu\text{m}$  particle size, 150  $\times$  1 mm; mobile phase: 0.025 M aqueous  $\text{KH}_2\text{PO}_4$ /acetonitrile (78:22 v/v); flow rate: 50  $\mu\text{L}/\text{min}$ ; injection volume: 0.5  $\mu\text{L}$ .

photodiode as well as dark currents on both photodiodes were negligible. The detection limits were determined as 10  $\mu\text{M}$  for tryptophan and 5  $\mu\text{M}$  for 4-hydroxybenzoic acid.

### 3.3 Applications with the 280 nm LED

The detector was then coupled to an HPLC setup to further evaluate its capability. This was assembled from a micropump, an online degasser, a six-port micro-injection valve, and a  $\text{C}_{18}$  separation column of 1 mm diameter and 15 cm length containing 3  $\mu\text{m}$  particles. Standard solutions of ascorbic acid, acetaminophen (paracetamol), and caffeine absorbing around 280 nm were separated in an isocratic elution and then quantified with the UV-LED detector. A chromatogram of the three substances detected at 280 nm is shown in Fig. 2. The quantitative data are given in Table 1. As demonstrated by the correlation coefficients shown in Table 1, linear responses were satisfactorily achieved with paracetamol and

**Table 1.** Quantitative data for detection at 280 nm

	Correlation coefficients for peak areas ( $r^a$ )	Reproducibility for peak area <sup>b</sup> (%)	LOD <sup>c</sup> ( $\mu\text{M}$ )
Ascorbic acid	0.9954	0.56	8
Paracetamol	0.9998	0.37	20
Caffeine	0.9997	0.46	8
Sulfathiazole	0.9998	0.24	5
Sulfamerazine	0.9997	0.20	10
Sulfamethazine	0.9998	0.41	10

a) For eight concentrations from 8 to 2000  $\mu\text{M}$  (ascorbic acid, paracetamol, caffeine) and 5 to 1000  $\mu\text{M}$  (the sulfa drugs).

b) RSD,  $n = 5$ ; 1000  $\mu\text{M}$ .

c) Concentrations corresponding to peaks whose heights are three times the baseline noise.

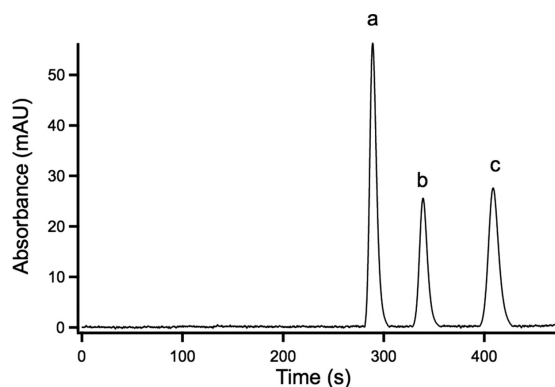


**Figure 3.** Chromatogram of a separation by gradient elution detected at 280 nm. (A) Sulfathiazole; (B) sulfamerazine; (C) sulfamethazine (all 1000  $\mu\text{M}$ ); column: as for Fig. 2; mobile phase:  $\text{H}_2\text{O}$  adjusted to pH 2.5 with  $\text{HCOOH}$ /methanol;  $t = 0$  min, 72:28 v/v;  $t = 8$  min, 60:40 v/v; flow rate: 40  $\mu\text{L}/\text{min}$ ; injection volume: 0.5  $\mu\text{L}$ .

caffeine in a wide range of concentrations up to 2 mM. For ascorbic acid, a slight curvature was obtained, which led to a lower correlation coefficient. This is due to spectral reasons, e.g. the imperfect monochromaticity of the light source. A detailed discussion can be found in one of our previous publications [21]. The effect need not be a problem as it can be dealt with by using a nonlinear calibration. The reproducibilities of the measurements were excellent with SDs of <1%. The baseline noise, measured as the maximum deviation for a period of five times the peak width (12 s), was determined as 80  $\mu\text{AU}$  when a low-pass filter with a cut-off frequency of 1 Hz was applied. The detection limits determined as concentrations giving peak heights corresponding to three times the baseline noise were 20  $\mu\text{M}$  for paracetamol and 8  $\mu\text{M}$  for both ascorbic acid and caffeine. The baseline was found to be very stable, as over the acquisition time of a chromatogram no drift could be discerned.

A separation of some sulfa drugs, namely sulfathiazole, sulfamerazine, and sulfamethazine, detected also at 280 nm, was carried out in gradient elution. The chromatogram given in Fig. 3 shows that the investigated detector is also suitable for quantification with HPLC instruments in this mode of operation. The quantitative data are also given in Table 1. The good correlation coefficients obtained for the quantification of the three compounds indicate good linearity for peak areas against concentration of the compounds. The noise level of the baseline was determined as 100  $\mu\text{AU}$ , and the LODs were as low as 5  $\mu\text{M}$  for sulfathiazole and 10  $\mu\text{M}$  for sulfamerazine as well as sulfamethazine. The baseline of the chromatogram was found not to be quite as stable as that of the isocratic separation as a drift amounting to a total of 0.46 mAU over the duration of the chromatogram was present. This must be due to a slight sensitivity of the detector to changes in the refractive index of the eluent, which is not constant during gradient elution. As shown in Table 1, the reproducibilities

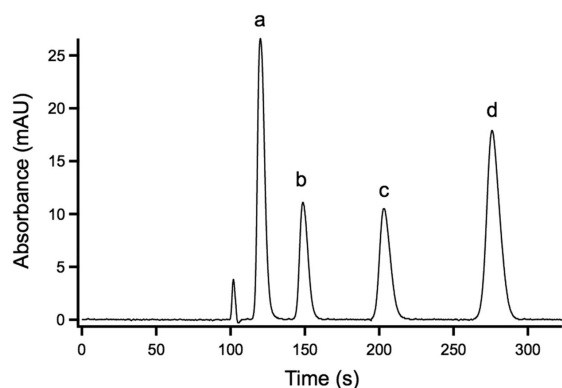


**Figure 4.** Chromatogram of a separation by isocratic elution detected at 255 nm. (A) Paracetamol (720  $\mu\text{M}$ ); (B) 4-hydroxybenzoic acid (240  $\mu\text{M}$ ); (C) 2-acetylsalicylic acid (4800  $\mu\text{M}$ ); (D) sorbic acid (480  $\mu\text{M}$ ); column: as for Fig. 2; mobile phase:  $\text{H}_2\text{O}/0.1\%$  TFA in methanol (47/53 v/v); flow rate: 50  $\mu\text{L}/\text{min}$ ; injection volume: 0.5  $\mu\text{L}$ .

for the peak areas of the three compounds were again found to be better than 1%.

### 3.4 Applications with the 255 nm UV-LED

The separation of the four model substances paracetamol, 4-hydroxybenzoic acid, 2-acetylsalicylic acid, and sorbic acid, monitored with an LED that emits at 255 nm is shown in Fig. 4. As the relevant data of Table 2 show, the performance

**Table 2.** Quantitative data for detection at 255 nm

	Correlation coefficients for peak areas ( $r^a$ )	Reproducibility for peak area <sup>b</sup> (%)	LOD <sup>c</sup> ( $\mu\text{M}$ )
Paracetamol	0.9999	0.41	5
4-Hydroxybenzoic acid	0.9999	0.47	5
2-Acetylsalicylic acid	0.9990	0.49	100
Sorbic acid	0.9992	0.29	5
Cytidine	0.9994	0.53	10
Uridine	0.9997	0.59	5
Guanosine	0.9997	0.18	10
Adenosine	0.9986	0.16	10
Xanthosine	0.9975	0.58	15

a) For eight concentrations for paracetamol (5–720  $\mu\text{M}$ ), 4-hydroxybenzoic acid (1.66–240  $\mu\text{M}$ ), 2-acetylsalicylic acid (33.3–4800  $\mu\text{M}$ ), sorbic acid (3.33 to between 8 and 2000  $\mu\text{M}$ ); nine concentrations for the nucleosides (5–1000  $\mu\text{M}$ ).

b) RSD,  $n = 5$ ; 720  $\mu\text{M}$  (paracetamol); 240  $\mu\text{M}$  (4-hydroxybenzoic acid); 4800  $\mu\text{M}$  (2-acetylsalicylic acid); 480  $\mu\text{M}$  (sorbic acid); 250  $\mu\text{M}$  (the nucleosides).

c) Concentrations corresponding to peaks whose heights are three times the baseline noise.

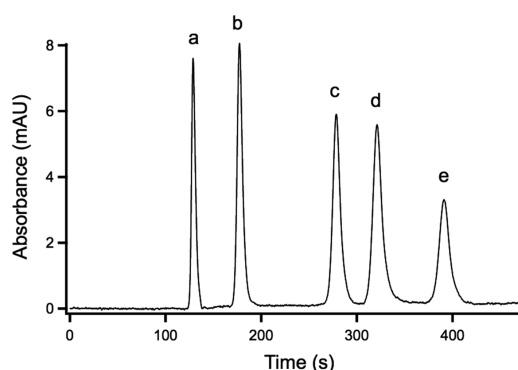


**Figure 5.** Chromatogram of a separation by gradient elution detected at 255 nm. (A) Cytidine; (B) uridine; (C) guanosine; (D) adenosine; (E) xanthosine (all 250  $\mu\text{M}$ ); column: as for Fig. 2; mobile phase: 0.025 M aqueous  $\text{KH}_2\text{PO}_4$  (pH 3.1)/acetonitrile;  $t = 0$  min, 98:2 v/v;  $t = 10$  min, 92:8 v/v; flow rate: 50  $\mu\text{L}/\text{min}$ ; injection volume: 0.5  $\mu\text{L}$ .

with the LED of this wavelength is comparable to that obtained with the LED emitting at 280 nm. The higher LOD for 2-acetylsalicylic acid is due to the relatively low absorptivity of this compound. In this application, the noise on the baseline was approximately 80  $\mu\text{AU}$ , equivalent to that recorded with the 280 nm light source. A systematic baseline drift was again not detectable for this isocratic separation.

The separation of some nucleosides by gradient elution and detection at 255 nm was also carried out (Fig. 5). The performance parameters for quantification, given in Table 2, in terms of linearity of the calibration curve, reproducibility, and LODs are again comparable to the results obtained for the other separations. The noise of the baseline was determined at value of 95  $\mu\text{AU}$ , but a baseline drift is also evident on the relatively sensitive absorbance scale of Fig. 5 and amounts to 0.17 mAU for the chromatogram. This again must be due to refractive index changes of the eluent.

## 4 Concluding remarks

It could be demonstrated that a viable absorption detector for miniaturized HPLC can be constructed using deep UV-LEDs as light sources. The stability and linearity of the detector is excellent and comparable to the earlier version designed for conventional HPLC [21]. The baseline noise was also found to be comparable with that of the earlier device, but the shorter optical pathlength led to the expected reduction in LODs in terms of concentration. Some baseline drifts, ascribed to refractive index effects, were found when gradient elution was employed. The extent of these will depend on the conditions but sloping baselines will not be a problem if they are not too pronounced. The detector should prove useful for applications in which a reduction of eluent consumption is desired, or where only limited sample volumes are available, and it is not necessary to obtain utmost sensitivity.



Financial support by the Swiss Federal Commission for Scholarships for Foreign Students and the Swiss National Science Foundation are gratefully acknowledged.

The authors have declared no conflict of interest.

## 5 References

- [1] Flaschka, H., McKeithan, C., Barnes, R., *Anal. Lett.* 1973, 6, 585–594.
- [2] Trojanowicz, M., Worsfold, P. J., Clinch, J. R., *Trends Anal. Chem.* 1988, 7, 301–305.
- [3] Hauser, P. C., Tan, S. S., Cardwell, T. J., Cattrall, R. W., Hamilton, I. C., *Analyst* 1988, 113, 1551–1555.
- [4] Wolfbeis, O. S., Weis, L. J., Leiner, M. J. P., Ziegler, W. E., *Anal. Chem.* 1988, 60, 2028–2030.
- [5] Hauser, P. C., Tan, S. S. S., *Analyst* 1993, 118, 991–995.
- [6] Müller, B., Hauser, P. C., *Analyst* 1996, 121, 339–343.
- [7] Li, S. T., Yu, Q. L., Lu, X., Zhao, S. L., *J. Sep. Sci.* 2009, 32, 282–287.
- [8] Johns, C., Macka, M., Haddad, P. R., *Electrophoresis* 2004, 25, 3145–3152.
- [9] Bruno, A. E., Maystre, F., Krattiger, B., Nussbaum, P., Gassmann, E., *Trends Anal. Chem.* 1994, 13, 190–198.
- [10] Butler, P. A. G., Mills, B., Hauser, P. C., *Analyst* 1997, 122, 949–953.
- [11] Walsh, Z., Levkin, P. A., Jain, V., Paull, B., Svec, F., Macka, M., *J. Sep. Sci.* 2010, 33, 61–66.
- [12] O'Toole, M., Diamond, D., *Sensors (Basel)* 2008, 8, 2453–2479.
- [13] Xiao, D., Yan, L., Yuan, H. Y., Zhao, S. L., Yang, X. P., Choi, M. M. F., *Electrophoresis* 2009, 30, 189–202.
- [14] Dasgupta, P. K., Eom, I. Y., Morris, K. J., Li, J. Z., *Anal. Chim. Acta* 2003, 500, 337–364.
- [15] Dasgupta, P. K., Bellamy, H. S., Liu, H. H., Lopez, J. L., Loree, E. L., Morris, K., Petersen, K., Mir, K. A., *Talanta* 1993, 40, 53–74.
- [16] Schmidt, G. J., Scott, R. P. W., *Analyst* 1984, 109, 997–1002.
- [17] Berthod, A., Glick, M., Winefordner, J. D., *J. Chromatogr.* 1990, 502, 305–315.
- [18] O'Toole, M., Lau, K. T., Shazmann, B., Shepherd, R., Nesterenko, P. N., Paull, B., Diamond, D., *Analyst* 2006, 131, 938–943.
- [19] Barron, L., Nesterenko, P. N., Diamond, D., O'Toole, M., Lau, K. T., Paull, B., *Anal. Chim. Acta* 2006, 577, 32–37.
- [20] Schmid, S., Macka, M., Hauser, P. C., *Analyst* 2008, 133, 465–469.
- [21] Bomastyk, B., Petrovic, I., Hauser, P. C., *J. Chromatogr. A* 2011, 1218, 3750–3756.
- [22] Krčmová, L., Stjernlof, A., Mehlen, S., Hauser, P. C., Abele, S., Paull, B., Macka, M., *Analyst* 2009, 134, 2394–2396.
- [23] Ryvolova, M., Preisler, J., Foret, F., Hauser, P. C., Krasensky, P., Paull, B., Macka, M., *Anal. Chem.* 2010, 82, 129–135.
- [24] Saito, Y., Jinno, K., Greibrokk, T., *J. Sep. Sci.* 2004, 27, 1379–1390.
- [25] Zotou, A., *Centr. Eur. J. Chem.* 2012, 10, 554–569.
- [26] Kubáň, P., Hauser, P. C., *J. Chromatogr. A* 2007, 1176, 185–191.
- [27] Gillespie, E., Connolly, D., Macka, M., Hauser, P., Paull, B., *Analyst* 2008, 133, 1104–1110.
- [28] Wilson, J., Hawkes, J. F. B., *Optoelectronics, An Introduction*, Prentice Hall, London 1983.

**3<sup>rd</sup> project:**

**Absorbance detector for capillary electrophoresis based on  
light-emitting diodes and photodiodes for the deep-ultraviolet range**

*Journal of Chromatography A (2015), 1421, 203-208*



Contents lists available at ScienceDirect

## Journal of Chromatography A

journal homepage: [www.elsevier.com/locate/chroma](http://www.elsevier.com/locate/chroma)

# Absorbance detector for capillary electrophoresis based on light-emitting diodes and photodiodes for the deep-ultraviolet range



Duy Anh Bui, Peter C. Hauser\*

Department of Chemistry, University of Basel, Spitalstrasse 51, 4056 Basel, Switzerland

## ARTICLE INFO

## Article history:

Received 22 April 2015  
 Received in revised form 2 June 2015  
 Accepted 3 June 2015  
 Available online 9 June 2015

## Keywords:

Capillary electrophoresis  
 Deep-UV LED  
 Photodiode

## ABSTRACT

A new absorbance detector for capillary electrophoresis featuring relatively high intensity light-emitting diodes as radiation sources and photodiodes for the deep-UV range was developed. The direct relationship of absorbance values and concentrations was obtained by emulating Lambert-Beer's law with the application of a beam splitter to obtain a reference signal and a log-ratio amplifier circuitry. The performance of the cell was investigated at 255 nm with the detection of sulfanilic, 4-nitrobenzoic, 4-hydroxybenzoic and 4-aminobenzoic acid and the indirect detection of acetate, propionate, butyrate and caproate using benzoate as the displacement dye molecule. Vanillic acid, L-tyrosine and DL-tryptophan as well as the sulfonamides sulfamerazine, sulfathiazole and sulfamethazine were determined at 280 nm. Good linearities over 3 orders of magnitude were obtained. The noise level recorded was as low as 50  $\mu$ AU and the drift typically <200  $\mu$ AU/5 min.

© 2015 Elsevier B.V. All rights reserved.

## 1. Introduction

Capillary electrophoresis is in principle very simple in that for separation essentially only an inexpensive capillary and a high voltage supply are required. For commercial instruments the standard method of detection is via molecular absorption in the UV and visible ranges. The source of radiation for these detectors is broadband emitters in the form of deuterium and tungsten lamps, monochromators are used for wavelength selection and photomultipliers for intensity measurement. Such a detector is then perhaps the most complex part of a CE-instrument.

Light-emitting diodes (LEDs) have been employed as alternative radiation sources in instrumentation for the analytical sciences since the first report on such a use by Flaschka et al. in 1973 [1]. As the emission bands of LEDs are relatively narrow (typically about 30 nm) monochromators or optical filters are not generally required when carrying out molecular absorption measurements as these spectral widths are well matched to the absorbance bands of molecules. Other advantages are compact size and robustness, low power consumption and low heat production. A further analytically important benefit is the high stability of the

output intensity of LEDs. The original work by Flaschka et al. [1] was based on a then available red LED, but since that time LEDs with progressively shorter emission wavelengths have become available and their analytical applications have been extended to many different fields. Two recent general reviews are available [2,3].

Tong and Yeung in 1995 were the first to describe a purpose built absorption detector for CE based on a green LED as radiation source [4]. The indirect detection of inorganic anions via the displacement of permanganate in the background electrolyte was demonstrated. Macka et al. in 1996 reported the direct detection of alkali and alkaline earth metals as their Arsenazo complexes using green and yellow LEDs fitted into a commercial detector in place of the conventional light source [5]. Butler et al. in 1997 demonstrated the use of a green LED for the direct detection of the complexes of transition metals with 4-(2-pyridylazo) resorcinol and the indirect detection of inorganic cations and anions using organic displacement dyes [6]. Macka and coworkers in 2002 also introduced the use of an LED emitting at 380 nm in the near UV-range, which was demonstrated for the indirect determination of inorganic anions via the displacement of chromate as a probe dye [7]. This is a common method for these ions when determined with conventional commercial CE instruments as otherwise they are not accessible by optical detection. A number of further reports on the use of LEDs in detectors for capillary electrophoresis have appeared over the years and the developments up to 2009 have been reviewed by Xiao et al. [8,9].

Abbreviations: CE, capillary electrophoresis; UV, ultraviolet; LED, light-emitting diode; HPLC, high performance liquid chromatography; AU, absorbance unit.

\* Corresponding author. Tel.: +41 61 267 10 03.

E-mail address: [Peter.Hauser@unibas.ch](mailto:Peter.Hauser@unibas.ch) (P.C. Hauser).

<http://dx.doi.org/10.1016/j.chroma.2015.06.005>

0021-9673/© 2015 Elsevier B.V. All rights reserved.

A limitation to the employment of LEDs for analytical purposes, including their use in capillary electrophoresis, has been the restriction to visible light and the near-UV range. Most organic molecules absorb in the deep-UV range below 300 nm, but not in the visible range, and for this reason absorption detectors for the separation methods of column chromatography and capillary electrophoresis employ wavelengths typically of 280, 255 or 210 nm. However, in recent years deep UV-LEDs down to wavelengths of about 250 nm have become commercially available. Schmid et al. [10] in 2008 and Bomastyk et al. [11] in 2011 reported detectors for standard HPLC instruments based on UV-LEDs of 280 and 255 nm. This was followed by a report on a detector for narrow bore HPLC [12]. Kraiczek et al. [13] reported a HPLC detector employing an array of different UV-LEDs which features wavelength flexibility through simple electronic switching. Very recently Sharma et al. [14] reported an absorption cell for capillary liquid chromatography employing a 260 nm UV-LED. With all of these detectors, low noise, high stability and detection limits were achieved which were comparable with that of more complex and expensive commercial detectors. The use of deep-UV LEDs has also been reported for the quantification of  $O_3$  [15,16] directly in the gas phase.

Macka and coworkers in 2009 in a short communication reported the first design of a detector for CE based on a 255 nm UV-LED as a light source and showed limited preliminary results for the detection of 4 nucleotides [17]. Due to the utilization of an early low intensity UV-LED a photomultiplier tube was employed to measure the light intensity. Rudaz and coworkers in 2009 also reported a UV-LED based detector for CE, but no details on the design of the detector nor its performance parameters were given [18,19]. The detector reported herein was fitted with newer LEDs of higher intensity than previously available and is based on photodiodes. Its performance in CE was evaluated for the commonly used wavelengths of 280 and 255 nm.

## 2. Experimental

### 2.1. Chemicals and reagents

All chemicals were of analytical grade. Sulfanilic acid was purchased from Merck (Zug, Switzerland). Sodium butyrate and sodium propionate were obtained from Lancaster Synthesis (White Lund, Morecambe, England) and Riedel-de Haën (Seelze, Germany), respectively. The other chemicals were products of Sigma-Aldrich (Buchs, Switzerland) or Fluka (Buchs, Switzerland). Deionized water from a NANO-Pure water purification system (Barnstead, IA, USA) was used throughout the experiments. Standard solutions were prepared in water, except for sulfamerazine, sulfathiazole and sulfamethazine, which were dissolved in methanol. All solutions were degassed in an ultrasonic bath and filtered through 0.2  $\mu\text{m}$  nylon filters purchased from BGB Analytic (Boeckten, Switzerland). The capillaries were preconditioned with 1 M NaOH for 10 min, rinsed with deionized water for 10 min and finally flushed with the electrolyte solutions for 30 min. After each separation, they were reconditioned with the electrolyte solutions for 5 min.

### 2.2. Instrumentation

The high intensity UV-LEDs emitting at 255 nm (model 7YS,  $P_{100\text{mA}} = 1.8\text{ mW}$ ) and 280 nm (model 74P,  $P_{100\text{mA}} = 1.5\text{ mW}$ ) were obtained from Crystal IS (Green Island, NY, USA). The UV-photodiodes (SG01L-C, SG01L-B18) were sourced from Sglux Solgel Technologies (Berlin, Germany). A polyimide coated fused-silica capillary (50  $\mu\text{m}$  ID, 360  $\mu\text{m}$  OD) from Polymicro Technologies (Phoenix, AZ, USA) and a fused-silica extended light path capillary (G1600-62232, 50  $\mu\text{m}$  ID, 360  $\mu\text{m}$  OD, bubble factor = 3) from

Agilent Technologies (Agilent, Waldbronn, Germany) were employed for separations. The beam splitter (G344312000) was sourced from Qioptiq Photonics (Munich, Germany). The 4 mm diameter fused-silica ball lens (No. 67385), and the 50  $\mu\text{m}$  and 100  $\mu\text{m}$  wide optical slits of 3 mm length (air slits Nos. 38559 and 38560, respectively) were products of Edmund Optics Germany (Karlsruhe, Germany). The mechanical parts (holders and adjustable positioning stages) were made in our workshop from black poly(methyl methacrylate) (PMMA) or from aluminium. The log-ratio amplifier (LOG102) was obtained from Texas Instruments (Austin, TX, USA). The separations of target ions were carried out by using a purpose-made portable capillary electrophoresis instrument, which is a refinement of the design first developed by Kubáň [20]. It consists of a case made from PMMA with dimensions of 310  $\times$  220  $\times$  260 mm. This was fitted with a microswitch to interrupt the high voltage for safety when opened for manipulations inside. It includes a dual polarity high voltage power supply (CZE2000, Spellman, Pulborough, UK), which has maximum output voltage of  $\pm 30\text{ kV}$  at 300  $\mu\text{A}$ , and associated control electronics. The signals were recorded and digitized with the use of an e-corder data acquisition system (Model ED401) and the Chart software package (both from EDAQ, Denistone East, NSW, Australia).

## 3. Results and discussion

### 3.1. Design of detector

The physical arrangement of the detector was a modification of the previously reported design for narrow bore chromatography [12] and the circuitry used was an adaptation of the one reported elsewhere [11]. The overall set-up of the cell is shown in Fig. 1A. The UV-LED was driven with a constant current source at 100 mA. The light beam was divided into signal and reference paths. This allows a compensation for the temperature dependence of the output

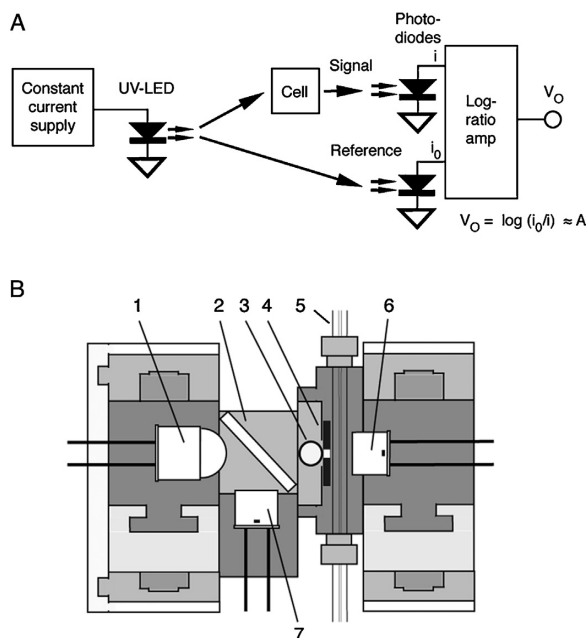


**Fig. 1.** Design of the detector. (A) Overview. (B) Assembly: 1) UV-LED in positioning stage, 2) beam splitter, 3) ball lens, 4) optical slit, 5) capillary, 6) signal photodiode in positioning stage, 7) reference photodiode.

**Table 1**  
Baseline noise for some LED-based detectors.

	Wavelength (nm)	Cut-off frequency of filter (Hz)	Peak-to-peak (p-p) or Standard deviation (SD)	Baseline period considered (s)	Noise level ( $\mu$ AU)	Reference
CE-Detector, photodiodes, referenced	255	2	p-p	60	50	This work
	255	2	SD	60	7.6	
	280	2	p-p	60	53	
	280	2	SD	60	7.9	
CE-detector, single photodiode	525	n.a.	p-p	n.a.	30	[6]
CE-detector, photomultiplier	255	n.a.	n.a.	n.a.	100	[17]
Standard HPLC Detector, (aperture of 1 mm diameter), photodiodes, referenced	255	20	p-p	20	61	[11]
	255	1	p-p	20	16	
	280	20	p-p	20	52	
	280	1	p-p	20	7.5	
Narrow Bore HPLC detector (150 $\mu$ m ID), single photodiode	260	0.1	SD	60	4.4	[14]
Narrow Bore HPLC detector (250 $\mu$ m ID), photodiodes, referenced	255	1	p-p	60	220	[12]
	280	1	p-p	60	250	

n.a. = not available.

intensity which is intrinsic to all LEDs. Photodiodes selective for the UVC (225–287 nm) and UVB (231–309 nm) ranges were employed for the LEDs emitting at 255 and 280 nm, respectively. The wavelength restriction of the photodiodes serves to prevent the detection of incidental bands at longer wavelengths which are present for the deep UV-LEDs [10,11,17]. The photodiodes produce the signal and reference photocurrents ( $i$  and  $i_0$ ), which are proportional to the light intensities ( $I$  and  $I_0$ ), and these were processed with a log-ratio amplifier, which directly implements Lambert-Beer's law and gives an output voltage corresponding to absorbance ( $A$ ) (1 V equals 1 absorbance unit). The circuitry also features an offset section to allow zero setting of the baseline and low pass filtering with a second order Butterworth filter with a  $-3$  dB cut-off frequency of 10 Hz to remove high frequency electronic noise.

A sketch of the mechanical arrangement of the detector is given in Fig. 1B. In order to restrict the light beam to the liquid filled core of the separation capillaries, an optical slit was mounted directly in front of the capillary. For the regular 50  $\mu$ m ID capillary a slit with a width of 50  $\mu$ m was used while for the capillary with bubble cell a slit with 100  $\mu$ m width was fixed in front of the capillary. The original lengths of the commercial slits were reduced to 1 mm by attaching pieces of adhesive copper tape. The LEDs have a built-in ball lens which focuses the emitted light to a point with about 1 mm diameter at a distance of approximately 15 mm. As this focussing area is much larger than the detection windows, a UV-transparent fused silica ball lens of 4 mm diameter was fixed in front of the aperture to improve the focus. This was mounted in a support which was attached to the capillary holder via a thread that allowed the optimization of the distance. Placed at the opposite sides of the detection window, the deep UV-LED and the signal photodiode were mounted on miniature positioning stages to adjust their placements in 3 axes in order to maximize the intensity of the transmitted light on the photodiode. These positioning stages were based on T-shaped grooves and their mating counterparts were fixed in place with screws. The beam splitter plate mounted at a 45° angle in front of the LED has splitting ratio of 80:20, hence 20% of the incident light was diverted to the reference photodiode which was placed in a fixed holder. All mechanical components were made with high precision in order to minimize any possible movement which could cause baseline fluctuations. A grounded

metal case with dimension of 137  $\times$  99  $\times$  77 mm was used to cover the base-plate on which the electronic and mechanical parts were mounted in order to eliminate interferences from ambient light and electromagnetic radiation.

### 3.2. Noise, linearity and detection limits of the detector

The baseline noise of the detector was evaluated by acquiring the signal with the e-corder data acquisition system and determining the fluctuations over a period of 60 s. A low pass filter with a 2 Hz cut-off frequency was applied by the input amplifier of the data-acquisition system in addition to the analog output filtering of the detector circuitry itself (10 Hz cut-off). The noise values for the detector determined in this way are given in Table 1 together with values for related LED based detectors reported in the literature. As an investigation of the data shows, the values of about 50  $\mu$ AU (peak-to-peak over 60 s) are comparable with that of an earlier CE detector based on a green LED, and better than that of the previously reported value for the deep UV-LED CE detector with photomultiplier tube. On the other hand, they are not as good as the best values reported for deep UV-LED based detectors for chromatography which generally have a larger available cross-section for the optical path. However, it has to be borne in mind that such a direct comparison of noise can only be approximate. As illustrated by the data of Table 1, not only are the values obtained very much dependent on the extent of low pass filtering applied, but also on the method used for their quantification (e.g. the time scale considered and whether peak-to-peak or standard deviation values are used). The baseline drift was also examined and found to be ranging from 80  $\mu$ AU to 200  $\mu$ AU for periods of 5 min. The variation of this value is presumably due to different fluctuations in ambient temperature.

The linearity performance of this detector was then investigated by filling it with standard solutions in a wide range of concentrations from 0 to 1000  $\mu$ M (twelve concentrations). 4-Hydroxybenzoic acid and L-tyrosine, which have strong absorption bands at 255 and 280 nm, respectively, were used to carry out this evaluation. The calibration curves were found to be linear up to the highest concentrations tested, which correspond to 119 mAU for 4-hydroxybenzoic acid and 255 nm and 48 mAU for L-tyrosine and

**Table 2**

Determination of aromatic acids at 255 nm.

	Correlation coefficient for peak areas ( $r^a$ )	Reproducibility for peak area <sup>b</sup> (%)	LOD <sup>c</sup> ( $\mu\text{M}$ )	Efficiency $N^d$
Standard capillary				
Sulfanilic Acid	0.9994	1.9	3.0	38100
4-Nitrobenzoic Acid	0.9993	1.9	7.5	8300
4-Hydroxybenzoic Acid	0.9993	1.7	2.5	62200
4-Aminobenzoic Acid	0.9991	1.8	3.2	58700
Extended light path capillary				
Sulfanilic Acid	0.9996	2.0	1.3	37100
4-Nitrobenzoic Acid	0.9994	1.8	3.0	8460
4-Hydroxybenzoic Acid	0.9997	1.6	1.1	61800
4-Aminobenzoic Acid	0.9993	1.8	1.4	59100

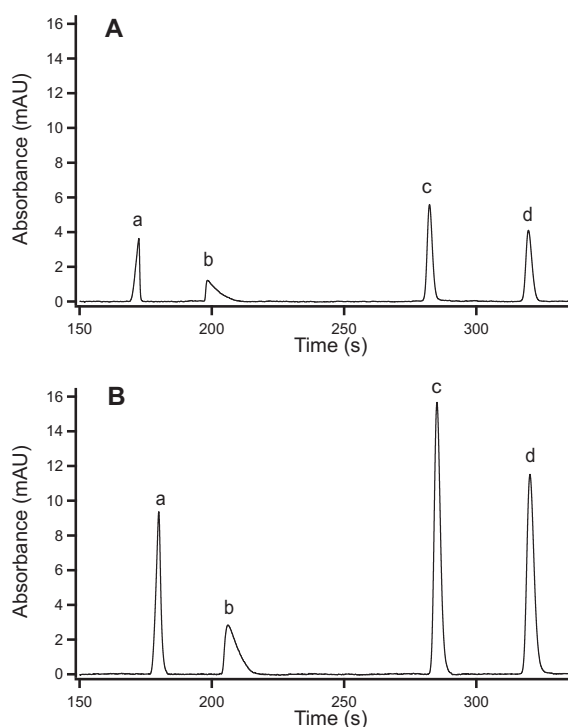
<sup>a</sup> 10 concentrations (10–500  $\mu\text{M}$ ).<sup>b</sup> RSD,  $n=5$ , 100  $\mu\text{M}$ .<sup>c</sup> Concentrations corresponding to peak heights of  $3\times$  the baseline noise.<sup>d</sup> Number of theoretical plates, calculated from the width at half maximum, 100  $\mu\text{M}$ .

280 nm. Higher absorbance values are rarely obtained in capillary zone electrophoresis. The correlation coefficients ( $r$ ) were determined as 0.9996 and 0.9995 for 4-hydroxybenzoic acid (255 nm) and L-tyrosine (280 nm), respectively. The good linearity confirms the adherence of the detector response to Lambert-Beer's law as well as negligible levels of stray light and dark current on the photodiodes for the relevant absorbance range. The detection limits, as the concentrations that gave signals corresponding to three times the baseline noise, were determined to be 2.5  $\mu\text{M}$  for 4-hydroxybenzoic acid (160  $\mu\text{AU}$ ) and 5.5  $\mu\text{M}$  for L-tyrosine (170  $\mu\text{AU}$ ). The reproducibility for signals was determined at concentrations of 100  $\mu\text{M}$  by refilling the cell 5 times. The standard deviation was determined as 1.9% for both systems.

### 3.3. Applications with the 255 nm UV-LED

The separation of the four aromatic compounds, sulfanilic acid, 4-nitrobenzoic acid, 4-hydroxybenzoic acid and 4-aminobenzoic acid by zone electrophoresis in a capillary with 50  $\mu\text{m}$  ID and direct detection at 255 nm is illustrated in Fig. 2A. Note, that while triangular peak shapes are common in zone electrophoresis the reason for the excessive tailing of the peak for 4-nitrobenzoic acid is not known. Calibration curves for peak areas were acquired for concentrations from 10  $\mu\text{M}$  up to 500  $\mu\text{M}$  and these were linear up to at least this level for all four compounds. The baseline noise under separation conditions was found to be similar to the values obtained without application of the separation voltage. The data for quantitative performance are given in Table 2. Good correlation coefficients are evident and reproducibilities of peak areas just under 2% were achieved. Limits of detection for the 4 compounds in the low  $\mu\text{M}$ -range were obtained. The measurements were repeated with an extended light path capillary which led to the expected increase in sensitivity as shown in Fig. 2B. The validation data is also given in Table 2. The reproducibility was comparable to that obtained with the standard capillary and the detection limits showed the anticipated improvement of approximately a factor of 3. Note, that the peak sharpness in terms of plate number ( $N$ ) was not deteriorated by the use of the extended light path capillary. The slight variance in the migration times obtained for the two capillaries (Fig. 2A and B) is thought to be due to a difference in the effectiveness of the dynamic coating with the quaternary amine (CTAB), which was carried out for reversal of the electroosmotic flow in the determination of the anions.

Also performed at 255 nm was the indirect detection of carboxylic acids, namely acetic acid, propionic acid, butyric acid and caproic acid, via the displacement of the UV-absorbing benzoate anion in the background electrolyte [21]. The separation of these species is illustrated in Fig. 3. A good linearity of peak areas with

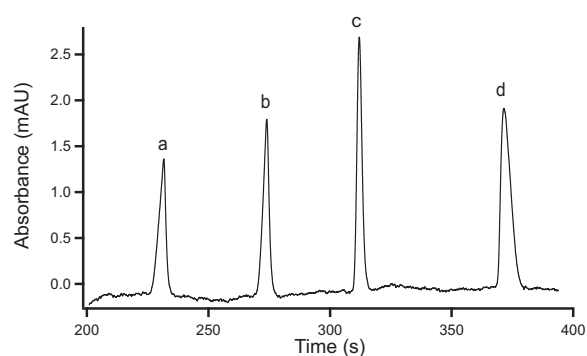
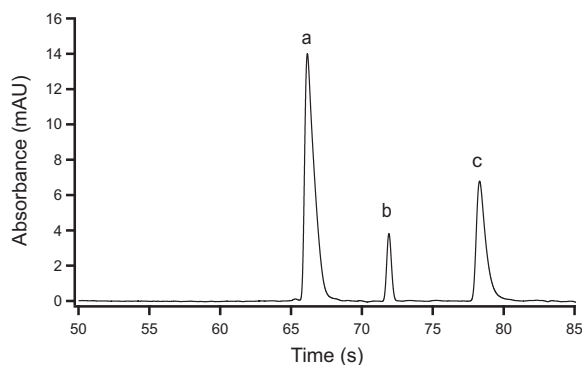


**Fig. 2.** Electropherograms for aromatic acids with detection at 255 nm: (A) Standard capillary, (B) Extended light path capillary. (a) Sulfanilic acid, (b) 4-nitrobenzoic acid, (c) 4-hydroxybenzoic acid, (d) 4-aminobenzoic acid (all 100  $\mu\text{M}$ ). Electrolyte: DL-alanine 250 mM adjusted to pH=4.2 with acetic acid, CTAB 25  $\mu\text{M}$ . Capillaries: 50  $\mu\text{m}$  ID, total length: 46 cm, effective length: 42 cm. Separation voltage:  $-25$  kV. Injection: hydrostatic, 10 s at 10 cm elevation.

concentrations up to 2000  $\mu\text{M}$  was obtained as indicated by the correlation coefficients given in Table 3. The LODs, also given in Table 3, were slightly higher for this indirect method than for the direct detection of the aromatic compounds. It was found that the baseline was less stable for this indirect detection. The extent of baseline fluctuations of approximately 0.2 mAU over the analysis time presumably relates to changes in absorption due to the probe molecule as this is more pronounced than the typical baseline noise observed otherwise. The reproducibilities for peak areas were in agreement with those obtained for the aromatic acids (RSD  $\approx$  2%).

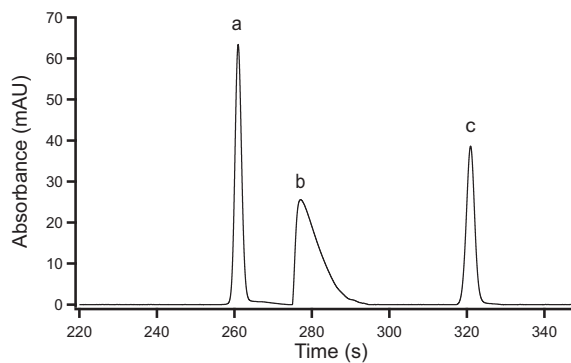
**Table 3**  
Indirect determination of aliphatic carboxylic acids at 255 nm.

	Correlation coefficient for peak areas ( $r^a$ )	Reproducibility for peak area <sup>b</sup> (%)	LOD <sup>c</sup> ( $\mu\text{M}$ )	Efficiency $N^d$
Acetic acid	0.9998	2.1	12	29500
Propionic acid	0.9995	2.0	11	53900
Butyric acid	0.9998	1.9	10	81400
Caproic acid	0.9997	2.3	10	40500

<sup>a</sup> 8 concentrations (25–2000  $\mu\text{M}$ ).<sup>b</sup> RSD,  $n=5$ , 100  $\mu\text{M}$ .<sup>c</sup> Concentrations corresponding to peak heights of  $3\times$  the baseline noise.<sup>d</sup> Number of theoretical plates, calculated from the width at half maximum, 100  $\mu\text{M}$ .**Fig. 3.** Electropherogram for the indirect detection of carboxylic acids at 255 nm: (a) acetate, (b) propionate, (c) butyrate, (d) caproate (all 250  $\mu\text{M}$ ). Electrolyte: Sodium benzoate 10 mM adjusted to pH = 7.8 with Tris, CTAB 0.2 mM. Capillary: extended light path capillary, 50  $\mu\text{m}$  ID, total length: 46 cm, effective length: 42 cm. Separation voltage:  $-20$  kV; Injection: hydrostatic, 15 s at 10 cm elevation.**Fig. 4.** Electropherogram for the detection of aromatic compounds at 280 nm: (a) vanillic acid (100  $\mu\text{M}$ ), (b) L-tyrosine (200  $\mu\text{M}$ ), (c) DL-tryptophan (100  $\mu\text{M}$ ). Electrolyte: sodium tetraborate 35 mM and 5% acetonitrile (v/v) adjusted to pH = 9.2 with boric acid, CTAB 0.5 mM. Capillary: extended light path capillary, 50  $\mu\text{m}$  ID, total length: 46 cm, effective length: 42 cm. Separation voltage:  $-25$  kV. Injection: hydrostatic, 15 s at 10 cm elevation.

### 3.4. Applications with the 280 nm UV-LED

The performance of this detector was further tested in the detection of vanillic acid, L-tyrosine and DL-tryptophan at 280 nm and this separation using the extended light path capillary is demonstrated in Fig. 4. Photodiodes for the UVB range were employed which have a maximum spectral response at this wavelength. As shown by the correlation coefficients given in Table 4, the absorbance values were well linear for concentrations up to 1000  $\mu\text{M}$  for tyrosine, and 500  $\mu\text{M}$  for vanillic acid and DL-tryptophan. The quantitative data shown in Table 4 were comparable to those given in Table 2 indicating that its performance with this emission wavelength is as good as that achieved with the 255 nm light source. The reproducibilities of peak areas was acceptable with a RSD < 3%. A further application at 280 nm is illustrated in Fig. 5 in the separation of the sulfonamides sulfamethazine, sulfathiazole and sulfamerazine according to a slight modification of a method previously reported by Lin et al. [22].

**Fig. 5.** Electropherogram of sulfonamides with detection at 280 nm: (a) sulfamerazine, (b) sulfathiazole, (c) sulfamethazine (all 300  $\mu\text{M}$ ). Electrolyte: trisodium citrate 60 mM adjusted to pH = 7 with citric acid, CTAB 0.1 mM. Capillary: extended light path capillary, 50  $\mu\text{m}$  ID, total length: 46 cm, effective length: 42 cm. Separation voltage:  $-15$  kV. Injection: hydrostatic, 15 s at 10 cm elevation.**Table 4**  
Determination of vanillic acid and aromatic amino acids at 280 nm.

	Correlation coefficient for peak areas ( $r^a$ )	Reproducibility for peak area <sup>b</sup> (%)	LOD <sup>c</sup> ( $\mu\text{M}$ )	Efficiency $N^d$
Vanillic acid	0.9997	2.2	0.5	47800
L-Tyrosine	0.9998	2.6	5.6	179700
DL-Tryptophan	0.9998	2.9	1.4	66200

<sup>a</sup> 7 concentrations for vanillic acid and DL-tryptophan (10–500  $\mu\text{M}$ ), 8 concentrations for L-tyrosine (20–1000  $\mu\text{M}$ ).<sup>b</sup> RSD,  $n=5$ , 100  $\mu\text{M}$  (vanillic acid), 200  $\mu\text{M}$  (L-tyrosine), 100  $\mu\text{M}$  (DL-tryptophan).<sup>c</sup> Concentrations corresponding to peak heights of  $3\times$  the baseline noise.<sup>d</sup> Number of theoretical plates, calculated from the width at half maximum; 100  $\mu\text{M}$  (vanillic acid), 200  $\mu\text{M}$  (L-tyrosine), 100  $\mu\text{M}$  (DL-tryptophan).

#### 4. Conclusions

With newer higher intensity deep-UV LEDs it was possible to construct a detector for CE based on photodiodes, rather than the photomultiplier tube previously used. Its performance in terms of baseline noise (50  $\mu$ AU) matches that of significantly more complex and expensive commercial UV-detectors for current capillary electrophoresis instruments (<50  $\mu$ AU for the Agilent 7100 Capillary Electrophoresis system [23], <30  $\mu$ AU for the PrinCE-C 700 system [24]). Similarly, drift and linearity are also excellent. The low current consumption and compactness makes the LED based detector also suitable for use in portable, battery operated CE instruments.

#### Acknowledgements

Duy Anh Bui gratefully acknowledges a scholarship by the Canton of Basel City.

#### References

- [1] H. Flaschka, M.C. R. Barnes, Light emitting diodes and phototransistors in photometric modules, *Anal. Lett.* 6 (1973) 585–594.
- [2] M. Macka, T. Piasecki, P.K. Dasgupta, Light-emitting diodes for analytical chemistry, *Annu. Rev. Anal. Chem.* 7 (2014) 183–207.
- [3] D.A. Bui, P.C. Hauser, Analytical devices based on light-emitting diodes—a review of the state-of-the-art, *Anal. Chim. Acta* 853 (2015) 46–58.
- [4] W. Tong, E.S. Yeung, Simple double-beam absorption detection systems for capillary electrophoresis based on diode lasers and light-emitting diodes, *J. Chromatogr. A* 718 (1995) 177–185.
- [5] M. Macka, P. Andersson, P.R. Haddad, Linearity evaluation in absorbance detection: the use of light-emitting diodes for on-capillary detection in capillary electrophoresis, *Electrophoresis* 17 (1996) 1898–1905.
- [6] P.A.G. Butler, B. Mills, P.C. Hauser, Capillary electrophoresis detector using a light emitting diode and optical fibres, *Analyst* 122 (1997) 949–953.
- [7] M. King, B. Paull, P.R. Haddad, M. Macka, Performance of a simple UV LED light source in the capillary electrophoresis of inorganic anions with indirect detection using a chromate background electrolyte, *Analyst* 127 (2002) 1564–1567.
- [8] D. Xiao, S.L. Zhao, H.Y. Yuan, X.P. Yang, CE detector based on light-emitting diodes, *Electrophoresis* 28 (2007) 233–242.
- [9] D. Xiao, L. Yan, H.Y. Yuan, S.L. Zhao, X.P. Yang, M.M.F. Choi, CE with LED-based detection: an update, *Electrophoresis* 30 (2009) 189–202.
- [10] S. Schmid, M. Macka, P.C. Hauser, UV-absorbance detector for HPLC based on a light-emitting diode, *Analyst* 133 (2008) 465–469.
- [11] B. Bomastyk, I. Petrovic, P.C. Hauser, Absorbance detector for high-performance liquid chromatography based on light-emitting diodes for the deep-ultraviolet range, *J. Chromatogr. A* 1218 (2011) 3750–3756.
- [12] D.A. Bui, B. Bomastyk, P.C. Hauser, Absorbance detector based on a deep UV light emitting diode for narrow-column HPLC, *J. Sep. Sci.* 36 (2013) 3152–3157.
- [13] K.G. Kraiczek, R. Bonjour, Y. Salvadé, R. Zengerle, Highly flexible UV-Vis radiation sources and novel detection schemes for spectrometric HPLC detection, *Anal. Chem.* 86 (2014) 1146–1152.
- [14] S. Sharma, H.D. Tolley, P.B. Farnsworth, M.L. Lee, LED-based UV absorption detector with low detection limits for capillary liquid chromatography, *Anal. Chem.* 87 (2015) 1381–1386.
- [15] L.E. Kalnajs, L.M. Avallone, A novel lightweight low-power dual-beam ozone photometer utilizing solid-state optoelectronics, *J. Atmos. Ocean. Tech.* 27 (2010) 869–880.
- [16] Y. Aoyagi, M. Takeuchi, K. Yoshida, M. Kurouchi, T. Araki, Y. Nanishi, H. Sugano, Y. Ahiko, H. Nakamura, High-sensitivity ozone sensing using 280 nm deep ultraviolet light-emitting diode for detection of natural hazard ozone, *J. Environ. Protect.* 3 (2012) 695–699.
- [17] L. Krcmova, A. Stjernlof, S. Mehlen, P.C. Hauser, S. Abele, B. Paull, M. Macka, Deep-UV-LEDs in photometric detection: a 255 nm LED on-capillary detector in capillary electrophoresis, *Analyst* 134 (2009) 2394–2396.
- [18] R.D. Marini, E. Rozet, M.L.A. Montes, C. Rohrbasser, S. Roht, D. Rheme, P. Bonnabry, J. Schappler, J.L. Veuthey, P. Hubert, S. Rudaz, Reliable low-cost capillary electrophoresis device for drug quality control and counterfeit medicines, *J. Pharmaceut. Biomed. Anal.* 53 (2010) 1278–1287.
- [19] C. Rohrbasser, D. Rheme, S. Decastel, S. Roth, M.D.A. Montes, J.L. Veuthey, S. Rudaz, A new capillary electrophoresis device with deep UV detector based on LED technology, *Chimia* 63 (2009) 890–891.
- [20] P. Kubáň, H.T.A. Nguyen, M. Macka, P.R. Haddad, P.C. Hauser, New fully portable instrument for the versatile determination of cations and anions by capillary electrophoresis with contactless conductivity detection, *Electroanalysis* 19 (2007) 2059–2065.
- [21] J. Romano, P. Jandik, W.R. Jones, P.E. Jackson, Optimization of inorganic capillary electrophoresis for the analysis of anionic solutes in real samples, *J. Chromatogr.* 546 (1991) 411–421.
- [22] C.E. Lin, C.C. Chang, W.C. Lin, Migration behavior and separation of sulfonamides in capillary zone electrophoresis. 3. Citrate buffer as a background electrolyte, *J. Chromatogr. A* 768 (1997) 105–112.
- [23] Datasheet for the Agilent 7100 Capillary Electrophoresis System, Agilent, Waldbronn, Germany, 2015.
- [24] Data Sheet for the PrinCE-C700 Instrument, Prince Technologies, Emmen, The Netherlands, 2015.



**4<sup>th</sup> project:**

**A deep-UV light-emitting diode-based absorption detector  
for benzene, toluene, ethylbenzene and the xylene compounds**

*Sensors and Actuators B: Chemical (2016), manuscript in press*



# A deep-UV light-emitting diode-based absorption detector for benzene, toluene, ethylbenzene, and the xylene compounds

Duy Anh Bui, Peter C. Hauser\*

Department of Chemistry, University of Basel, Spitalstrasse 51, CH-4056 Basel, Switzerland

## ARTICLE INFO

### Article history:

Received 29 January 2016  
Received in revised form 19 May 2016  
Accepted 24 May 2016  
Available online xxx

### Keywords:

Btex  
Photometric detection  
Deep-UV LED  
Photodiode

## ABSTRACT

The BTEX detector employs the emission band of an ultraviolet light-emitting diode at 260 nm as monochromatic light source and photodiodes for the deep UV-range as reference and signal detectors. Optical fibres are used for coupling the light to the absorption cell of 40 cm length as well as to the reference photodiode. The use of an integrated circuit log-ratio amplifier allows the direct determination of absorbance values according to Lambert-Beer's law. Linear calibration curves over two orders of magnitude, between about 1 ppm and 100 ppm, were obtained for benzene, toluene, ethylbenzene, *o*-xylene, *m*-xylene and *p*-xylene. There is some variation of the sensitivity between the six species, which correlate with differences in the absorption spectra, with toluene, ethylbenzene, *o*-xylene and *m*-xylene showing close values between 150  $\mu$ AU/ppm and 185  $\mu$ AU/ppm, while benzene with 62  $\mu$ AU/ppm has a somewhat lower and *p*-xylene with 235  $\mu$ AU/ppm a somewhat higher sensitivity. The limits of detection were determined as approximately 1 ppm.

© 2016 Published by Elsevier Ltd.

## 1. Introduction

The BTEX compounds, namely benzene, toluene, ethylbenzene and the xylenes, are natural components of crude oil and belong to the most abundantly produced chemicals because of their widespread use as solvents and additives in industry. However, these aromatic hydrocarbons are a concern because of their risk for human health, especially the potential carcinogenicity of benzene, and their promotion of photochemical smog in urban air [1]. Anthropogenic activities are the major sources of benzene and its derivatives in air. It has been determined that these compounds are also released to the atmosphere via the exhaust of motor vehicles, which is considered the dominant source in cities [1].

Gas chromatography (GC) has been the commonly used analytical technique for the determination of these aromatic hydrocarbons in air. This separation method has the advantages of selectivity and excellent detection limits, in particular if on-line preconcentration techniques such as cryogenic sampling are employed [2]. However, as the aromatic compounds absorb well in the UV-range, their spectrophotometric determination is an attractive alternative. Direct absorbance measurements are simpler than gas-chromatographic separations and therefore instruments based on this method can be cheaper. Tunnicliff et al. in 1949 demonstrated the determination of the individual BTEX components based on absorption photometry at several wavelengths in the UV range [3]. Since then, a variety of absorbance based devices have been developed for their determination. Barber et al. in 1995 described an absorbance cell with 30 cm path length employed

on a soil remediation site, which was based on a deuterium lamp with a conventional monochromator and a photodiode for detection [4]. A detection limit of 13 ppm for benzene in air and good agreement with the off-line analyses in the laboratory were reported. Ueno in 2001 introduced a miniature detection cell for BTEX operating in the 230–275 nm region with an optical path length of only 2 cm, but used a preconcentration unit to obtain a comparable detection limit of 4 ppm [5]. They also employed a deuterium lamp and a conventional monochromator. Allouch et al. in 2013 presented a review on BTEX detection systems in which these and more recent developments have been summarized [6].

In recent years light-emitting diodes (LEDs) for the deep UV-range have become available. These devices have emission bandwidths which are relatively narrow (typically <30 nm) and well matched to the absorption bands of molecules. If these are employed as light sources for spectroscopic detectors, monochromators or optical filters are not required, resulting in significantly lower complexity and cost compared to conventional systems with deuterium or tungsten lamps. LEDs have other advantages, such as high output stability, robustness, low power consumption and low heat production which are of great benefit for analytical applications. Since the first report in 1973 of Flaschka et al. on the use of a red LED as a light source in spectrometry [7], LED-based devices have been introduced for a variety of analytical purposes following the progression of the development of LEDs with shorter wavelengths and higher intensities. For recent reviews on the use of LEDs in analytical instruments see the articles by Macka, Piasecki and Dasgupta [8] and Bui and Hauser [9].

In gas phase sensing, LEDs have mostly been employed for absorption measurements in the infrared (IR) range. Johnston in 1992 introduced IR-LEDs based sensors for monitoring carbon dioxide (CO<sub>2</sub>) at 4.25  $\mu$ m and hydrocarbons at 3.3–3.4  $\mu$ m [10]. Since then, a number of reports using IR and mid-IR-LEDs for the determination

**Abbreviations:** BTEX, benzene toluene ethylbenzene *o*-xylene *m*-xylene *p*-xylene; UV, ultraviolet; LED, light-emitting diode

\* Corresponding author.

Email address: Peter.Hauser@unibas.ch (P.C. Hauser)

<http://dx.doi.org/10.1016/j.snb.2016.05.122>

0925-4005/© 2016 Published by Elsevier Ltd.

of CO<sub>2</sub>, carbon monoxide (CO), and water vapour [11] as well as methane (CH<sub>4</sub>) [12–14] have appeared in the literature and some commercial devices are available [9]. The use of visible and UV-LEDs for gas sensing has also been reported. Fowles already in 1981 described a photometric sensor for ozone (O<sub>3</sub>) based on a yellow-orange LED as a light source [15]. Schorsch et al. employed a blue LED and a UV-LED for the detection of CH and OH radicals at the bands of 430 nm and 310 nm, respectively [16]. Hawe in 2008 demonstrated a multi-pass absorption detector for nitrogen dioxide (NO<sub>2</sub>) in which a UV-LED with an emission band at 370 nm and a photodiode was mounted on two sides of a spherical chamber employed as a reflection cell [17]. A detection limit for NO<sub>2</sub> below 5 ppm was achieved with a calculated optical path length of 55 cm. Degner et al. [18], Kalnajs and Avallone [19], as well as Aoyagi et al. [20] reported purpose built photometric devices for O<sub>3</sub> employing 255 nm and 280 nm UV-LEDs as radiation sources. Detection limits below 100 ppb could be obtained. Degner et al. also introduced UV-LEDs based configurations for the real-time monitoring of SO<sub>2</sub> and NO<sub>2</sub> in exhaust gases from combustion engines by their absorption bands at 280 nm and 400 nm, respectively [21].

The newer deep UV-LEDs of higher intensity released recently are expected to also allow the construction of the simple absorption based devices without requiring a monochromator for the determination of aromatic hydrocarbons. To our knowledge the use LEDs for the direct detection of volatile aromatic compounds has not previously been investigated. Reported herein is a detector suitable for the BTEX compounds based on an LED with an emission band at 260 nm.

## 2. Experimental

### 2.1. Chemicals

All chemicals were of analytical grade. Benzene, toluene, *o*-xylene, *m*-xylene, *p*-xylene and isooctane were products of Sigma-Aldrich (Buchs, Switzerland). Ethylbenzene was purchased from Fluka (Buchs, Switzerland). Compressed nitrogen was sourced from PanGas (Dagmersellen, Switzerland). The BTEX analytical standard mixture in nitrogen (each component 10 ppm) was obtained from Fluka.

### 2.2. Instrumentation

A high intensity 260 nm UV-LED (model: Optan260J, P<sub>100mA</sub> = 1 mW) was sourced from Crystal IS (Green Island, NY, USA). The photodiodes for the UV range (SG01XL-C5, 4 mm<sup>2</sup> active area for the signal and SG01L-C, 1 mm<sup>2</sup> active area for the reference) were obtained of Sglux Solgel Technologies (Berlin, Germany). The aluminium tube with 2 mm i.d. and 4 mm o.d. was purchased from Advent (Oxford, UK). A multimode optical fibre for the range from 190 to 325 nm (UM22-300, 300 µm core diameter) from Thorlabs (Dachau, Munich, Germany) was used for light transmission. A log-ratio amplifier (LOG102) was purchased from Texas Instruments (Austin, TX, USA). The mass flow controllers (model 1179) were products of MKS Instruments (Berlin, Germany). The vacuum pump (model PM20405-86) was obtained from VWR (Dietikon, Switzerland). The precision balance (model PB1502) was a product of Mettler Toledo (Greifensee, Switzerland). A diode array spectrometer (model Maya 2000 Pro) and a deuterium light source (model DH-2000), both from Ocean Optics (Dunedin, FL, USA), were used to determine the absorption spectra of the BTEX species in solution and the emission spectrum of the UV-LED. The mechanical parts, including holders for the LED, photodiodes and the absorption cell

were made in our workshop from aluminium. An Arduino microcontroller board (Nano 3.1) (RS Components, Wädenswil, Switzerland) with a purpose made interface circuitry was employed for setting the mass flow controllers from a personal computer. The in-house written software package *Instrumentino* was used for this purpose [22,23]. An e-corder data acquisition system (model ED401) and the Chart software package from EDAQ (Denistone East, NSW, Australia) running on a personal computer were employed for the digitization and recording of signals. A low pass filter with a cut-off frequency of 2 Hz was applied.

### 2.3. Vaporization and dilution

Gas mixtures in nitrogen were prepared using the evaporation and dilution unit shown in Fig. 1. First the laboratory glass bottle used for dilution (approximately 1.1 L total internal volume) was evacuated with the vacuum pump. Then the desired amount of the BTEX compound was injected into the sealed glass bottle with a micro-syringe (approximately 1 µL). This was followed by the controlled introduction of nitrogen with the help of mass flow controller 1 (maximum flow rate 200 mL/min) to about 1.5 bar in order to produce the pressure required for the subsequent metering. The amount of nitrogen added (approximately 2 g) was determined from the mass difference obtained with the balance placed underneath the container. The diluted vapour was then passed to the measuring cell via mass flow controller 2 (maximum flow rate 10 mL/min) and further diluted as required by adding a controlled flow of nitrogen with mass flow controller 3 (maximum flow rate 200 mL/min). Note, that the ppm and ppb concentration values given herein denote gas phase volume fractions.

## 3. Results and discussion

### 3.1. Design of detector

The general arrangement of the detector is shown in Fig. 2A. It was designed to directly obtain the absorbance value (*A*) according to Lambert-Beer's law, which is given by  $A = \log(I_0/I)$  where *I*<sub>0</sub> and *I* are the incident and transmitted light intensities, respectively. The radiation from the LED is directed to the absorption cell and then to a photodiode serving as detector. Part of the light is passed to a reference photodiode. The photocurrents (*i* and *i*<sub>0</sub>) obtained from the two photodiodes are then processed with a log-ratio amplifier which produces an output voltage (*V*<sub>0</sub>) which directly corresponds to absorbance according to  $V_0 = \log(i_0/i)$ . In order to limit variations in emission intensity, the deep UV-LED was powered with a constant current source at 100 mA. The circuitry also features an offset unit

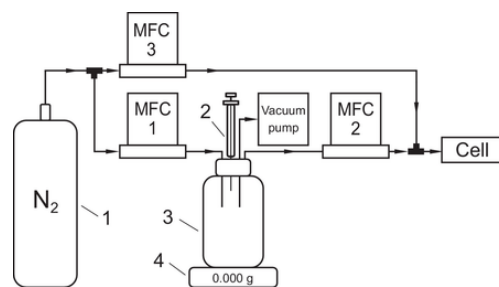


Fig. 1. Overall arrangement of the vaporization and dilution system: MFC = mass flow controller, (1) cylinder of compressed nitrogen, (2) syringe for injection of standard, (3) laboratory glass bottle with about 1.1 L internal volume, (4) balance.

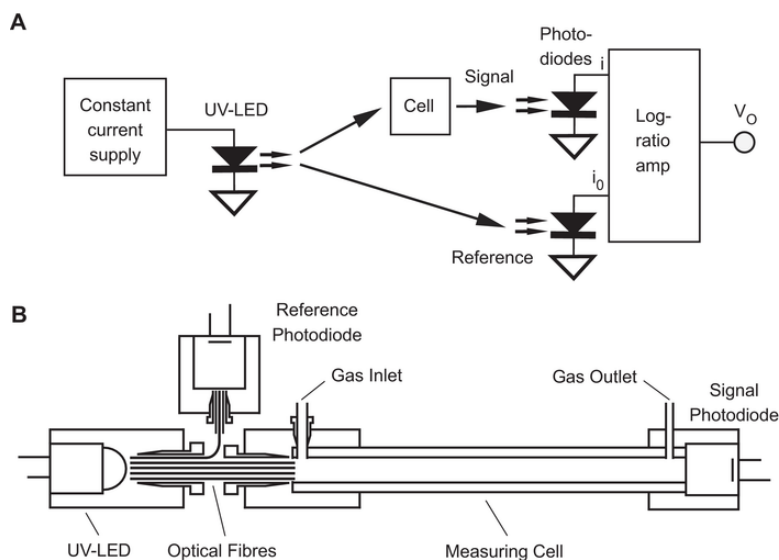


Fig. 2. Design of the detector. (A) Overview. (B) Mechanical arrangement (not drawn to scale).

for zero setting of the baseline and a low-pass filter with a 10 Hz cut-off frequency to remove high-frequency electronic noise. More details on the circuitry can be found in previous reports [24–27].

The optical and mechanical setup is detailed in Fig. 2B. One end of a 7 cm long bundle of 20 optical fibres was placed at a distance of 4 mm from the surface of the LED, which features a built in lens. Each fibre has an outer diameter of 370  $\mu\text{m}$  and the diameter of the resulting bundle was approximately 1.9 mm. A single fibre was directed to the reference photodiode, while the other 19 fibres of the bundle were placed at the inlet of a 40 cm long aluminium tube with an internal diameter of 2 mm, which served as a flow through detection cell. The signal photodiode was placed directly at the far end of this cell. All parts were aligned in precisely machined holders of high stability in order to minimize baseline shifts due to mechanical movements. The assembly was housed in a grounded metal case to exclude ambient light and electromagnetic interference on the circuitry. The case was lined with thermal insulating material to also minimize temperature fluctuations.

### 3.2. Spectral considerations

The emission band of the UV-LED and the absorption spectra of the BTEX species are shown in Fig. 3. As can be seen, the emission band of the LED with a bandwidth of approximately 12 nm (full width at half maximum), centred at 260 nm, represents a good compromise for the monitoring of the BTEX species. It closely matches the absorption maxima of the broad absorption bands of ethylbenzene (260 nm), toluene (261 nm), *o*-xylene (262 nm) and *m*-xylene (264 nm). It also overlaps with a flank of the broad band of the more strongly absorbing *p*-xylene which at 260 nm still has a maximum which is about 35–40% higher than that of the 4 species mentioned afore. Benzene, on the other hand, exhibits only a relatively weak and narrow absorption band at 260 nm.

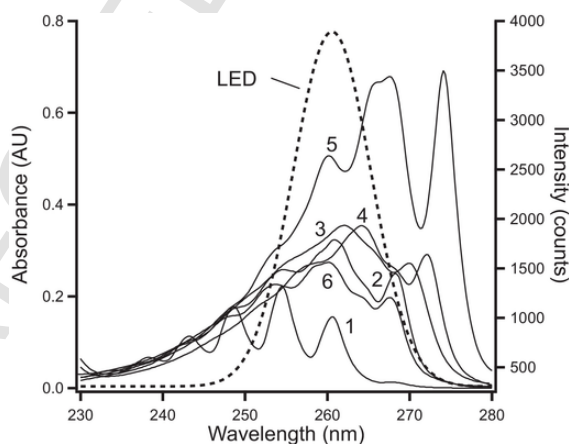


Fig. 3. Emission spectrum of the deep UV-LED (dashed line) and absorption spectra of the BTEX species in isoctane (solid lines): (1) benzene, (2) toluene, (3) *o*-xylene, (4) *m*-xylene, (5) *p*-xylene, (6) ethylbenzene (all 1.5 mM).

### 3.3. Calibration

The performance of detector was first evaluated with the absorption measurement of vapours produced from each of the BTEX species. As an example, measurements for toluene vapours between 550 ppb and 25.3 ppm are shown in Fig. 4. The measurement sequence started by flushing with pure nitrogen followed by the introduction of the vapours of the different concentrations for about 30–40 s and interspersed by flushing with nitrogen for 30 s. As can be seen from the inset of Fig. 4, illustrating the detection of 550 ppb toluene vapour at an expanded scale, the baseline noise, taken as the maximum deviations over a period of 60 s, was amounting to about 40  $\mu\text{AU}$ . Incidentally, this value is comparable to those obtained with

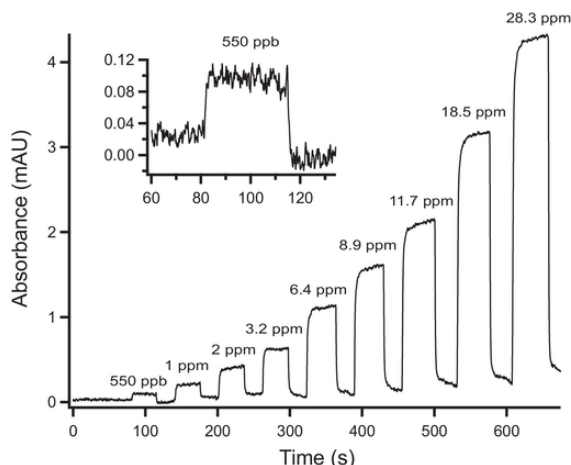


Fig. 4. Absorption measurements of toluene vapour. The inset shows an expanded view of the measurement for the 550 ppb dilution.

our earlier detector for capillary electrophoresis based on 255 and 280 nm UV-LEDs (50 and 53  $\mu$ AU respectively) for the same filter settings for the data recording (low pass with 2 Hz cut-off) and quantification method (peak-to-peak) [24]. This indicates that the performance in this regard is dictated by the optoelectronic and electronic setup.

Given in Table 1 is the quantitative data of measurements for the six BTEX species. The response was found to be linear for each species up to the highest concentration of 110 ppm measured and the correlation coefficients were determined to be 0.999 or better. This indicates a good adherence to Lambert-Beer's law and negligible levels of stray light and dark currents on the photodiodes. Evidently, the UV-LED based detector shows the highest sensitivity for *p*-xylene, while its sensitivity for benzene is lowest, and the other species showed relatively close values. This is in agreement with the expected from the spectral data discussed above. The reproducibilities are good and the detection limits, which are below 1 ppm, except for benzene, reflect the differences in sensitivity. The latter values compare well with the value of 13 ppm reported by Barber et al. [4] for benzene using a device based on a deuterium lamp and a monochromator and an optical path length of 30 cm. Also determined was the baseline drift, which was found to be typically in the range from 620 to 750  $\mu$ AU for periods of 15 min. Temperature instabilities are thought to be the reason for this behaviour. For critical determina-

Table 1  
Detection of BTEX Vapours.

Compound	Correlation coefficients ( $r^a$ )	Sensitivity <sup>b</sup> ( $\mu$ AU/ppm)	Reproducibility of absorbance values <sup>c</sup> (%)	LOD <sup>d</sup> (ppb)
Benzene	0.9990	62	2.3	1194
Toluene	0.9997	152	1.9	658
<i>o</i> -Xylene	0.9998	185	2.2	600
<i>m</i> -Xylene	0.9998	169	1.8	607
<i>p</i> -Xylene	0.9997	235	1.7	457
Ethylbenzene	0.9997	166	2.1	612

<sup>a</sup> 13 concentrations between 500 ppb and 110 ppm.

<sup>b</sup> As obtained from the regression equation.

<sup>c</sup> RSD,  $n = 5$ , determined at 5 ppm.

<sup>d</sup> Concentrations corresponding to signals whose values are 3 times higher than the baseline noise.

tions it is therefore desirable to establish the baseline inbetween measurements.

### 3.4. Verification

The response of the detector to BTEX was verified by measuring a 60 ppm BTEX standard consisting of 10 ppm each of benzene, toluene, *o*-xylene, *m*-xylene, *p*-xylene and ethylbenzene. The absorbance value of 9.55 mAU compares well with the value expected from the calibration data given in Table 1, *i.e.* the sum of the expected absorbance values for each of the compounds at 10 ppm, of 9.7 mAU. The deviation is less than 2%. The measurement for BTEX mixtures obtained by dilution from the 60 ppm standard showed good linearity with a correlation coefficient of 0.9990 (11 concentrations from 934 ppb–60 ppm). The response to the lower end of this calibration range is illustrated in Fig. 5. The reproducibility was determined as 1.8% (relative standard deviation,  $n = 5$ , for the dilution at 5.7 ppm). The LOD for the BTEX mixture was determined as 680 ppb.

## 4. Conclusions

It was found possible to construct a simple photometric detector for the BTEX species by employing a deep UV-LED and photodiodes. The detection limit of the device was by about one order of magnitude lower than that of an earlier reported instrument based on a conventional deuterium lamp and monochromator. The low power consumption allows the construction of battery based portable instruments for detections in which the utmost sensitivity is not required. While the detection limits of the device are not adequate for all applications its combination with a preconcentration system is also a possibility. If higher precision is desired, careful thermostating should be adopted. This would not only overcome a remaining temperature dependence of the optoelectronic setup, which presumably is the reason for the observed drifts, but also take care of a significant temperature effect on the absorption coefficients of the analytes [3].

## Acknowledgements

Duy Anh Bui gratefully acknowledges the Canton of Basel City for financial support. The authors are also expressing their gratitude

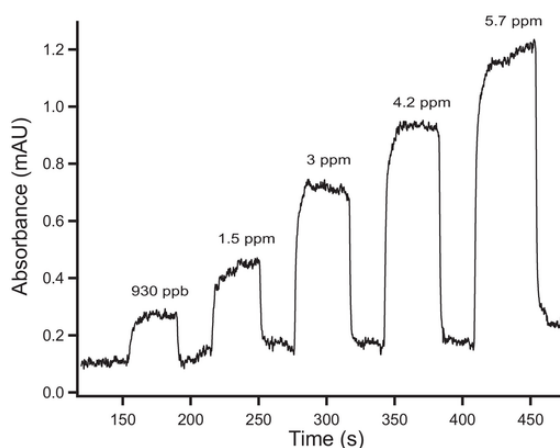


Fig. 5. Absorption measurements of dilutions of the BTEX standard mixture. The concentration values refer to the total concentration of the 6 compounds.

to Yoel Koenka for help with setting up the mass-flow controller software.

## References

- [1] R. Volkamer, T. Etzkorn, A. Geyer, U. Platt, Correction of the oxygen interference with UV spectroscopic (DOAS) measurements of monocyclic aromatic hydrocarbons in the atmosphere, *Atmos. Environ.* 32 (1998) 3731–3747.
- [2] J. Dewulf, H. VanLangenhove, Analytical techniques for the determination and measurement data of 7 chlorinated C-1- and C-2-hydrocarbons and 6 monocyclic aromatic hydrocarbons in remote air masses: an overview, *Atmos. Environ.* 31 (1997) 3291–3307.
- [3] D.D. Tunnicliff, R.R. Brattain, L.R. Zumwalt, Benzene, toluene ethylbenzene, o-xylene, m-xylene and p-xylene, determination by ultraviolet spectrophotometry, *Anal. Chem.* 21 (1949) 890–894.
- [4] T.E. Barber, W.G. Fisher, E.A. Wachter, Online monitoring of aromatic hydrocarbons using a near-ultraviolet fiber optic absorption sensor, *Environ. Sci. Technol.* 29 (1995) 1576–1580.
- [5] Y. Ueno, T. Horiuchi, T. Morimoto, O. Niwa, Microfluidic device for airborne BTEX detection, *Anal. Chem.* 73 (2001) 4688–4693.
- [6] A. Allouch, S. Le Calvé, C.A. Serra, Portable, miniature, fast and high sensitive real-time analyzers: BTEX detection, *Sens. Actuators B* 182 (2013) 446–452.
- [7] H. Flaschka, C. McKeithan, R. Barnes, Light emitting diodes and phototransistors in photometric modules, *Anal. Lett.* 6 (1973) 585–594.
- [8] M. Macka, T. Piasecki, P.K. Dasgupta, Light-emitting diodes for analytical chemistry, *Annu. Rev. Anal. Chem.* 7 (2014) 183–207.
- [9] D.A. Bui, P.C. Hauser, Analytical devices based on light-emitting diodes—a review of the state-of-the-art, *Anal. Chim. Acta* 853 (2015) 46–58.
- [10] S.F. Johnston, Gas monitors employing infrared leds, *Meas. Sci. Technol.* 3 (1992) 191–195.
- [11] B.A. Matveev, G.A. Gavrilov, V.V. Evstropov, N.V. Zotova, S.A. Karandashov, G.Y. Sotnikova, N.M. Stus, G.N. Talalakin, J. Malinen, Mid-infrared (3–5  $\mu\text{m}$ ) LEDs as sources for gas and liquid sensors, *Sens. Actuators B* 39 (1997) 339–343.
- [12] A.A. Popov, M.V. Stepanov, V.V. Sherstnev, Y.P. Yakovlev, 3.3- $\mu\text{m}$  LEDs for measuring methane, *Tech. Phys. Lett.* 23 (1997) 828–830.
- [13] B. Matveev, M. Aidaraliev, G. Gavrilov, N. Zotova, S. Karandashov, C. Sotnikova, N. Stus, G. Talalakin, N. Il'inskaya, S. Aleksandrov, Room temperature InAs photodiode-InGaAs LED pairs for methane detection in the mid-IR, *Sens. Actuators B* 51 (1998) 233–237.
- [14] A. Krier, V.V. Sherstnev, Powerful interface light emitting diodes for methane gas detection, *J. Phys. D: Appl. Phys.* 33 (2000) 101–106.
- [15] M. Fowles, R.P. Wayne, Ozone monitor using an led source, *J. Phys. E: Sci. Instrum.* 14 (1981) 1143–1145.
- [16] S. Schorsch, J. Kiefer, A. Leipertz, Z.S. Li, M. Alden, Detection of flame radicals using light-emitting diodes, *Appl. Spectrosc.* 64 (2010) 1330–1334.
- [17] E. Hawe, C. Fitzpatrick, P. Chambers, G. Dooly, E. Lewis, Hazardous gas detection using an integrating sphere as a multipass gas absorption cell, *Sens. Actuators A* 141 (2008) 414–421.
- [18] M. Degner, N. Damaschke, H. Ewald, S. O'Keefe, E. Lewis, UV LED-based fiber coupled optical sensor for detection of ozone in the ppm and ppb range, *IEEE Sens. Conf.* 9 (2009) 5–9 (9).
- [19] L.E. Kalnajs, L.M. Avallone, A novel lightweight low-Power dual-Beam ozone photometer utilizing solid-State optoelectronics, *J. Atmos. Ocean. Technol.* 27 (2010) 869–880.
- [20] Y. Aoyagi, M. Takeuchi, K. Yoshida, M. Kurouchi, T. Araki, Y. Nanishi, H. Sugano, Y. Ahiko, H. Nakamura, High-sensitivity ozone sensing using 280 nm deep ultraviolet light-emitting diode for detection of natural hazard ozone, *J. Environ. Prot.* 3 (2012) 5.
- [21] M. Degner, N. Damaschke, H. Ewald, E. Lewis, Real time exhaust gas sensor with high resolution for onboard sensing of harmful components, *IEEE Sens. Conf.* 97 (2008) 3–97 (6).
- [22] I.J. Koenka, J. Sáiz, P.C. Hauser, Instrumentino: an open-source modular Python framework for controlling Arduino based experimental instruments, *Comput. Phys. Commun.* 185 (2014) 2724–2729.
- [23] I.J. Koenka, J. Sáiz, P.C. Hauser, Instrumentino: an open-source software for scientific instruments, *Chimia* 69 (2015) 172–175.
- [24] D.A. Bui, P.C. Hauser, Absorbance detector for capillary electrophoresis based on light-emitting diodes and photodiodes for the deep-ultraviolet range, *J. Chromatogr. A* 1421 (2015) 203–208.
- [25] D.A. Bui, P.C. Hauser, Absorbance measurements with light-emitting diodes as sources: silicon photodiodes or light-emitting diodes as detectors?, *Talanta* 116 (2013) 1073–1078.
- [26] D.A. Bui, B. Bomastyk, P.C. Hauser, Absorbance detector based on a deep UV light emitting diode for narrow-column HPLC, *J. Sep. Sci.* 36 (2013) 3152–3157.
- [27] B. Bomastyk, I. Petrovic, P.C. Hauser, Absorbance detector for high-performance liquid chromatography based on light-emitting diodes for the deep-ultraviolet range, *J. Chromatogr. A* 1218 (2011) 3750–3756.

**Duy Anh Bui** obtained his MSc in Environmental Sciences from the Hanoi University of Science (Hanoi, Vietnam) with an interest in soil and water contaminations. From 2011 to 2013 he joined the Analytical and Bioanalytical Sciences research group at the University of Basel (Switzerland) as an exchange student with a focus on applications of deep UV-LEDs for miniature analytical devices. Since September 2013 he has been pursuing his PhD at the University of Basel.

**Peter C. Hauser** carried out his undergraduate studies in Switzerland and then obtained a MSc at the University of British Columbia (UBC) under Prof. M. W. Blades (1985), followed by a PhD at LaTrobe University (Melbourne, Australia) under Prof. R. W. Catrall (1988). Following a lectureship at Auckland University (New Zealand) in 1996 he took up his current position as Associate Professor at the University of Basel. His research interests in the analytical sciences have always included electronic aspects and he has been designing analytical devices employing LEDs since the 1980s.

## **Appendix**

### **Review:**

**Analytical devices based on light-emitting diodes - a review of the state-of-the-art**

*Analytica Chimica Acta (2015), 853, 46-58*



Review

# Analytical devices based on light-emitting diodes – a review of the state-of-the-art



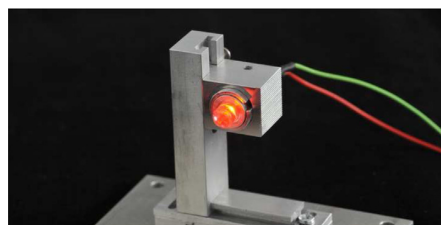
Duy Anh Bui, Peter C. Hauser\*

Department of Chemistry, University of Basel, Spitalstrasse 51, 4056 Basel, Switzerland

## HIGHLIGHTS

- A review of the current status of the use of LEDs in analytical devices is given.
- Fundamental aspects with relevance to quantitative measurements are discussed.
- A broad overview of the reported applications is given.

## GRAPHICAL ABSTRACT



## ARTICLE INFO

### Article history:

Received 1 July 2014

Received in revised form 22 September 2014

Accepted 25 September 2014

Available online 28 September 2014

### Keywords:

Light-emitting diode

Analytical devices

Review

Photodiode

Absorbance

Fluorescence

## ABSTRACT

A general overview of the development of the uses of light-emitting diodes in analytical instrumentation is given. Fundamental aspects of light-emitting diodes, as far as relevant for this usage, are covered in the first part. The measurement of light intensity is also discussed, as this is an essential part of any device based on light-emitting diodes as well. In the second part, applications are discussed, which cover liquid and gas-phase absorbance measurements, flow-through detectors for chromatography and capillary electrophoresis, sensors, as well as some less often reported methods such as photoacoustic spectroscopy.

© 2014 Elsevier B.V. All rights reserved.

## Contents

1. Introduction	47
2. Fundamental considerations	48
2.1. Characteristics of LEDs	48
2.2. Detection of light	50
2.2.1. Detection devices	50
2.2.2. Intensity measurements	50
2.2.3. Measurement of absorbance	51
3. Applications	52

Abbreviations: LED, light-emitting diode; IR, infrared; LDR, light-dependant resistor; PMT, photo-multiplier tube; PEDD, paired emitter detector diodes; AU, absorbance unit; ADC, analogue-to-digital convertor.

\* Corresponding author. Tel.: +41 61 267 1003; fax: +41 61 267 1013.

E-mail address: [peter.hauser@unibas.ch](mailto:peter.hauser@unibas.ch) (P.C. Hauser).

<http://dx.doi.org/10.1016/j.aca.2014.09.044>

0003-2670/© 2014 Elsevier B.V. All rights reserved.



3.1.	Molecular absorption spectrometry	52
3.1.1.	Batch measurements	52
3.1.2.	Titrations	52
3.1.3.	Flow systems	53
3.1.4.	Chromatography	53
3.1.5.	Absorption detection in capillaries/capillary electrophoresis	53
3.1.6.	Gas phase	54
3.2.	Fluorescence	54
3.3.	Membrane based sensors	55
3.4.	Microfluidic devices	55
3.5.	Photoacoustics	56
3.6.	Other applications	56
4.	Conclusions	56
	Acknowledgments	56
	References	56



**Duy Anh Bui** obtained his MSc in Environmental Sciences from the Hanoi University of Science (Hanoi, Vietnam) with an interest in soil and water contaminations. From 2011 to 2013 he joined the Analytical and Bioanalytical Sciences research group at the University of Basel (Switzerland) as an exchange student with a focus on applications of deep-UV-LEDs for miniature analytical devices. Since September 2013 he has been pursuing his PhD at the University of Basel.



**Peter C. Hauser** carried out his undergraduate studies in Switzerland and then obtained an MSc at the University of British Columbia (UBC) under Prof. M.W. Blades (1985), followed by a PhD at LaTrobe University (Melbourne, Australia) under Prof. R.W. Cattrall (1988). Following a lectureship at Auckland University (New Zealand) in 1996 he took up his current position as Associate Professor at the University of Basel. His research interests in the analytical sciences have always included electronic aspects and he has been designing analytical devices employing LEDs since the 1980s.

## 1. Introduction

Light-emitting diodes became commercially available in the 1960s [1]. The early devices emitted red light and this was followed by the introduction of LEDs of shorter wavelengths, i.e. orange, yellow and green. Blue LEDs were first sold in the mid-1980s, near-UV (ultraviolet) devices at 370 nm in about 2000 and only in recent years deep-UV devices, i.e. with wavelengths below 320 nm, have become available. Currently LEDs with wavelengths down to 240 nm can be obtained commercially. The shorter the wavelength, the higher the energy, which requires the more difficult creation of semiconductor junctions with higher bandgaps. Along with the move to lower wavelengths has also been a trend to higher intensities. Parallel to these developments occurred an extension to longer wavelengths, so that now devices with wavelengths up to about 4.6  $\mu\text{m}$  in the mid-IR (infrared) range are also available commercially.

The general applications of LEDs are manifold. Prominent is their use as indicating lights for electronic circuitry, but increasingly LEDs are also used for lighting applications, in particular in form of white light emitting devices (which either contain a fluorescent compound to achieve wide band emission or a combination of LED substrates of different colours). Invisible near-IR LEDs are used for remote controls and automatic door openers, and also, along with semiconductor lasers, for fibre optic telecommunications. Near-UV-LEDs are used for examination of banknotes for forgery and invisible owner markings. Deep-UV-LEDs have potential for use in disinfection. The brightest visible LEDs now have such intensity that radio amateurs were able to demonstrate audio communications links based on the transmission of the modulated light of single LEDs over free space through distances of 83 km during daytime [2] and 167 km at night [3].

The development of applications of LEDs in analytical chemistry naturally has followed the progression in wavelengths and intensity. The first report on an analytical LED device appears to

be a publication by Flaschka et al. [4]. The photometric instrument was based on a red LED and a phototransistor [4]. Analytical devices based on blue LEDs were first reported in about 1986 [5], while first instruments employing deep-UV-LEDs were reported about 5 years ago [6,7]. The development of deep-UV-LEDs is very significant for analytical applications as most organic molecules absorb in this range, but not in the near-UV or visible wavelength regions. LEDs in the IR range have been found to be most useful for the detection of small gas molecules such as  $\text{CO}_2$ . Many of the reported devices based on LEDs are low cost alternatives to commercial instruments, but on the other hand, due to the inherent properties of the LEDs, well designed devices are capable of delivering the highest performance, often surpassing that of instruments based on conventional light sources.

The use of LEDs in analytical devices has been reviewed repeatedly. As the field is very wide, most of these have been focussed on specific areas, but there are some more general overviews. Dasgupta et al. in 1993 [8] wrote a review concerning absorption measurements in flow through detectors based on LEDs, and again in 2003 [9] covered the topic with the inclusion of fluorescence and spectroelectrochemical techniques. Capitán-Valvey and Palma have summarized developments in handheld and portable analytical instruments based on optical sensing [10]. Their review does not exclusively cover LED-based devices, but due to their utility for battery operated portable instruments, they feature very prominently. O'Toole and Diamond have reviewed sensors and sensing devices based on absorbance measurements with LEDs in 2008 [11]. During the preparation of this article a further review by Dasgupta and coauthors has appeared which is focussed mainly on the developments of absorbance and fluorescence measurements in liquids with LEDs over the period from 2008 to 2013 [12]. The interested reader is advised to also consult this complementary publication.

This review is intended to give a broad overview of the state-of-the-art concerning analytical uses of LEDs. Fundamentals are

covered as far as relevant for the basic construction of analytical devices, without delving into the underlying semiconductor physics. Given the breadth of the subject it naturally cannot comprehensively cover all publications in the field. Often publications are cited as examples to illustrate a point, but it should not be taken to imply that there are not other equally valid publications as well. Not discussed are applications of LEDs in chemistry in general, such as for decomposition of molecules or curing epoxies. Also not discussed are purely physical sensing and detection with LEDs, nor are laser diodes.

## 2. Fundamental considerations

### 2.1. Characteristics of LEDs

A photograph of an LED in the most common package is shown in Fig. 1. This is referred to as a 5 mm, or T-1 3/4, package. The latter denotation stems from an earlier standard for tungsten filament lamps and corresponds to its diameter as a multiple of 1/8th of an inch [13]. The light originates from the semiconducting material contained in a reflective cup in the centre on top of one of the connecting leads. Note that there is a very thin wire contacting the semiconducting material from the top, which is connected to the second lead. The entire assembly is encapsulated in an epoxy resin. Different forms are available, such as miniature types, surface mount variants, or special high power versions. All forms have in common a much higher degree of robustness and miniaturization than the common light sources used in analytical instruments, which are usually either incandescent light bulbs or discharge lamps. The dome of the standard package shown in Fig. 1 forms a lens and disperses the light. LEDs with narrow or wider beam angles are available according to their intended purposes. For analytical applications it is usually not desirable to have the light dispersed but it should be focussed or collimated. It is possible to cut off the dome, followed by polishing of the surface, in order to get closer access to the emitter, but one must be careful not to break the top connecting wire in the process. Such polished LEDs are well suited for coupling to optical fibres, in particular the plastic fibres with 1 mm diameter. The latter corresponds to a readily available standard. However, tight focussing, e.g. for detection on capillaries or coupling into narrower optical fibres, or good collimation of the light, is difficult as the emitting substrates are not point sources. Ball lenses may be the best option for narrow focussing.



**Fig. 1.** Photograph of a blue LED in the common 5 mm package. The emitting chip is contained in the well on top of the pin on the right. The dome acts as a lens to disperse the light.

Other advantages are high current efficiency and therefore low heat production, which in turn reduces intensity drifts. Further advantageous features compared to conventional light sources used in analytical instruments are long lifetimes, and low cost. All these attributes make them attractive for use in analytical instrumentation, in particular for low power portable devices. A further important aspect, which strongly distinguishes LEDs from conventional light sources employed in analytical instruments, is the restriction of the emission to bands of typically 30 nm in width. This wavelength limitation further improves the efficiency of the light source. Note that, in contrast, laser diodes have much narrower emission lines. The emission spectra of a selection of LEDs covering the range from about the shortest currently available wavelength of 255 nm to about 900 nm are shown in Fig. 2. LEDs for wavelengths much further into the IR are also available. The emission bands are usually clean, but deep-UV-LEDs may also show spurious emissions at longer wavelength which would have to be considered in the design of a device. The wavelength selectivity is often the most important ground for choosing LEDs as light sources in instrumentation as this can eliminate a costly monochromator, which is generally needed with conventional lamps, and few other light sources with inherent wavelength restriction are available. Generally a good match of the emission bands of the LEDs with the broad absorbance bands of molecules can be obtained. On the other hand, of course, such a fixed emission band can also be a limitation. This can, to some extent, be overcome by the use of switchable LED arrays [14–16], while still benefitting from the other advantages of the LEDs. In recent years white LEDs have also become available. Some of these devices are based on the combination of three different substrates emitting the three primary colours. By balancing the intensities the impression of white light is achieved. A second type of white LEDs is based on the combination of a short wavelength emitter with an embedded fluorescent material to achieve emission over a wider wavelength range. Both types appear white to the human eye, but show gaps in the emission spectra. If used for analytical instruments a wavelength dispersive element would normally be required, as with a more conventional light source, and one would have to be aware of the gaps in the emission.

A further advantage is the possibility for fast switching. This feature is made use of in infrared remote controls and fibre optic communications, and bandwidths well into the MHz range are

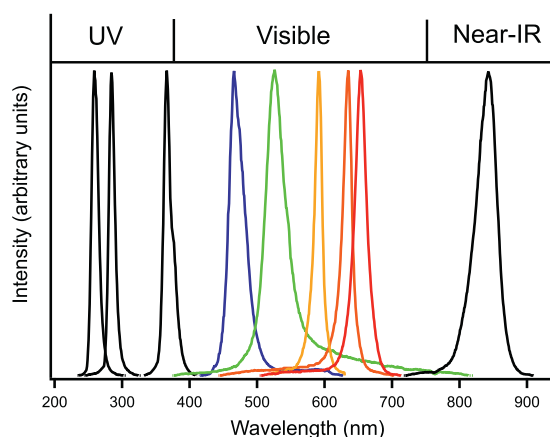


**Fig. 2.** Emission spectra of a selection of LEDs from the deep UV to the near IR. UV: 255 nm, 280 nm, 365 nm. Visible: blue at 464 nm, green at 516 nm, amber at 590 nm, red at 635 nm, dark red at 645 nm. IR: 850 nm.

possible [1]. This characteristic is also of interest when employing LEDs in analytical instrumentation as this means that for modulation of the light intensity it is not necessary to employ mechanical beam choppers, as is usually the case with conventional light sources due to their slow response, but this can be done with electronic oscillators. This is useful for lock-in amplification, e.g. for the suppression of ambient light interference, or for lifetime measurements in fluorescence.

Light-emitting diodes are non-linear devices and show the typical logarithmic current vs. voltage characteristics ( $i/V$ -curve) of a diode shown in Fig. 3. This means that they cannot be operated directly from a voltage source as slight changes in the supply voltage or drifts in the junction voltage (such as those due to temperature changes) can cause not only pronounced changes in output intensity, but may also lead to catastrophic failure of the device. Therefore they should be driven with a constant current source, rather than the common constant voltage source. Usually this is approximated by using a higher voltage and a current limiting resistor. For more precise operation it is better to use an active current control which can easily be achieved with a LM317 voltage regulator integrated circuit in the appropriate configuration, or an operational amplifier, as shown in Fig. 4. Other approaches are possible. The use of such a circuitry is particularly important when the voltage drop across the diode is very high, as is the case for deep-UV-LEDs (about 7 V), and it is driven from a standard low voltage source.

It should be noted, that, while the use of a constant current source reduces the temperature dependence of the output intensity of the LEDs, this effect is far from being perfect as shown in Fig. 5. Measurements for three LEDs of different colours operated with a current limiting resistor and with a constant current source are shown and it can be seen that the temperature stability is only slightly better for the constant current operation. The reason for this must be the fact that with temperature not only the voltage drop across the diode (and with it the current when operated with a current limiting resistor) changes, but also the conversion efficiency of the LED [1]. When good precision is required, it is therefore necessary to compensate for intensity drifts due to temperature changes by using a referenced measuring approach. Stable output intensities can also be achieved by using a servo circuitry which makes use of a photodiode for monitoring. Some commercially available LEDs even include a monitor photodiode in the same case. However, temperature changes may also cause a spectral drift, and for high precision work it may therefore be necessary to control the temperature of the LED with a Peltier (thermoelectric) element. A detailed discussion of the temperature dependence of LEDs and options for compensation can be found in Dasgupta et al. [9].

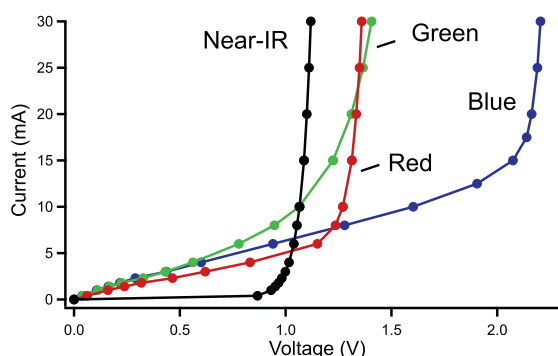


Fig. 3.  $i$ - $V$  curves determined for LEDs of different colours.

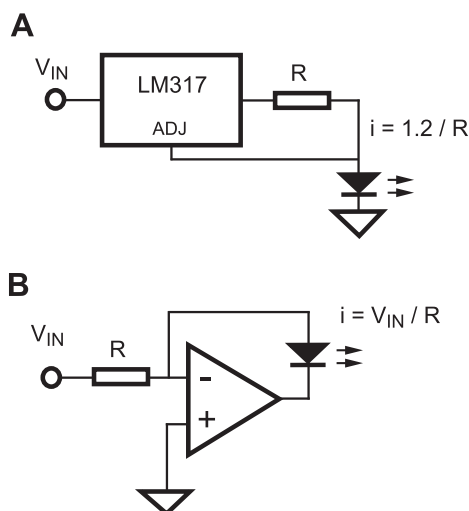


Fig. 4. Constant current circuitries for use with LEDs. (A) Based on the LM317 adjustable voltage regulator integrated circuit. (B) Based on an operational amplifier.

LEDs of vastly different intensities are available. Power LEDs for lighting applications can have optical output powers of up to several Watts (available e.g. from Avago, Philips Lumileds, King-bright or Osram Opto Semiconductors). However, at the far ends of

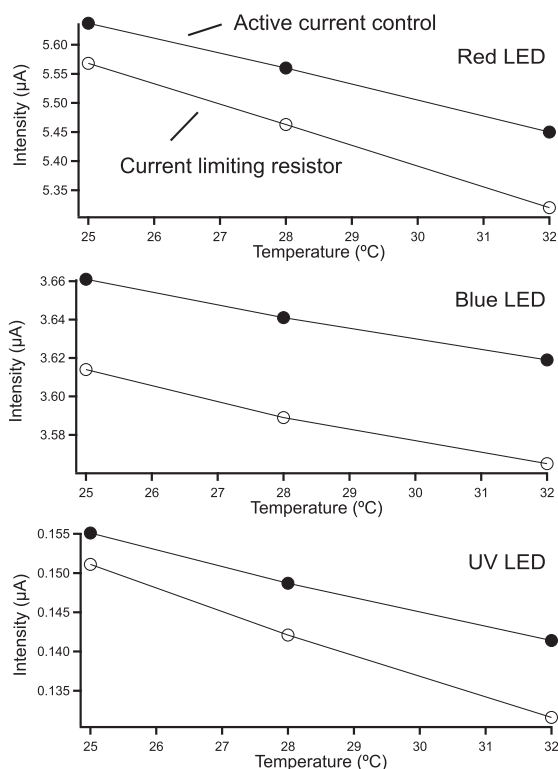


Fig. 5. Temperature dependencies measured for a red, blue and UV (365 nm) LED when operated either with a current limiting resistor from a fixed voltage supply of 5 V, or with a constant current supply according to the circuitry of Fig. 4A.

the spectrum covered by LEDs, *i.e.* the IR range above 3  $\mu\text{m}$  and the deep UV below 300 nm the maximum available output powers drop to the  $\mu\text{W}$  range (see for example [www.roither-laser.com](http://www.roither-laser.com)). Note that the intensities for visible LEDs are usually specified as luminous intensity (with the units of Candela, cd), which is a measure of the brightness as perceived by the human eye, *i.e.* it takes into account the dispersion of the light by the body of the LED and the wavelength dependence of the eye sensitivity.

## 2.2. Detection of light

### 2.2.1. Detection devices

When using LEDs as light sources in analytical devices it is also necessary to employ detectors for light. The exception are the thermo-optic methods. One of these is photoacoustic sensing, which is discussed in a later section. A discussion of the use of LEDs is not complete without a consideration of the other half of the set-up. In keeping with the simplicity of the LEDs photodiodes based on semiconductor p/n-junctions are usually employed. In these devices an annihilation of charge carriers occurs at the interface, but the absorption of photons releases the charges. The principle is the same as for photovoltaic cells employed for the production of electricity from sunlight. For visible, and immediately adjacent wavelengths Si-photodiodes work best. In construction, photodiodes are very similar to LEDs, they are solid state and small. Well performing devices can be obtained for as little as about 1 euro and these are therefore as inexpensive as the cheapest LEDs. Special devices, in precision cases, with extra low dark current (background signal when no light is present) or specific wavelength sensitivities, will, of course, be more expensive. Standard Si-photodiodes have a maximum in sensitivity close to 1000 nm, but as dictated by the bandgap of the junction a sharp cut-off at 1100 nm. For use in the UV below about 300 nm, special types with UV-transparent windows are needed. Several alternatives are available for the deep-UV range between about 200 nm and 300 nm, based on SiC, GaN, GaP or TiO<sub>2</sub>. For the IR-range photodiodes based on InGaAs, InAs, InSb or HgCdTe are available. They all have different intrinsic spectral sensitivities and must be chosen according to the wavelength range of interest for the application at hand. Some devices have been designed to cover only relatively narrow bands, and may contain optical filters, such as to allow the determination of the intensities of the UV-A, UV-B and UV-C ranges related to sun-light.

When very low intensities must be measured the more complex and more expensive photomultiplier tubes (PMT) may be employed. The combination of LEDs with PMTs is rare, but an example is a detector for capillary electrophoresis based on a deep-UV-LED which was only available with low intensity [17]. In practice the use of PMTs does not have to be difficult as simple modules which include all the necessary electronics are available. Phototransistors also have higher sensitivities than photodiodes, but are not well suited for reproducible intensity measurements. Note, that also light dependant resistors (LDR) can be used to measure light intensity. These are junctionless semiconductor devices which change their resistance in dependence of the light intensity. The performance of these components is inferior to that of photodiodes, due to non-linearity, hysteresis and slow response times, and they should not be used in modern devices.

While photodiodes do not emit light when a current is passed through, it has been known that LEDs also behave like photodiodes [18], although at lower sensitivity than real photodiodes [8]. An intriguing fact is that the sensitivity of LEDs when used as detectors is limited to a rather narrow wavelength range, with a width similar to their emission bands. But note that the sensitivity is shifted to lower wavelengths compared to their emission. The wavelength selectivity has been made use of in the

construction of inexpensive instruments where this is needed, *i.e.* for sun light spectrometers [18] and crop monitors [19]. Berry et al. have constructed a molecular absorption spectrometer based on a tungsten broadband emitter and an array of different LEDs as detectors to achieve wavelength selectivity [20]. However, when the wavelength selectivity in an analytical device is already determined by the employment of an LED as source, the use of an LED instead of a photodiode for detection has no clear general benefit, in particular when considering that well performing photodiodes can be obtained for a cost as low as that of inexpensive LEDs. For a detailed discussion and a comparison of the performance of LEDs used as detectors vs. photodiodes see [21]. Nevertheless the combination of two LEDs for analytical devices, one used as source, the other as detector, has been reported repeatedly and has been termed PEDD (paired emitter detector diodes) (see for example [22–24]). An interesting application of the use of LEDs for detection, other than for analytical instrumentation, is in bi-directional digital communication over light where the LEDs alternately function as emitters and as detectors [25].

### 2.2.2. Intensity measurements

A signal may be obtained from photodiodes in different modes of operation. These can be distinguished fundamentally between current measurements (the photocurrent mode) or voltage measurements (the photovoltaic mode) [26]. The photocurrent is proportional to light intensity, while in the photovoltaic mode a logarithmic response is obtained. For quantitative measurements the photocurrent mode is generally preferred as the photovoltaic mode has a poorer precision, mainly caused by a significant temperature dependence. The photocurrent can easily be measured with the help of an operational amplifier in the current-to-voltage convertor (or current follower) configuration as shown in Fig. 6A. The output voltage of the amplifier is then proportional to the light intensity. In the photovoltaic mode shown in Fig. 6B, the diode voltage is measured, usually with an operational amplifier as a buffer to avoid loading, *i.e.* drawing a significant current from the photodiode. A further, indirect approach is also possible [27]. The photodiode is first reverse biased, that is a voltage is applied in the polarity which is blocked by the device, in order to charge its intrinsic junction capacitance. In the second step the voltage source is disconnected, and the remaining voltage across the device is monitored. As the junction capacitance is discharged by the photocurrent, the time for decay of the voltage is dependant on the light level. While this appears to

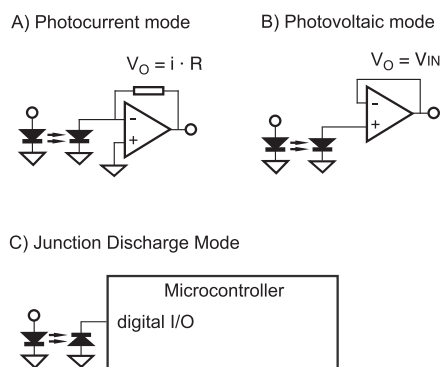


Fig. 6. The different reported modes of measuring light intensities with photodiodes.

be rather complicated, the approach can be implemented easily, essentially in software, using a digital input–output pin of a modern microcontroller without requiring any additional circuitry as illustrated in Fig. 6C. The method has also been employed with LEDs used as detectors [28]. Special photodiodes are also available, such as avalanche photodiodes for low light level measurements, photodiodes with built in amplifiers, and photodiodes with a built in circuitry that gives a light level dependant frequency output for ease of interfacing with a microcontroller. Interference by ambient light can be overcome by intensity modulation of the LED and lock-in detection. This does not need to be complicated, nor expensive, as it can be implemented with a synchronous detector available as an integrated circuit [29,30].

### 2.2.3. Measurement of absorbance

Analytical measurements based on the absorption of light by the analyte make use of the absorbance ( $A$ ) parameter, which is directly related to concentration ( $c$ ), but obtained only indirectly from the light intensities before ( $I_0$ ) and after ( $I$ ) passage through the absorbing material as described by the well known Lambert–Beer law:

$$A = \log \frac{I_0}{I} = \varepsilon \times b \times c \quad (1)$$

$\varepsilon$  is the molar absorptivity coefficient of the analyte, and  $b$  the optical pathlength.

If the light intensities are measured with photodiodes, the intensities ( $I_0$  and  $I$ ) are converted to currents ( $i_0$  and  $i$ ), and therefore in practice the absorbance is then given by:

$$A = \log \frac{i_0}{i} \quad (2)$$

The Lambert–Beer law in the common form is, however, strictly only true for monochromatic radiation. For non-monochromatic light sources an extended form of the equation is applicable, which takes into account the variation of the intensity ( $I_0$ ) of the source, of the detector sensitivity ( $S$ ) and of the absorptivity ( $\varepsilon$ ) across the wavelength ( $\lambda$ ) band of the source:

$$A = \log \frac{i_0}{i} = \log \frac{\int_{\lambda_0}^{\lambda_1} S(\lambda) \times I_0(\lambda) d\lambda}{\int_{\lambda_0}^{\lambda_1} S(\lambda) \times I_0(\lambda) \times 10^{-\varepsilon(\lambda)bc} d\lambda} \quad (3)$$

As illustrated in Fig. 7, this can in practice lead to more or less strongly pronounced non-linear calibration curves when LEDs are employed for absorbance measurements. The deviation from linearity depends on how well the absorbance bands are matched with the LED emission spectra. If the molar absorptivity,  $\varepsilon$ , varies only slightly across the emission band of the LED, then the deviation from linearity is usually small. For this reason the two spectra should be compared carefully when choosing an LED for a given application. A further discussion of this effect can be found in Macka et al. [31] as well as in two of our earlier publications [16,32].

Absorbance measurements are best implemented with a log ratio amplifier as illustrated in Fig. 8. These amplifiers give an output voltage ( $V_O$ ) that is logarithmically related to the ratio of two input currents ( $i_1$  and  $i_2$ ):

$$V_O \approx \log \frac{i_1}{i_2} \quad (4)$$

As shown in the figure, two photodiodes, one of which provides the reference signal, can be connected directly in the photocurrent mode to the log ratio amplifier. The output voltage represents directly Absorbance,  $A$ , i.e. typically 1 V equals an absorbance of 1 (or 1 absorbance unit, 1 AU). The referenced approach will

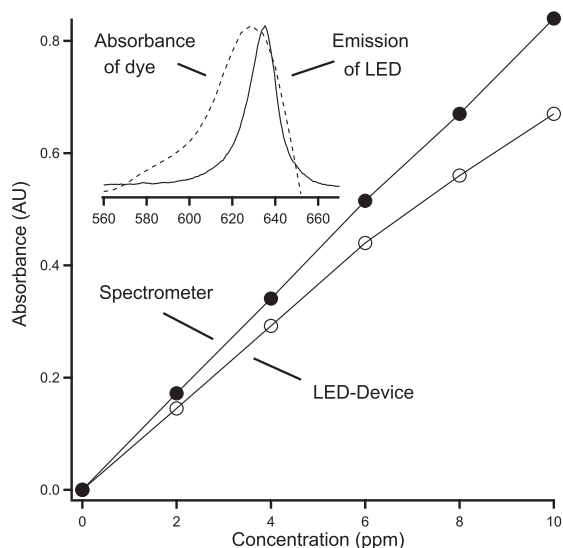


Fig. 7. Absorbances measured for methyl green measured with a device based on a red LED and a photodiode against absorbances measured with a conventional spectrometer. The non-linearity is a violation of Lambert–Beer's law, occurs despite the peaks of absorbance and emission being very close ( $\lambda_{\max} = 629$  nm and 635 nm), and is due mainly to the changing absorptivity of the dye across the emission spectrum of the LED.

significantly reduce drifts such as those caused by temperature changes, but can, of course, not completely eliminate them. Residual drifts between  $0.3 \text{ mAU h}^{-1}$  and  $5 \text{ mAU h}^{-1}$  were reported, for example, by Bomastyk et al. for such an arrangement [32]. Absorbances down to the low  $\mu\text{AU}$  level can be measured with a log ratio amplifier and short term noise levels as low as about  $10 \mu\text{AU}$  are readily possible [32]. Integrated logarithmic amplifiers used to be fairly expensive, and thus not suitable for the low-cost applications typical for many of the reported analytical uses of LEDs, but they are now available for about 10–20 US\$ when sourced through catalogue distributors. Log amps suitable for absorbance measurements are presently available from at least three suppliers (Texas Instruments, Analog Devices and Maxim Integrated). Note, that for absorbance measurements there is not much to be gained by using LEDs with intensities higher than average (due to the ratio measurement). Shot noise would ultimately be obtained for low light levels, but even the low intensities of current deep-UV-LEDs are far from this limit [33].

For less demanding applications the reference photodiode can be omitted, but the log amplifier is still useful for carrying out the logarithmic conversion demanded by Lambert–Beer's law. Again for unexacting tasks a logarithmic signal that is inversely

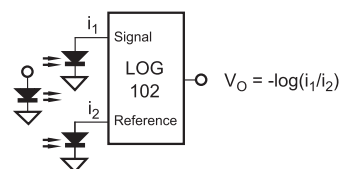


Fig. 8. The use of a log-ratio amplifier to obtain a voltage signal that directly represents absorbance.

proportional to absorbance may also be obtained by using a photodiode in the photovoltaic mode. As has been shown by Bui and Hauser [21] for a LED–photodiode pair this measurement may be carried out directly with a multimeter, instead of a circuitry based on an operational amplifier, as the load by such a standard voltmeter was found tolerable. A variation of this approach is suggested here. Most microcontrollers, such as the AVR-series from Atmel employed on the open source Arduino electronics platform ([www.arduino.cc](http://www.arduino.cc)) include an analogue-to-digital convertor (ADC). It is possible to directly connect a photodiode to such an input in order to carry out measurements in the photovoltaic mode, an approach which to our knowledge has not been reported before. The results of such measurements are shown in Fig. 9.

For many of the devices intended for absorption measurements reported in the literature a logarithmic conversion has not been implemented and simply a measurement of light intensity has been used. This parameter is proportional to Transmittance,  $T$ , which does not have a linear relationship to concentration. It is, of course, to some extent possible to work with non-linear calibration curves, and furthermore, for a limited concentration range (corresponding to small maximal absorbances) the deviation from linearity may be tolerable (see also the discussion by Dasgupta et al. [8]).

### 3. Applications

#### 3.1. Molecular absorption spectrometry

##### 3.1.1. Batch measurements

The photometric determination of metal ions following their complexation with colour forming reagents is versatile and widely used and several common anions can also be determined with this long established technique. The absorption bands of molecules, and of the metal complexes, are generally broad and therefore can be well matched to the emission bands of LEDs. However, surprisingly few of the original publications on molecular absorption measurements with LEDs as light source deal with the construction of photometers for batchwise measurements, *i.e.* with replacements of standard photometers. A reason for this must be the appeal of LEDs for miniaturization

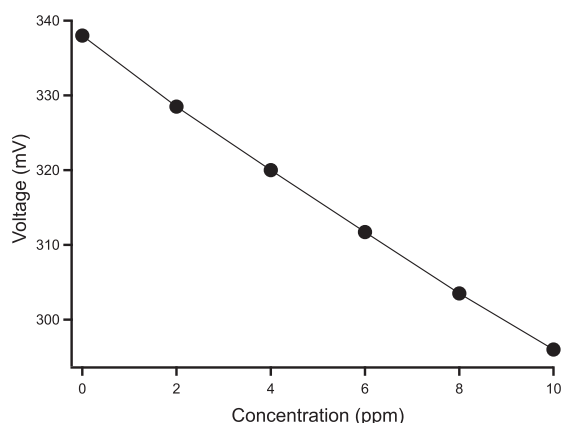


**Fig. 9.** Voltages on a photodiode operated in the photovoltaic mode measured directly using the analogue-to-digital convertor (ADC) of the microcontroller (ATmega328 from Atmel) on the Arduino Uno platform. Thymol blue in 0.1 M NaOH. LED:  $\lambda_{\text{max}} = 595 \text{ nm}$ .

which led to a focus especially on detector cells for flow-injection analysis. However, LED based photometers for the measurement of individual samples are still useful and the first publication on the use of LEDs in analytical chemistry by Flaschka et al. indeed described such a device [4]. Real applications were not reported but the cell was evaluated with solutions of a Cu(II)–aquo complex using a red LED. An early report by Imasaka et al. [34] on batchwise measurements concerned the sensitive determination of phosphate with the molybdenum blue method. A detection limit in the sub-ppb level was achieved. LED-based photometers can be compact and battery operated and such field portable instruments are now commercially available from various suppliers (for example from Hach-Lange, Hanna Instruments, Windaus Labor-technik, WTW Wissenschaftlich-Technische Werkstätten, Chemetrics, etc.). Typical applications are the determination of chlorine or ozone in swimming pools, or the determination of ammonium or phosphate in waste water treatment plants or in environmental samples. LEDs have also been adopted as light sources into commercial benchtop robotic analyzers for the microtiter format (*e.g.* from Tecan, Biorad, Biochrom, Labexim Products, etc.) with their main applications in the clinical field or in life science research, or in a clinical analyser based on a rotary sample tray (Eurolyser). In these routine applications wavelength flexibility is not required.

The fixed wavelength of LEDs can indeed be seen as a disadvantage, and to address this limitation a number of authors have reported switchable multi-wavelength photometers based on dual- or triple-colour LEDs, *i.e.* components which contain two or three emitting chips of different colours, or photometers which combine several standard LEDs [14–16]. The challenge to efficiently combine the light from a number of LEDs into one spot can be solved by employing fibre bundles or fibre splitters. Such LED-array photometers have been reported for the simultaneous determination of binary mixtures of analytes with overlapping spectra in combination with multivariate calibration [15,35]. Another approach to obtain wavelength flexibility from LEDs is to use white LEDs in combination with a wavelength selective device. Veras et al. combined such an LED with a compact disc (CD) as an inexpensive wavelength dispersive device, in order to construct a simple spectrophotometer for molecular absorption spectroscopy [36]. Piasecki et al. replaced the standard deuterium lamp in a commercial diode array detector for capillary electrophoresis with a white LED [37]. For the LED less noise was present compared to the standard light source, which demonstrates that this arrangement still can be advantageous despite the loss of the wavelength selectivity inherent to the light source.

A very special but well established application of absorbance measurements with LEDs is pulse oximetry, in which the oxygen content of blood is measured with a red LED at 600 nm via the colouration of haemoglobin. A probe is clipped directly onto a finger or an earlobe for direct non-invasive *in-vivo* measurement. To account for such variations as the length of the light path and light scattering, a second measurement is made with an IR-LED at 950 nm and the two measurements are ratioed [38].

##### 3.1.2. Titrations

Another early reported analytical application of LEDs was in probes for end-point detection in titrations [39]. This approach has also been adopted commercially and is implemented in state-of-the-art automatic titrators (Metrohm, Mettler-Toledo). One of the advantages of the optical end-point detection in titrations, instead of employing electrochemical sensors, is the possibility of automation of older methods which had been validated for use with indicator dyes.

### 3.1.3. Flow systems

An important field of application of absorbance measurements with LED based devices is detection in analytical flow-through systems. Some of the earliest applications reported concerned detectors for flow-injection analysis (FIA), where a reagent is added to produce a coloured product, and these have been reviewed by Trojanowicz et al. [40]. For such cells attention has to be paid to potential refractive index effects (changes of intensity due to changes in the refractive index of the solution when the sample passes through the cell). Such interferences may be minimized by optimizing the cell geometry [8]. It is also possible to use a referenced approach in which a second wavelength at which the analyte does not absorb is employed for, at least, partial correction of refractive index effects or turbidity [41]. The use of LEDs lends itself well to the construction of miniature devices, and even flow through cells constructed by drilling appropriate holes into the body of an LED have been reported (see for example Dasgupta et al. [8]). Flow-through process analysers with LED based absorbance detectors are now commercially available (e.g. from Metrohm). Process monitoring without adding reagents is also possible if the stream shows an absorbance in dependence of the analyte concentration at a wavelength accessible with LEDs [42].

### 3.1.4. Chromatography

LED based detectors have also been reported for column chromatography. Early reports were based on visible LEDs. Schmidt and Scott in 1984 reported a detector based on a green LED for the determination of heavy metal ions as their complexes with 4-(2-pyridylazo) resorcinol (PAR) [43], a method which was later also used with a PEDD device [44]. Berthod et al. in 1990 described an indirect HPLC detector which was based on the displacement of methylene blue in the eluent by the analytes [45]. Standard photometric detection in HPLC is based on UV-light below 300 nm as most analytes are not coloured and absorb light only in the lower UV-range, and therefore only the commercial introduction of deep-UV-LEDs a few years ago really opened up the field. Detectors based on 255 nm and 280 nm LEDs were reported by Hauser and co-workers [7,32,33]. A detector for conventional HPLC showed detection limits of 0.4 mAU, excellent linearity (correlation coefficients of 0.9999) and reproducibilities of between 0.1 and 0.2%; performance data which is comparable to that of a commercial diode-array detector with a significantly higher purchase price [32]. A photo of a prototype detector for narrow bore separation columns is shown in Fig. 10 and a chromatogram acquired with this device is given in Fig. 11. Note, that for this application special visible light blind photodiodes were employed, in order to suppress a background signal due to secondary emission at longer wavelengths present for the UV-LEDs. Kraiczek et al. recently described an HPLC detector which featured an array of UV-LEDs for flexibility of the wavelength [14].

### 3.1.5. Absorption detection in capillaries/capillary electrophoresis

Absorption measurements in capillaries are a challenge for three reasons. First of all, in the usual transversal measurement, the optical pathlengths are very short (the internal diameters are 100  $\mu\text{m}$  or less in capillary electrophoresis), which according to Lambert–Beer's law imparts a low sensitivity. It also means that the light source should be highly stable to achieve good precision and low limits of detection. Secondly, the light path needs to be restricted to the narrow internal diameter of the capillary in order to avoid stray light. A carefully produced and aligned optical slit is needed. Thirdly, the assembly has to be very stable mechanically as slight changes in the alignment can strongly influence the intensity of light falling on the detector. On the other hand, the inherent stability, high intensity, and small size of LEDs are an advantage for such applications and a number of LED based absorption detectors

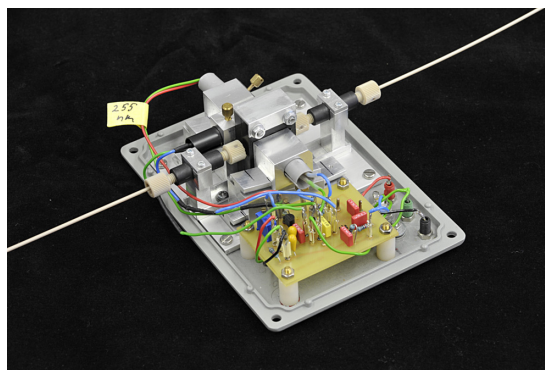


Fig. 10. Detector for narrow bore HPLC based on a deep-UV-LED.

for capillary electrophoresis (CE) and other flow methods employing capillaries have been developed. The first report on the use of such a cell in CE by Tong and Yeung in 1995 described the employment of yellow and red LEDs and a cell that included focusing optics (a camera lens and two ball lenses) [46]. Direct absorption detection, as well as indirect detection were demonstrated. The latter refers to the use of a charged dye in the separation buffer which is displaced by the analyte ions leading to negative going peaks [46]. This approach is commonly used in CE, also when employing conventional absorption detectors, when ions which do not absorb light are to be detected. This early report was followed in 1996 by a study by Macka et al. in which the mercury vapour lamp in a conventional CE detector was replaced by an LED and the superior performance of the solid state light source was demonstrated [31]. Boring and Dasgupta in 1997 described a compact purpose made cell that did not require any focussing optics [47]. A different arrangement, which was based on fibre optic cables butted perpendicularly to the separation capillary, was also reported in 1997 [48]. The latter approach dispenses with the need of placing an optical aperture in front of the capillary as the size of the fibre core can be made to match the internal diameter of the separation capillary.

To improve the sensitivity of absorbance measurements in capillaries Mishra and Dasgupta in 2007 reported a multi-reflection cell [49]. Another approach to increasing the sensitivity for optical detection in capillaries is by passing the light axially along the capillary, instead of the usual transversal arrangement. This is possible by employing capillaries which are made from a

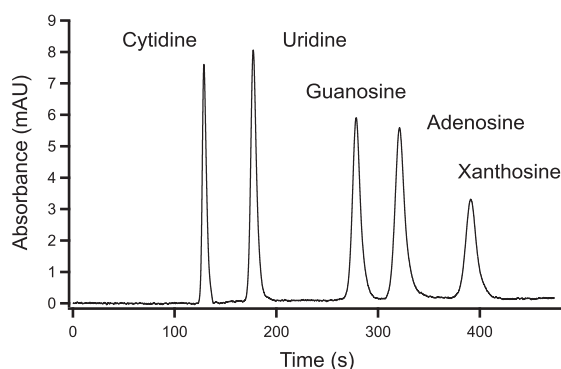


Fig. 11. Chromatogram for nucleosides at 25  $\mu\text{M}$  acquired with the detector shown in Fig. 10.

low refractive index material (Teflon AF), or which are internally coated with such a material, in order to obtain a liquid-core waveguide. Wada et al. [50] reported such a set-up for a study in capillary electrophoresis in which the light could be guided along its entire length, but it is difficult to see how this could be implemented for the usual end-of-capillary detection in electrophoresis. However, other analytical applications of liquid-core waveguides in capillaries have been described, some of them involving LEDs as light sources, and these have been reviewed by Dallas and Dasgupta [51].

Macka and co-workers have also remained active in the field of LED based absorption detectors for CE and over the years have demonstrated a range of applications [52–61]. This included, for example, a study of the use of a near-UV-LED (380 nm) with chromate, which is frequently used as displacement dye in the indirect detection of inorganic anions [62]. The developments of LED based detectors in CE up to 2009 have been reviewed by Xiao et al. [63,64].

As for HPLC, in capillary electrophoresis the deep UV range is the most important wavelength region. A detector employing an LED with an emission band at 255 nm which was based on a modified cell from a conventional CE detector, was reported by Krčmová et al. in 2009 [17]. Due to the relatively low intensity of the early deep-UV device, and the loss of light at the narrow cell aperture, a photomultiplier tube had to be employed for the measurement of the transmitted light intensity. A similar detector based on a 255 nm LED was also reported by Rudaz and co-workers [65,66], but unfortunately very little detail, other than that it employed a deep-UV-LED as light source was given.

LED based detectors for CE are, to our knowledge, presently not commercially available, but a suitable capillary cell which may be used with LEDs is on sale (Ocean Optics). This employs butted fibre optic cables and is based on a commercial cross-type tubing coupler.

### 3.1.6. Gas phase

The determination of small analytes by absorption measurement in the gas phase is a well established technique. A prominent species is carbon dioxide (CO<sub>2</sub>), but many others, such as methane (CH<sub>4</sub>) and other hydrocarbons, ozone (O<sub>3</sub>), NO<sub>x</sub> compounds, sulphur dioxide (SO<sub>2</sub>), hydrogen sulfide (H<sub>2</sub>S), ammonia (NH<sub>3</sub>), or carbon monoxide (CO) are also of interest. For a review on optical gas sensing see for example [67]. These analytes show groups of very narrow absorption lines in the mid-IR range (2.5–14 μm) due to the vibrational and rotational modes of the molecules. Spectral matching to a single line requires the narrow emission line of a laser, and indeed powerful laser based techniques are available, which allow sensitive determination and may even be used for the distinction between molecules composed of different isotopes. For the construction of simple instruments or sensors, broadband sources, such as incandescent lamps, are employed. Typical applications are air monitoring in industrial settings or in mining. These give good results for not too challenging limits of detection despite the not perfect spectral match. Different cell arrangements are used and these usually include an optical filter to limit the wavelength range and often relatively long pathlengths to achieve good sensitivity. Another difficulty is the presence of a background radiation in the IR-range, and for this reason the light source is generally intensity-modulated to allow discrimination via synchronous detection [68]. The replacement of thermal sources with LEDs is advantageous not only due to their inherent wavelength selectivity but also because they can be electronically modulated. The presence of the background radiation also makes the use of wavelength selective detectors sensible for this wavelength range in order to suppress some of the unwanted baseline signal, and for example Matveev

have described the use of specially designed spectrally matched pairs of LEDs and wavelength restricted photodiodes for optical gas sensing [68].

Probably the earliest report on a gas sensor based on a direct absorbance measurement and employing an IR-LED was published by Johnston in 1992 [69]. Two devices for monitoring carbon dioxide at 4.25 μm and hydrocarbons in the range from 3.3–3.4 μm were described. Since then, a variety of photometric absorbance sensors employing mid-IR LEDs have been reported, for example for the detection of CH<sub>4</sub> [70–72], CO and CO<sub>2</sub> [73], and water vapour [73]. The commercial adoption of the mid-IR LEDs for this purpose has been relatively slow, possibly because these devices are not mass-produced for other applications, but some products are commercially available (e.g. from LED Microsensor NT, Gas Sensing Solutions, and Mipex). An added advantage of these devices is the lower power consumption compared to the ones based on thermal radiation sources, so that this approach is of particular interest for portable gas detectors.

Photometric gas sensing with LEDs is mainly the domain of IR-LEDs, but some fruitful spectral matches outside the mid-IR have also been reported. Fowles and Wayne reported already in 1981 a photometric detector for ozone employing a yellow–orange LED as light source and a silicon photodiode as light sensor [74]. It was reported that the detection limit in the ppm range was achieved with a relatively short optical pathlength for gases of 10 mm. The introduction of UV-LEDs opened up some further possibilities. Degner et al. [6], Kalnajs and Avallone [75], as well as Aoyagi et al. [76] reported ozone sensors based on deep-UV-LEDs with 280 or 255 nm emission bands and achieved detection limits below 100 ppb. Degner et al. also reported the determination of SO<sub>2</sub> and NO<sub>2</sub> in exhaust gases from internal combustion engines via their absorbance bands at 280 nm and 400 nm respectively using LEDs [77]. Schorsch et al. reported the use of a blue and a UV-LED of 370 nm for the detection of OH and CH radicals in flames [78].

### 3.2. Fluorescence

LEDs may also be employed as excitation sources in molecular fluorescence spectrometry. For this application the shorter wavelengths are more important as most fluorescent compounds require blue or ultraviolet light for excitation. In contrast to molecular absorbance measurements for fluorescence measurements LEDs of the highest intensities are desirable as the signal, and therefore the detection limit, is directly proportional to the intensity of the excitation source. Generally, much lower detection limits are achieved in fluorescence than in absorption measurements. The intensities of LEDs tend not to be as high as those of lasers, but this is, at least partially, compensated by a higher stability. The suitability of LEDs for fluorescence measurements is illustrated in Fig. 12.

In a very early report in 1975 an instrument based on a red LED for the measurement of the fluorescence of chlorophyll directly in leaves was described [79]. Another early report on the use of an LED for a fluorescence measurement in 1986 described a fibre optic end-point detection system for acid–base titrations employing a coumarin indicator dye [5]. Smith et al. pursued more standard fluorimetry and presented a simple fluorimeter with a green LED and a photodiode employing a conventional cuvette [80]. Their study was focussed on the improved noise and stability that could be obtained with LEDs compared to conventional light sources.

A prominent application over the years has been fluorescence detection in capillary electrophoresis. The first publication by Bruno et al. [81] demonstrated the simple detection of rhodamine B standard excited with a green LED, but the method is particularly useful for the determination of fluorescently labelled biochemical species, such as amino acids, peptides, proteins, DNA fragments,



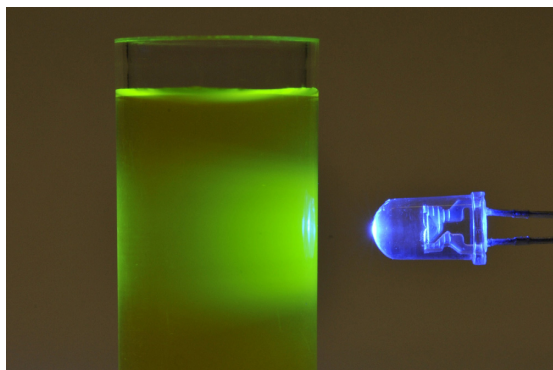


Fig. 12. Excitation of fluorescence from fluorescein using a blue LED.

catecholamines, and others. The developments up to 2009 have been summarized by Xiao et al. in their reviews on the use of LEDs in capillary electrophoresis [63,64]. This work has mostly been carried out with blue LEDs which are available with high intensity and match the excitation wavelengths of common fluorescent labels, such as fluorescein.

In fundamental studies of fluorescence frequently lifetime measurements are made using pulsed light sources. LEDs are again well suited for this task as they can be electronically modulated reaching into the nanosecond domain. This approach was first demonstrated by Araki and Misawa in 1995 with a blue LED using a special pulse shaping circuitry and a ultrafast digitizing oscilloscope [82]. Harms et al. soon after demonstrated a more affordable set-up based on a commercial lock-in amplifier [83]. An example of an application for such measurements is the detection of polycyclic aromatic hydrocarbons (PAHs) in environmental samples [84]. Recently the time domain technology has also been implemented in a very compact portable format [85].

The fact that in fluorescence the sensitivity is directly proportional to the intensity of the excitation source has been exploited for single molecule detection using lasers. It has also been shown more recently by different authors that single molecule detection can also be achieved with high intensity LEDs [86–88]. Also possible is gas-phase fluorescence with LED sources. Sadanga et al. have described the determination of atmospheric nitrogen dioxide with a blue light-emitting diode via its fluorescence [89]. The use of LEDs for the excitation of fluorescence has not been limited to molecules, atomic fluorescence of alkali and alkaline earth metals in the inductively coupled plasma with these sources has also been reported [90].

A very useful application of LEDs is as light sources in fluorescence microscopy for the investigation of stained biological samples. According to Marzouk et al. in such applications LEDs are a replacement for conventional mercury lamps with improved spectral properties and higher intensities, which eliminates the need for a darkened room [91]. This provides, for example, easier access to sputum tests for tuberculosis in developing countries [92]. Such microscopes are now commercially available as are LED based instruments for time domain fluorescence studies (e.g. from Photon System Instruments), special instruments for algae or chlorophyll determination (e.g. from Qubit), handheld portable instruments for environmental testing such as the determination of optical brighteners in waste water or cyanobacteria in fresh water (e.g. from Turner Designs), portable instruments for chlorophyll measurements in leaves (e.g. from Walz Mess- und Regeltechnik),

instruments for total DNA quantification (e.g. from Biotium) or for determination of DNA fragments following PCR (e.g. from Biosan) and others.

### 3.3. Membrane based sensors

Optical chemical sensors (“optodes” or “optrodes”) generally are based on membranes which interact specifically with an analyte and in the process change an optical property. Fluorescence measurements are more easily implemented than absorbance measurements as both, the excitation and the measurement of the signal, cannot be carried out from the back of the membrane which is not exposed to the sample. An early report on an LED-based all solid-state instrument for use with optical sensors was presented by Guthrie et al. 1988 [93]. Among the many examples reported in the literature the most prominent application is the determination of dissolved oxygen via fluorescence quenching of, for example, ruthenium complexes [94] and such sensors are now commercially available from different suppliers. The end of a fibre optic probe, which was used in our laboratory, is shown in Fig. 13 [29]. It was employed with fluorescent membranes, for example for the determination of nitrate. The probe consisted of a bifurcated fibre bundle, one half of the bundle was used to bring light from the LED to the sensing membrane, while the other half served to bring light back to the detector. Lock-in amplification allowed the distinction from ambient light. Taib and Narayanaswamy in 1995 [95] reviewed fibre optic sensors employing solid state instrumentation, which largely implies LEDs or laser diodes as light sources.

### 3.4. Microfluidic devices

The small volumes of microfluidic devices pose the same challenges as capillaries. As the optical path lengths tend to be even shorter, absorbance measurements are relatively seldom used in favour of fluorescence measurements. Götz and Karst in 2007 wrote a review on optical detection methods for microchip separations which includes the LED based methods [96]. A nice example is the compact microchip electrophoresis analyzer for creatinine in urine following labelling with fluorescein isothiocyanate described by Wang et al. [97]. The compact instrument was based on a blue LED and a photodiode for quantification.

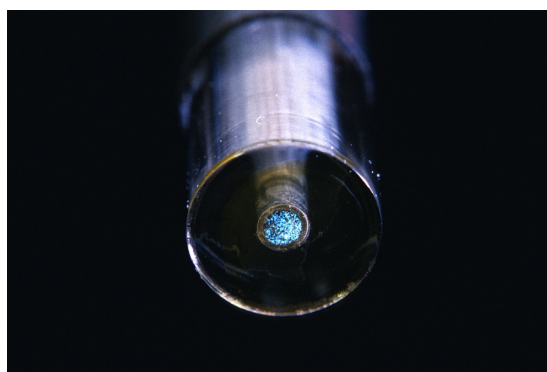


Fig. 13. The end of a bifurcated fibre optic probe for use with fluorescent sensor membranes.

### 3.5. Photoacoustics

Photoacoustic spectroscopy is a thermo-optic method in which the absorption of light is measured indirectly via the heat waves created when the sample is irradiated with intensity modulated light. The heat waves translate into pressure waves, *i.e.* the propagation of sound according to the frequency at which the light source is modulated. The sound can then be picked up with a microphone or a piezoelectric transducer. As it is not a differential measurement, high intensity light sources lead to low limits of detection, a feature shared with fluorimetry. Lasers are often also used for this reason, but the introduction of high intensity LEDs brought about some examples of instruments based on these as well. Lay-Ekuakille et al. described a gas monitor based on mid-IR LEDs (4–4.5  $\mu\text{m}$ ) for applications in a hospital such as the determination of the anaesthetics sevoflurane and nitrous oxide ( $\text{N}_2\text{O}$ ) [98]. Water vapour may be determined with a near-IR LED (1450 nm) [99].  $\text{NO}_2$  in air can be determined with a blue LED (about 460 nm) also by photoacoustics [100–102], and ozone in air is accessible with a deep-UV-LED (285 nm) [103]. Rabasovic et al. reported a low-cost photoacoustic instrument for solid samples employing a white LED [104].

### 3.6. Other applications

An unusual spectrometric application of LEDs is their use in Raman spectroscopy, which was reported by Adami and Kiefer [105]. Note that in order to achieve good spectral resolution, a further narrowing of the emission band of the LED was necessary, which was achieved by placing an interference filter in front of the LED.

It was recognised already in 1978 by Betteridge et al. that LED based transducers can be employed for refractive index measurements on liquids in flow through systems [106] and Pawliszyn studied this effect further in 1987 [107]. This application has now also been implemented commercially. Refractive index detectors for HPLC with LEDs as light sources are produced (*e.g.* by Waters), and benchtop instruments for the batchwise determination of the refractive index of solutions and solvents employing LEDs are also available (*e.g.* from Schmidt + Haensch).

Turbidimetry and nephelometry may also be carried out with LEDs. Schnable et al. [108], for example, in 1998 described a portable nephelometer featuring LEDs of different wavelengths. dos Santos et al. reported an LED-based instrument for concurrent turbidimetric and nephelometric measurements of pharmaceutical formulations [109]. Strzelak and Koncki described a flow-through cell for turbidimetry/nephelometry of urine proteins [110]. Benchtop and portable turbidimeters (employing near-IR LEDs) are now available commercially (*e.g.* from Hanna and Hach).

## 4. Conclusions

The development of analytical applications of light-emitting diodes has been very successful as evidenced by the diversity of reported methods. There is a clear trend to the replacement of conventional light sources in commercial instruments for applications where wavelength flexibility is not required. It has also been a great success story for academic research in analytical chemistry, indeed an endorsement, as many of the approaches first published in the scientific literature have later become implemented in routinely used commercial instrumentation. Further progress can be expected, in particular with regard to the important deep-UV range where most organic molecules show an absorbance.

## Acknowledgments

The authors are grateful to the Swiss National Science Foundation (Grant No. 200020-149068/1) and the Canton of Basel City for a scholarship to Duy Anh Bui.

## References

- [1] E.F. Schubert, *Light-Emitting Diodes*, 2nd ed., Cambridge University Press, New York, 2006.
- [2] [http://www.barry-chambers.staff.shef.ac.uk/LED\\_files/led.html](http://www.barry-chambers.staff.shef.ac.uk/LED_files/led.html) (accessed 31.03.14).
- [3] [http://modulatedlight.org/Modulated\\_Light\\_DX/MODULATED\\_LIGHT\\_DX.html](http://modulatedlight.org/Modulated_Light_DX/MODULATED_LIGHT_DX.html) (accessed 31.03.14).
- [4] H. Flaschka, C. McKeithan, R. Barnes, Light emitting diodes and phototransistors in photometric modules, *Anal. Lett.* 6 (1973) 585–594.
- [5] O.S. Wolfbeis, B.P.H. Schaffar, E. Kaschnitz, Optical fiber titrations 3. Construction and performance of a fluorometric acid–base titrator with a blue LED as light source, *Analyst* 111 (1986) 1331–1334.
- [6] M. Degner, N. Damaschke, H. Ewald, S. O’Keeffe, E. Lewis, *IEEE, Proceedings of the 8th IEEE Conference on Sensors*, Oct. 25–28, 2009, Christchurch, New Zealand, IEEE Sensors Council, New York, 2009, pp. 95–99, doi:<http://dx.doi.org/10.1109/icsens.2009.5398230>.
- [7] S. Schmid, M. Macka, P.C. Hauser, UV-absorbance detector for HPLC based on a light-emitting diode, *Analyst* 133 (2008) 465–469.
- [8] P.K. Dasgupta, H.S. Bellamy, H.H. Liu, J.L. Lopez, E.L. Loree, K. Morris, K. Petersen, K.A. Mir, Light-emitting diode based flow-through optical-absorption detectors, *Talanta* 40 (1993) 53–74.
- [9] P.K. Dasgupta, I.Y. Eom, K.J. Morris, J.Z. Li, Light emitting diode-based detectors absorbance, fluorescence and spectroelectrochemical measurements in a planar flow-through cell, *Anal. Chim. Acta* 500 (2003) 337–364.
- [10] L.F. Capitán-Vallvey, A.J. Palma, Recent developments in handheld and portable optosensing – a review, *Anal. Chim. Acta* 696 (2011) 27–46.
- [11] M. O’Toole, D. Diamond, Absorbance based light emitting diode optical sensors and sensing devices, *Sensors* 8 (2008) 2453–2479.
- [12] M. Macka, T. Piasecki, P.K. Dasgupta, Light-emitting diodes for analytical chemistry, *Annu. Rev. Anal. Chem.* 7 (2014) 183–207.
- [13] S. Gage, D. Evans, M. Hodapp, H. Sorensen, D. Jamison, B. Krause, *Optoelectronics/Fiber-Optics Applications Manual*, 2nd ed., McGraw-Hill, New York, 1981.
- [14] K.G. Kraiczek, R. Bonjour, Y. Salvadé, R. Zengerle, Highly flexible UV–vis radiation sources and novel detection schemes for spectrometric HPLC detection, *Anal. Chem.* 86 (2014) 1146–1152.
- [15] A. Fonseca, I.M. Raimundo, A multichannel photometer based on an array of light emitting diodes for use in multivariate calibration, *Anal. Chim. Acta* 522 (2004) 223–229.
- [16] P.C. Hauser, T.W.T. Rupasinghe, N.E. Cates, A multi-wavelength photometer based on light-emitting diode, *Talanta* 42 (1995) 605–612.
- [17] L. Krčmová, A. Stjernlof, S. Mehlen, P.C. Hauser, S. Abele, B. Paull, M. Macka, Deep-UV-LEDs in photometric detection: a 255 nm LED on-capillary detector in capillary electrophoresis, *Analyst* 134 (2009) 2394–2396.
- [18] F.M. Mims III, Sun photometer with light emitting diode as spectrally selective detectors, *Appl. Opt.* 31 (1992) 3.
- [19] C. Weber, J.O. Tocho, E.J. Rodríguez, H.A. Acciaresi, LEDs used as spectral selective light detectors in remote sensing techniques, *J. Phys. Conf. Ser.* 274 (2011) 1–6.
- [20] R.J. Berry, J.E. Harris, R.R. Williams, Light-emitting diodes as sensors for colorimetric analysis, *Appl. Spectrosc.* 51 (1997) 1521–1524.
- [21] D.A. Bui, P.C. Hauser, Absorbance measurements with light-emitting diodes as sources: silicon photodiodes or light-emitting diodes as detectors? *Talanta* 116 (2013) 1073–1078.
- [22] K.T. Lau, S. Baldwin, R.L. Shepherd, P.H. Dietz, W.S. Yezunis, D. Diamond, Novel fused-LEDs devices as optical sensors for colorimetric analysis, *Talanta* 63 (2004) 167–173.
- [23] L. Tymecki, M. Pokrzywnicka, R. Koncki, Paired emitter detector diode (PEDD)-based photometry – an alternative approach, *Analyst* 133 (2008) 1501–1504.
- [24] M. Czugała, C. Fay, N.E. O’Connor, B. Corcoran, F. Benito-Lopez, D. Diamond, Portable integrated microfluidic analytical platform for the monitoring and detection of nitrite, *Talanta* 116 (2013) 997–1004.
- [25] P. Dietz, W. Yezunis, D. Leigh, in: A.K. Dey, A. Schmidt, J.F. McCarthy (Eds.), *Ubicomp 2003: Ubiquitous Computing*, 2864, Springer-Verlag, Berlin, 2003, pp. 175–191.
- [26] J. Wilson, J.F.B. Hawkes, *Optoelectronics: An Introduction*, Prentice Hall, London, 1983.
- [27] G. de Graaf, R.F. Woffenbittel, Light-to-frequency convertor using integrating mode photodiodes, *IEEE T. Instrum. Meas.* 46 (1997) 933–936.
- [28] K.T. Lau, S. Baldwin, M. O’Toole, R. Shepherd, W.J. Yezunis, S. Izuo, S. Ueyama, D. Diamond, A low-cost optical sensing device based on paired emitter detector light emitting diodes, *Anal. Chim. Acta* 557 (2006) 111–116.
- [29] P.C. Hauser, S.S.S. Tan, All-solid-state instrument for fluorescence-based fibre-optic chemical sensors, *Analyst* 118 (1993) 991–995.
- [30] P.C. Hauser, C.L.C. Liang, B. Müller, A solid-state instrument for fluorescence chemical sensors using a blue-light emitting diode of high intensity, *Meas. Sci. Technol.* 6 (1995) 1081.

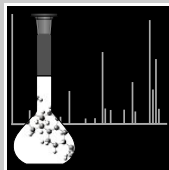
- [31] M. Macka, P. Andersson, P.R. Haddad, Linearity evaluation in absorbance detection: the use of light-emitting diodes for on-capillary detection in capillary electrophoresis, *Electrophoresis* 17 (1996) 1898–1905.
- [32] B. Bomastyk, I. Petrovic, P.C. Hauser, Absorbance detector for high-performance liquid chromatography based on light-emitting diodes for the deep-ultraviolet range, *J. Chromatogr. A* 1218 (2011) 3750–3756.
- [33] D.A. Bui, B. Bomastyk, P.C. Hauser, Absorbance detector based on a deep UV light emitting diode for narrow-column HPLC, *J. Sep. Sci.* 36 (2013) 3152–3157.
- [34] T. Imasaka, T. Kamikubo, Y. Kawabata, N. Ishibashi, Ultratrace photometric determination of phosphate with a solid-state emitter as light source, *Anal. Chim. Acta* 153 (1983) 261–263.
- [35] P.C. Hauser, T.W.T. Rupasinghe, Simultaneous determination of metal ion concentrations in binary mixtures with a multi-LED photometer, *Fresen. J. Anal. Chem.* 357 (1997) 1056–1060.
- [36] G. Veras, E.C. Silva, W.S. Lyra, S.F.C. Soares, T.B. Guerreiro, S.R.B. Santos, A portable, inexpensive and microcontrolled spectrophotometer based on white LED as light source and CD media as diffraction grid, *Talanta* 77 (2009) 1155–1159.
- [37] T. Piasecki, M.C. Breadmore, M. Macka, White LEDs as broad spectrum light sources for spectrophotometry: demonstration in the visible spectrum range in a diode-array spectrophotometric detector, *Electrophoresis* 31 (2010) 3737–3744.
- [38] J.P. Dekock, L. Tarasenko, Pulse oximetry – theoretical and experimental models, *Med. Biol. Eng. Comput.* 31 (1993) 291–300.
- [39] T. Anfält, A. Granéli, M. Strandberg, Probe photometer based on optoelectronic components for the determination of total alkalinity in seawater, *Anal. Chem.* 48 (1976) 357–360.
- [40] M. Trojanowicz, P.J. Worsfold, J.R. Clinch, Solid-state photometric detectors for flow-injection analysis, *Trac-Trends Anal. Chem.* 7 (1988) 301–305.
- [41] H.H. Liu, P.K. Dasgupta, Dual-wavelength photometry with light-emitting diodes – compensation of refractive-index and turbidity effects in flow-injection analysis, *Anal. Chim. Acta* 289 (1994) 347–353.
- [42] P.C. Hauser, T.W.T. Rupasinghe, C.C. Lucas, A. McClure, Process monitor for an ammoniacal nickel solution employing an infrared light-emitting diode and a log-ratio amplifier, *Analyst* 120 (1995) 2635–2638.
- [43] G.J. Schmidt, R.P.W. Scott, Simple and sensitive ion chromatograph for trace metal determination, *Analyst* 109 (1984) 997–1002.
- [44] M. O'Toole, K.T. Lau, B. Shazmann, R. Shepherd, P.N. Nesterenko, B. Paull, D. Diamond, Novel integrated paired emitter detector diode (PEDD) as a miniaturized photometric detector in HPLC, *Analyst* 131 (2006) 938–943.
- [45] A. Berthod, M. Glick, J.D. Winefordner, Sensitive, indirect photometric detector for high-performance liquid-chromatography using a light-emitting diode, *J. Chromatogr.* 502 (1990) 305–315.
- [46] W. Tong, E.S. Yeung, Simple double-beam absorption detection systems for capillary electrophoresis based on diode lasers and light-emitting diodes, *J. Chromatogr. A* 718 (1995) 177–185.
- [47] C.B. Boring, P.K. Dasgupta, An affordable high-performance optical absorbance detector for capillary systems, *Anal. Chim. Acta* 342 (1997) 123–132.
- [48] P.A.G. Butler, B. Mills, P.C. Hauser, Capillary electrophoresis detector using a light emitting diode and optical fibres, *Analyst* 122 (1997) 949–953.
- [49] S.K. Mishra, P.K. Dasgupta, Capillary scale light emitting diode based multi-reflection absorbance detector, *Anal. Chim. Acta* 605 (2007) 166–174.
- [50] A. Wada, M. Harada, T. Okada, Kinetic monitoring of electrophoretically induced solute reaction by axial absorption detection with liquid-core waveguide, *Anal. Chem.* 78 (2006) 4709–4712.
- [51] T. Dallas, P.K. Dasgupta, Light at the end of the tunnel: recent analytical applications of liquid-core waveguides, *Trac-Trends Anal. Chem.* 23 (2004) 385–392.
- [52] M. Macka, B. Paull, P. Andersson, P.R. Haddad, Determination of barium and strontium by capillary zone electrophoresis using an electrolyte containing sulfonazo III, *J. Chromatogr. A* 767 (1997) 303–310.
- [53] M. Macka, B. Paull, D.P. Bogan, P.R. Haddad, Role of ligand purity in separations of alkaline earth metals as arsenazo I complexes by capillary zone electrophoresis, *J. Chromatogr. A* 793 (1998) 177–185.
- [54] M. Macka, P. Nesterenko, P. Andersson, P.R. Haddad, Separation of uranium (VI) and lanthanides by capillary electrophoresis using on-capillary complexation with arsenazo III, *J. Chromatogr. A* 803 (1998) 279–290.
- [55] M. Macka, P. Nesterenko, P.R. Haddad, Investigation of solute-wall interactions in separation of uranium(VI) and lanthanides by capillary electrophoresis using on-capillary complexation with arsenazo III, *J. Microcolumn Sep.* 11 (1999) 1–9.
- [56] N. Vachirapatana, M. Macka, P.R. Haddad, Separation and determination of vanadium in fertilizer by capillary electrophoresis with a light-emitting diode detector, *Anal. Bioanal. Chem.* 374 (2002) 1082–1085.
- [57] C. Johns, M. Macka, P.R. Haddad, Design and performance of a light-emitting diode detector compatible with a commercial capillary electrophoresis instrument, *Electrophoresis* 25 (2004) 3145–3152.
- [58] F. Momenbeik, C. Johns, M.C. Breadmore, E.F. Hilder, M. Macka, P.R. Haddad, Sensitive determination of carbohydrates labelled with p-nitroaniline by capillary electrophoresis with photometric detection using a 406 nm light-emitting diode, *Electrophoresis* 27 (2006) 4039–4046.
- [59] A.R. Fakhari, M.C. Breadmore, M. Macka, P.R. Haddad, Non-aqueous capillary electrophoresis with red light emitting diode absorbance detection for the analysis of basic dyes, *Anal. Chim. Acta* 580 (2006) 188–193.
- [60] M.C. Breadmore, R.D. Henderson, A.R. Fakhari, M. Macka, P.R. Haddad, Separation of Nile blue-labelled fatty acids by CE with absorbance detection using a red light-emitting diode, *Electrophoresis* 28 (2007) 1252–1258.
- [61] P. Balding, M.C. Boyce, M.C. Breadmore, M. Macka, Light-emitting diode-compatible probes for indirect detection of anions in CE, *Electrophoresis* 28 (2007) 3453–3460.
- [62] M. King, B. Paull, P.R. Haddad, M. Macka, Performance of a simple UV-LED light source in the capillary electrophoresis of inorganic anions with indirect detection using a chromate background electrolyte, *Analyst* 127 (2002) 1564–1567.
- [63] D. Xiao, L. Yan, H. Yuan, S. Zhao, X. Yang, M.M.F. Choi, CE with LED-based detection: an update, *Electrophoresis* 30 (2009) 189–202.
- [64] D. Xiao, S. Zhao, H. Yuan, X. Yang, CE detector based on light-emitting diodes, *Electrophoresis* 28 (2007) 233–242.
- [65] R.D. Marini, E. Rozet, M.L.A. Montes, C. Rohrbasser, S. Roht, D. Rheme, P. Bonnabry, J. Schappler, J.L. Veuthey, P. Hubert, S. Rudaz, Reliable low-cost capillary electrophoresis device for drug quality control and counterfeit medicines, *J. Pharm. Biomed. Anal.* 53 (2010) 1278–1287.
- [66] C. Rohrbasser, D. Rheme, S. Decastel, S. Roth, M.D.A. Montes, J.L. Veuthey, S. Rudaz, A new capillary electrophoresis device with deep UV detector based on LED technology, *Chimia* 63 (2009) 890–891.
- [67] J. Hodgkinson, R.P. Tatam, Optical gas sensing: a review, *Meas. Sci. Technol.* 24 (2013) .
- [68] B.A. Matveev, Mid-Infrared Semiconductor Optoelectronics, in: A. Krier (Ed.), Springer, London, 2006, pp. 395–428.
- [69] S.F. Johnston, Gas monitors employing infrared LEDs, *Meas. Sci. Technol.* 3 (1992) 191–195.
- [70] A.A. Popov, M.V. Stepanov, V.V. Sherstnev, Y.P. Yakovlev, 3.3  $\mu\text{m}$  LEDs for measuring methane, *Tech. Phys. Lett.* 23 (1997) 4.
- [71] B. Matveev, M. Aidaraliev, G. Gavrilov, N. Zotova, S. Karandashov, G. Sotnikova, N. Stus, G. Talalakin, N. Ilinskaya, S. Aleksandrov, Room temperature InAs photodiode-InGaAs LED pairs for methane detection in the mid-IR, *Sens. Actuators B: Chem.* 51 (1998) 5.
- [72] A. Krier, V.V. Sherstnev, Powerful interface light emitting diodes for methane gas detection, *J. Phys. D: Appl. Phys.* 33 (2000) 101–106.
- [73] B. Matveev, G. Gavrilov, V.V. Evstropov, N. Zotova, S. Karandashov, G.Y. Sotnikova, N.M. Stus, G.N. Talalakin, J. Malinen, Mid-infrared (3–5  $\mu\text{m}$ ) LEDs as sources for gas and liquid sensors, *Sens. Actuators B: Chem.* 38–39 (1997) 5.
- [74] M. Fowles, R.P. Wayne, Ozone monitor using an LED source, *J. Phys. E: Sci. Instrum.* 14 (1981) 1143–1145.
- [75] L.E. Kalnajs, L.M. Avallone, A novel lightweight low-power dual-beam ozone photometer utilizing solid-state optoelectronics, *J. Atmos. Ocean Technol.* 27 (2010) 869–880.
- [76] Y. Aoyagi, M. Takeuchi, K. Yoshida, M. Kurouchi, T. Araki, Y. Nanishi, H. Sugano, Y. Ahiko, H. Nakamura, High-sensitivity ozone sensing using 280 nm deep ultraviolet light-emitting diode for detection of natural hazard ozone, *J. Environ. Protect.* 3 (2012) 5.
- [77] M. Degner, N. Damaschke, H. Ewald, Real time exhaust gas sensor with high resolution for onboard sensing of harmful components, *IEEE Sens. Conf.* (2008) 4.
- [78] S. Schorsch, J. Kiefer, A. Leipertz, Z.S. Li, M. Alden, Detection of flame radicals using light-emitting diodes, *Appl. Spectrosc.* 64 (2010) 1330–1334.
- [79] U. Schreiber, L. Groberman, W. Vidaver, Portable, solid-state fluorometer for the measurement of chlorophyll fluorescence induction in plants, *Rev. Sci. Instrum.* 46 (1975) 538–542.
- [80] B.W. Smith, B.T. Jones, J.D. Winefordner, High-precision fluorimetry with a light-emitting diode source, *Appl. Spectrosc.* 42 (1988) 1469–1472.
- [81] A.E. Bruno, F. Maystre, B. Krattiger, P. Nussbaum, E. Gassmann, The pigtailling approach to optical-detection in capillary electrophoresis, *Trac-Trends Anal. Chem.* 13 (1994) 190–198.
- [82] T. Araki, H. Misawa, Light emitting diode-based nanosecond ultraviolet light source for fluorescence lifetime measurements, *Rev. Sci. Instrum.* 66 (1995) 5469–5472.
- [83] P. Harms, J. Sipiør, N. Ram, G.M. Carter, G. Rao, Low cost phase-modulation measurements of nanosecond fluorescence lifetimes using a lock-in amplifier, *Rev. Sci. Instrum.* 70 (1999) 1535–1539.
- [84] S. Landgraf, Use of ultrabright LEDs for the determination of static and time-resolved fluorescence information of liquid and solid crude oil samples, *J. Biochem. Biophys. Methods* 61 (2004) 125–134.
- [85] H. Wang, Y. Qi, T.J. Mountziaris, C.D. Salthouse, A portable time-domain LED fluorimeter for nanosecond fluorescence lifetime measurements, *Rev. Sci. Instrum.* 85 (2014) 055003.
- [86] J. Gerhardt, L. Mai, A. Lamas-Linares, C. Kurtsiefer, Detection of single molecules illuminated by a light-emitting diode, *Sensors* 11 (2011) 905–916.
- [87] A. Hattori, S. Habuchi, M. Vacha, Single-molecule imaging with an inexpensive UV-LED source, *Chem. Lett.* 38 (2009) 234–235.
- [88] J.S. Kuo, C.L. Kuyper, P.B. Allen, G.S. Fiorini, D.T. Chiu, High-power blue/UV light-emitting diodes as excitation sources for sensitive detection, *Electrophoresis* 25 (2004) 3796–3804.
- [89] Y. Sadanga, K. Suzuki, T. Yoshimoto, H. Bandow, Direct measurement system of nitrogen dioxide in the atmosphere using a blue-emitting diode induced fluorescence technique, *Rev. Sci. Instrum.* 85 (2014) 064101.
- [90] A. Young, L. Pitts, S. Greenfield, M. Foulkes, A preliminary comparison of radial and axial excitation fluorescence in the ICP using non-laser sources, *J. Anal. Atom. Spectrom.* 18 (2003) 44–48.

- [91] M. Marzouk, A. Ferjani, M. Dhaou, M.H. Ali, N. Hannachi, J. Boukadida, Comparison of LED and conventional fluorescence microscopy for detection of acid-fast bacilli in an area with high tuberculosis incidence, *Diagn. Micr. Infect. Dis.* 76 (2013) 306–308.
- [92] J.P. Tripathy, LED fluorescence microscopy for diagnosis of tuberculosis in countries with high disease burden, *Curr. Sci.* 105 (2013) 441–442.
- [93] A.J. Guthrie, R. Narayanaswamy, N.A. Welti, Solid-state instrumentation for use with optical-fibre chemical sensors, *Talanta* 35 (1988) 157–159.
- [94] O.S. Wolfbeis, M.J.P. Leiner, H.E. Posch, A new sensing material for optical oxygen measurement, with the indicator embedded in an aqueous phase, *Mikrochim. Acta III* (1986) 359–366.
- [95] M.N. Taib, R. Narayanaswamy, Solid-state instruments for optical fibre chemical sensors – a review, *Analyst* 120 (1995) 1617–1625.
- [96] S. Götz, U. Karst, Recent developments in optical detection methods for microchip separations, *Anal. Bioanal. Chem.* 387 (2007) 183–192.
- [97] S.P. Wang, X.C. Li, J.P. Yang, X.J. Yang, F.H. Hou, Z.G. Chen, Rapid determination of creatinine in human urine by microchip electrophoresis with LED induced fluorescence detection, *Chromatographia* 75 (2012) 1287–1293.
- [98] A. Lay-Ekuakille, G. Vendramin, A. Trotta, LED-based sensing system for biomedical gas monitoring: design and experimentation of a photoacoustic chamber, *Sens. Actuators B: Chem.* 135 (2009) 411–419.
- [99] J.M. Rey, M.W. Sigrist, New differential mode excitation photoacoustic scheme for near-infrared water vapour sensing, *Sens. Actuators B: Chem.* 135 (2008) 161–165.
- [100] J. Saarela, T. Sorvajärvi, T. Laurila, J. Toivonen, Phase-sensitive method for background-compensated photoacoustic detection of NO<sub>2</sub> using high-power LEDs, *Opt. Express* 19 (2011) A725–A732.
- [101] R. Bernhardt, G.D. Santiago, V.B. Slezak, A. Peuriot, M.G. Gonzalez, Differential LED-excited, resonant NO<sub>2</sub> photoacoustic system, *Sens. Actuators B: Chem.* 156 (2010) 533–536.
- [102] M. Gonzalez, G. Santiago, V. Slezak, A. Peuriot, Novel optical method for background reduction in resonant photoacoustics, *Rev. Sci. Instrum.* 78 (2007) 4.
- [103] S. Böttger, M. Köhring, U. Willer, W. Schade, Off-beam quartz-enhanced photoacoustic spectroscopy with LEDs, *Appl. Phys. B* 113 (2013) 227–232.
- [104] M.D. Rabasovic, M.G. Nikolic, M.D. Dramicanin, M. Franko, D.D. Markushev, Low-cost, portable photoacoustic setup for solid samples, *Meas. Sci. Technol.* 20 (2009) 6.
- [105] R. Adami, J. Kiefer, Light-emitting diode based shifted-excitation Raman difference spectroscopy (LED-SERDS), *Analyst* 138 (2013) 6258–6261.
- [106] D. Betteridge, E.L. Dagless, B. Fields, N.F. Graves, A highly sensitive flow-through phototransducer for unsegmented continuous-flow analysis demonstrating high-speed spectrophotometry at the parts per 10exp9 level and a new method of refractometric determinations, *Analyst* 103 (1978) 897–908.
- [107] J. Pawliszyn, LEDs and laser-diodes in schlieren optics, *Rev. Sci. Instrum.* 58 (1987) 245–248.
- [108] J.G. Schnable, P.J. Grochowski, L. Wilhelm, C. Harding, M. Kiefer, R.S. Orr, Portable LED-array VIS-NIR spectrophotometer/nephelometer, *Field Anal. Chem. Technol.* 2 (1998) 21–28.
- [109] V.B. dos Santos, T.B. Guerreiro, W.T. Suarez, R.C. Faria, O. Fatibello, Evaluation of turbidimetric and nephelometric techniques for analytical determination of *N*-acetylcysteine and thiamine in pharmaceutical formulations employing a lab-made portable microcontrolled turbidimeter and nephelometer, *J. Braz. Chem. Soc.* 22 (2011) 1968–1978.
- [110] K. Strzelak, R. Koncki, Nephelometry and turbidimetry with paired emitter detector diodes and their application for determination of total urinary protein, *Anal. Chim. Acta* 788 (2013) 68–73.

**Highlights of Analytical Sciences in Switzerland:**

**Deep UV-LED based absorbance detectors for narrow-bore HPLC  
and capillary electrophoresis**

*Chimia (2015), 69, 806*



## Highlights of Analytical Sciences in Switzerland

Division of Analytical Sciences

A Division of the Swiss Chemical Society

### Deep UV-LED Based Absorbance Detectors for Narrow-Bore HPLC and Capillary Electrophoresis

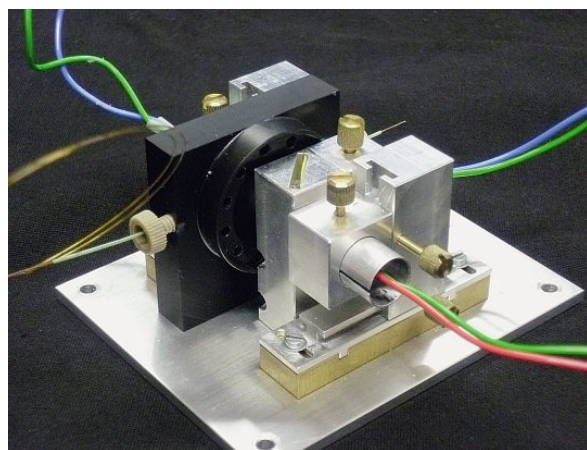
Duy Anh Bui and Peter C. Hauser\*

\*Correspondence: Prof. P.C. Hauser, Department of Chemistry, University of Basel, Spitalstrasse 51, CH-4051 Basel, E-mail: Peter.Hauser@unibas.ch

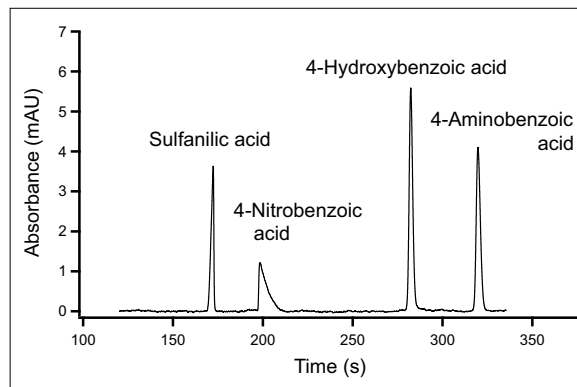
**Keywords:** Capillary detection · CE · Deep UV-LED · HPLC · UV photodiode

The most common detection method for the analytical separation techniques of HPLC and capillary electrophoresis (CE) is absorbance measurement in the deep-UV range (below 300 nm) as a large number of organic species absorb in this wavelength region. Conventional UV detectors are based on deuterium discharge lamps coupled to a monochromator for wavelength selection. Light-emitting diodes (LEDs) for this wavelength range have been produced in recent years. They have bandwidths of typically 30 nm, which makes them well suited for direct absorbance measurements of molecules without requiring a monochromator. Only UV-photodiodes and a log-ratio amplifier integrated circuit for emulating Lambert-Beer's law are required to complete the electronic circuitry.

Narrow-bore HPLC has primarily been developed for use with mass-spectrometric detection, for which only small amounts of analytes are sufficient. However, the savings in eluent consumption makes this approach also attractive for use with optical detection when ultimate sensitivity is not required. In CE narrow channels are essential to limit the Joule heating associated with the ionic current along the separation path.



The detector cell for capillary electrophoresis.



Detection of aromatic acids in capillary electrophoresis using a 50  $\mu\text{m}$  ID capillary with a 255 nm LED.

The design of LED-based detectors for these narrow gauge methods is more challenging than for standard HPLC. Due to the small available volumes, the construction of dedicated Z-shaped flow cells is not possible and the measurement has to be made transverse to the flow path. The narrowness of the necessary apertures requires careful attention to efficient light coupling and avoidance of stray light. High mechanical stability is also required in order to minimize noise due to mechanical fluctuations. Despite these hurdles excellent performance with regard to baseline noise (low  $\mu\text{AU}$  range), reproducibility of peak areas ( $\sim 1\%$ ), and linearity of calibration curves (correlation coefficients  $>0.999$ ) could be obtained with LEDs of the commonly used wavelengths of 255 and 280 nm for both, narrow-bore HPLC (250  $\mu\text{m}$  ID) and CE (50  $\mu\text{m}$  ID).

**The inexpensive LED-based devices display a capability comparable to standard commercial detectors. Their compact size and low power requirements make them also suitable for portable battery-powered instruments.**

Received: September 30, 2015

#### References

- B. Bomastyk, I. Petrovic, P. C. Hauser, *J. Chromatogr. A* **2011**, *1218*, 3750.  
 D. A. Bui, B. Bomastyk, P. C. Hauser, *J. Sep. Sci.* **2013**, *36*, 3152.  
 D. A. Bui, P. C. Hauser, *J. Chromatogr. A*, **2015**, *1421*, 203..

#### Can you show us your analytical highlight?

Please contact: Dr. Veronika R. Meyer, Unterstrasse 58, CH-9000 St. Gallen  
 Tel.: +41 71 222 16 81, E-mail: VRMeyer@bluewin.ch

### 3. References

1. L.S. Ettre, *Chromatographia*, 2001, 54, p. 409-414.
2. A.J.P. Martin, *Nobel Lecture*, 1952, p. 359-371.
3. R. Consden, A.H. Gordon and A.J.P. Martin, *Biochem. J*, 1944, 38, p. 224-232.
4. E.V. Piel, *Anal. Chem*, 1966, 38, p. 670-672.
5. P.D. McDonald, *Waters Corporation*, 2008, p. 1-20.
6. R.E. Majors, *Anal. Chem*, 1972, 44, p. 1722-1726.
7. H. Small, T.S. Stevens and W.C. Bauman, *Anal. Chem*, 1975, 47, p. 1801-1809.
8. J.J. Kirkland, *Anal. Chem*, 1971, 43, p. 36-48.
9. M.E. Swartz, *J. Liq. Chromatogr. R. T*, 2005, 28, p. 1253-1263.
10. C.G. Horvath and S.R. Lipsky, *Anal. Chem*, 1967, 39, p. 1893.
11. J. Porath, *Nature*, 1959, 183, p. 1657-1659.
12. J. Porath, *Clin. Chim. Acta*, 1959, 4, p. 776-778.
13. P.G.M. Flodin, *United States Patent Office*, 1965, 3208994, p. 1-6.
14. J. Martosella, P. Duong and A. Zhu, *Chromatography Today*, 2013, 6, p. 38-41.
15. M.A. Alabdalla, *J. Clin. Forensic. Med*, 2005, 12, p. 310-315.
16. C.K. Lai, T. Lee, K.M. Au and A.Y. Chan, *Clin. Chem*, 1997, 43, p. 312-325.
17. T. Tuzimski, *J. Sep. Sci*, 2008, 31, p. 3537-3542.
18. P. Persson, J. Andersson, L. Gorton, S. Larsson, N.O. Nilvebrant and L.J. Jonsson, *J. Agric. Food Chem*, 2002, 50, p. 5318-5325.
19. A. Berthod, S.S.C. Chang, J.P.S. Kullman and D.W. Armstrong, *Talanta*, 1998, 47, p. 1001-1012.
20. M. Karkacier, M. Erbas, M.K. Uslu and M. Aksu, *J. Chromatogr. Sci*, 2003, 41, p. 331-333.
21. J. Wen, T. Arakawa and J.S. Philo, *Anal. Biochem*, 1996, 240, p. 155-166.
22. T. Zetterstrom, T. Sharp, C.A. Marsden and U. Ungerstedt, *J. Neurochem*, 1983, 41, p. 1769-1773.

23. H. Weicker, M. Feraudi, H. Hagele and R. Pluto, *Clin. Chim. Acta*, 1984, 141, p. 17-25.
24. T.H. Mourey and L.E. Oppenheimer, *Anal. Chem*, 1984, 56, p. 2427-2434.
25. N.C. Megoulas and M.A. Koupparis, *Crit. Rev. Anal. Chem*, 2005, 35, p. 301-316.
26. P. Bhandari, N. Kumar, B. Singh and V.K. Kaul, *J. Chromatogr. A*, 2008, 1194, p. 257-261.
27. E. Dvorackova, M. Snoblova and P. Hrdlicka, *J. Sep. Sci*, 2014, 37, p. 323-337.
28. C.F. Torres, L. Vazquez, F.J. Senorans and G. Reglero, *J. Chromatogr. A*, 2005, 1078, p. 28-34.
29. W.M. Indrasena, K. Henneberry, C.J. Barrow and J.A. Kralovec, *J. Liq. Chromatogr. R. T*, 2005, 28, p. 2581-2595.
30. Y. Mengerink, R. Peters, C.G. deKoster, S. van der Wal, H.A. Claessen and C.A. Cramers, *J. Chromatogr. A*, 2001, 914, p. 131-145.
31. X.L. Jiang, V. Lima and P.J. Schoenmakers, *J. Chromatogr. A*, 2003, 1018, p. 19-27.
32. P. Kebarle, *J. Mass. Spectrom*, 2000, 35, p. 804-817.
33. M. Holcapek, R. Jirasko and M. Lisa, *J. Chromatogr. A*, 2012, 1259, p. 3-15.
34. H. Hoja, P. Marquet, B. Verneuil, H. Lotfi, B. Penicaut and G. Lachatre, *J. Anal. Toxicol*, 1997, 21, p. 116-126.
35. B.L. Ackermann, M.J. Berna, J.A. Eckstein, L.W. Ott and A.K. Chaudhary, *Annu. Rev. Anal. Chem*, 2008, 1, p. 357-396.
36. S.J. Hird, B.P.Y. Lau, R. Schuhmacher and R. Krska, *Trend. Anal. Chem*, 2014, 59, p. 59-72.
37. O. Vesterberg, *J. Chromatogr*, 1989, 480, p. 3-19.
38. A. Tiselius, *Trans. Faraday Soc*, 1937, 33, p. 524-530.
39. E.L. Durrum, *J. Am. Chem. Soc*, 1950, 72, p. 2943-2948.
40. O. Smithies, *Biochem. J*, 1955, 61, p. 629-641.
41. S. Raymond and L. Weintraub, *Science*, 1959, 130, p. 711.
42. A.L. Shapiro, M.D. Scharff, J.V. Maizel, Jr and J.W. Uhr, *Proc. Natl. Acad. Sci. USA*, 1966, 56, p. 216-221.



43. S. Hjerten, *Chromatogr. Rev*, 1967, 9, p. 122-219.
44. F.E.P. Mikkers, F.M. Everaerts and T.P.E.M. Verheggen, *J. Chromatogr*, 1979, 169, p. 11-20.
45. J.W. Jorgenson and K.D. Lukacs, *Anal. Chem*, 1981, 53, p. 1298-1302.
46. S. Terabe, K. Otsuka, K. Ichikawa, A. Tsuchiya and T. Ando, *Anal. Chem*, 1984, 56, p. 111-113.
47. T.J. Kasper, M. Melera, P. Gozel and R.G. Brownlee, *J. Chromatogr*, 1988, 458, p. 303-312.
48. T. Tsuda, J.V. Sweedler and R.N. Zare, *Anal. Chem*, 1990, 62, p. 2149-2152.
49. J.P. Chervet, R.E.J. Vansoest and M. Ursem, *J. Chromatogr*, 1991, 543, p. 439-449.
50. Y.J. Xue and E.S. Yeung, *Anal. Chem*, 1994, 66, p. 3575-3580.
51. T.S. Wang, J.H. Aiken, C.W. Huie and R.A. Hartwick, *Anal. Chem*, 1991, 63, p. 1372-1376.
52. S.D. Gilman and A.G. Ewing, *Anal. Chem*, 1995, 67, p. 58-64.
53. M.S. Heywood and P.B. Farnsworth, *Appl. Spectrosc*, 2010, 64, p. 1283-1288.
54. E. Okerberg and J.B. Shear, *Anal. Biochem*, 2001, 292, p. 311-313.
55. F. Prost, J. Caslavská and W. Thormann, *J. Sep. Sci*, 2002, 25, p. 1043-1054.
56. C. Horstkotter, D. Schepmann and G. Blaschke, *J. Chromatogr. A*, 2003, 1014, p. 71-81.
57. H.T. Chang and E.S. Yeung, *Anal. Chem*, 1995, 67, p. 1079-1083.
58. S.J. Lillard, E.S. Yeung and M.A. McCloskey, *Anal. Chem*, 1996, 68, p. 2897-2904.
59. A. Nann and E. Pretsch, *J. Chromatogr. A*, 1994, 676, p. 437-442.
60. M. Macka, G. Gerhardt, P. Andersson, D. Bogan, R.M. Cassidy and P.R. Haddad, *Electrophoresis*, 1999, 20, p. 2539-2546.
61. C. Haber, I. Silvestri, S. Roosli and W. Simon, *Chimia*, 1991, 45, p. 117-121.
62. W. Jin, L.T. Jin, G.Y. Shi and J.N. Ye, *Anal. Chim. Acta*, 1999, 382, p. 33-37.
63. M.E. Hadwiger, S.R. Torchia, S. Park, M.E. Biggin and C.E. Lunte, *J. Chromatogr. B*, 1996, 681, p. 241-249.

64. Y. Guo, L.A. Colon, R. Dadoo and R.N. Zare, *Electrophoresis*, 1995, 16, p. 493-497.
65. J. Wang, S. Mannino, C. Camera, M.P. Chatrathi, M. Scampicchio and J. Zima, *J. Chromatogr. A*, 2005, 1091, p. 177-182.
66. L.A. Colon, R. Dadoo and R.N. Zare, *Anal. Chem*, 1993, 65, p. 476-481.
67. A.J. Zemmann, E. Schnell, D. Volgger and G.K. Bonn, *Anal. Chem*, 1998, 70, p. 563-567.
68. P. Kuban and P.C. Hauser, *Electroanalysis*, 2004, 16, p. 2009-2021.
69. V. Solinova and V. Kasicka, *J. Sep. Sci*, 2006, 29, p. 1743-1762.
70. A.A. Elbashir and H.Y. Aboul-Enein, *Biomed. Chromatogr*, 2010, 24, p. 1038-1044.
71. P. Kuban and P.C. Hauser, *Electrophoresis*, 2009, 30, p. 176-188.
72. V. Kasicka, *Electrophoresis*, 2003, 24, p. 4013-4046.
73. D.C. Simpson and R.D. Smith, *Electrophoresis*, 2005, 26, p. 1291-1305.
74. M. Moini, *Anal. Bioanal. Chem*, 2002, 373, p. 466-480.
75. G. Bonvin, J. Schappler and S. Rudaz, *J. Chromatogr. A*, 2012, 1267, p. 17-31.
76. J.Y. Cai and J. Henion, *J. Chromatogr. A*, 1995, 703, p. 667-692.
77. W.F. Smyth, *Electrophoresis*, 2006, 27, p. 2051-2062.
78. A. von Brocke, G. Nicholson and E. Bayer, *Electrophoresis*, 2001, 22, p. 1251-1266.
79. C. Simo, C. Barbas and A. Cifuentes, *Electrophoresis*, 2005, 26, p. 1306-1318.
80. A. Kula, M. Krol and R. Wietecha-Posluszny, *Talanta*, 2014, 128, p. 92-101.
81. I. Newton, *Phil. Trans*, 1671, 6, p. 3075-3087.
82. G. Kirchhoff and R. Bunsen, *Ann. Phys*, 1860, 6, p. 161-189.
83. N. Bohr, *Phil. Mag. S. 6*, 1913, 26, p. 476-502.
84. A. Beer, *Ann. Phys*, 1852, 86, p. 78-88.
85. I.R. Altemose, *J. Chem. Educ*, 1896, 63, p. 216-223.
86. J. Buie, <http://www.labmanager.com>, 2011, p. 24-25.

87. E.F. Schubert, *Cambridge University Press, NewYork*, 2003, 1st ed.
88. N. Zheludev, *Nature Photon*, 2007, 1, p. 189-192.
89. R. Braunstein, *Phys. Rev*, 1955, 99, p. 1892-1893.
90. T.M. Okon and J.R. Biard, *The Edison Tech Center*, 2015, p. 1-14.
91. N. Holonyak and S.F. Bevacqua, *Appl. Phys. Lett*, 1962, 1, p. 82-83.
92. T.S. Perry, *IEEE Spectr*, 1995, 32, p. 52-55.
93. S. Nakamura, T. Mukai and M. Senoh, *Appl. Phys. Lett*, 1994, 64, p. 1687-1689.
94. E.F. Schubert, *Cambridge University Press, NewYork*, 2006, 2nd ed.
95. M. Cooke, *Semiconductor Today*, 2010, p. 82-88.
96. H. Flaschka, C. Mckeitha and R. Barnes, *Anal. Lett*, 1973, 6, p. 585-594.
97. P.C. Hauser and D.W.L. Chiang, *Talanta*, 1993, 40, p. 1193-1200.
98. S.F. Johnston, *Meas. Sci. Technol*, 1992, 3, p. 191-195.
99. B.A. Matveev, G.A. Gavrilov, V.V. Evstropov, N.V. Zotova, S.A. Karandashov, G.Y. Sotnikova, N.M. Stus, G.N. Talalakin and J. Malinen, *Sens. Actuator B-Chem*, 1997, 39, p. 339-343.
100. B.A. Matveev, M. Aidaraliev, G. Gavrilov, N. Zotova, S. Karandashov, C. Sotnikova, N. Stus, G. Talalakin, N. Il'inskaya and S. Aleksandrov, *Sens. Actuator B-Chem*, 1998, 51, p. 233-237.
101. A.A. Popov, M.V. Stepanov, V.V. Sherstnev and Y.P. Yakovlev, *Tech. Phys. Lett*, 1997, 23, p. 828-830.
102. A. Krier and V.V. Sherstnev, *J. Phys. D: Appl. Phys*, 2000, 33, p. 101-106.
103. P.K. Dasgupta, H.S. Bellamy, H.H. Liu, J.L. Lopez, E.L. Loree, K. Morris, K. Petersen and K.A. Mir, *Talanta*, 1993, 40, p. 53-74.
104. P.K. Dasgupta, I.Y. Eom, K.J. Morris and J.Z. Li, *Anal. Chim. Acta*, 2003, 500, p. 337-364.
105. M. O'Toole and D. Diamond, *Sensors*, 2008, 8, p. 2453-2479.
106. D. Xiao, S.L. Zhao, H.Y. Yuan and X.P. Yang, *Electrophoresis*, 2007, 28, p. 233-242.

107. D. Xiao, L. Yan, H.Y. Yuan, S.L. Zhao, X.P. Yang and M.M.F. Choi, *Electrophoresis*, 2009, 30, p. 189-202.
108. S. Schmid, M. Macka and P.C. Hauser, *Analyst*, 2008, 133, p. 465-469.
109. L. Krcmová, A. Stjernlof, S. Mehlen, P.C. Hauser, S. Abele, B. Paull and M. Macka, *Analyst*, 2009, 134, p. 2394-2396.
110. B. Bomastyk, I. Petrovic and P.C. Hauser, *J. Chromatogr. A*, 2011, 1218, p. 3750-3756.
111. S. Sharma, H. D. Tolley, P.B. Farnsworth and M.L. Lee, *Anal. Chem*, 2015, 87, p. 1381-1386.
112. D.D. Tunnicliff, R.R. Brattain and L.R. Zumwalt, *Anal. Chem*, 1949, 21, p. 890-894.
113. M. Degner, N. Damaschke, H. Ewald, S. O'Keefe and E. Lewis, *IEEE. Sens. Conf*, 2009, p. 95-99.
114. L.E. Kalnajs and L.M. Avallone, *J. Atmos. Ocean. Tech*, 2010, 27, p. 869-880.
115. Y. Aoyagi, M. Takeuchi, K. Yoshida, M. Kurouchi, T. Araki, Y. Nanishi, H. Sugano, Y. Ahiko and H. Nakamura, *J. Environ. Prot*, 2012, 3, p. 695-699
116. M. Degner, N. Damaschke and H. Ewald, *IEEE. Sensors. Conf*, 2008, p. 973-976
117. T. Schmid, *Anal. Bional. Chem*, 2006, 384, p. 1071-1086.
118. P. Patimisco, G. Scarmarcio, F.K. Tittel and V. Spagnolo, *Sensors*, 2014, 14, p. 6165-6206.
119. M.A. Gondal, A. Dastageer and Z.H. Yamani, *J. Environ. Sci. Heal. A*, 2009, 44, p. 1457-1464.
120. S. Bottger, M. Kohring, U. Willer and W. Schade, *Appl. Phys. B*, 2013, 113, p. 227-232.
121. T.E. Barber, W.G. Fisher and E.A. Wachter, *Environ. Sci. Technol*, 1995, 29, p. 1576-1580.

## 4. Curriculum Vitae

Full name	DUY ANH BUI
Date of Birth	05.12.1984
Gender	Male
Nationality	Vietnamese
Marital status	Married
Address	Room 217, Herbergsgasse 7, 4051 Basel, Switzerland
Mobile Tel	(+41) 787 435 489
Email address	<a href="mailto:duyanh.bui@stud.unibas.ch">duyanh.bui@stud.unibas.ch</a> ; <a href="mailto:buiduyanhl25@gmail.com">buiduyanhl25@gmail.com</a>

### Education and Qualifications

2013 - now	Doctoral study at University of Basel, Switzerland <i>Field of study: Analytical &amp; Bioanalytical sciences</i>
2011 - 2013	Post-graduate research at University of Basel, Switzerland <i>Field of research: Analytical &amp; Bioanalytical sciences</i>
2006 - 2008	Master study at Hanoi University of Science, Vietnam National University of Hanoi <i>Field of study: Environmental Sciences</i> <i>Grade: Very good</i>
2002 - 2006	Bachelor study at Hanoi University of Science, Vietnam National University of Hanoi <i>Field of study: Environmental Sciences</i> <i>Grade: Very good</i>

### Work experience

2013 - now	Doctoral student at Department of Chemistry, University of Basel, Switzerland. <i>Project: Development of deep UV-LED based absorbance detectors for analytical instruments</i>
2011 - 2013	Postgraduate researcher at University of Basel, Switzerland <i>Specialty: Analytical Sciences</i>
2008 - 2011	Manager and chief consultant for VinaControl Environment Consultancy and Appraisal Joint Stock Company, Vinacontrol Group, Vietnam ( <a href="http://www.vinacontrol.com.vn">www.vinacontrol.com.vn</a> ).

*Specialty: Environmental impact and risk assessment, environmental protection plan, clean development mechanism, environmental monitoring.*

### **Language and computer competences**

Language	Proficiency in spoken and written English
Informatics	Microsoft office and special programs for the analytical research

### **Awards and Scholarships**

2013 - 2016	Doctoral scholarship for foreign students funded by Canton of Basel city, Switzerland
2011 - 2013	Post-graduate research scholarship funded by Swiss Federal Commission for Scholarships for Foreign students (ESKAS)
2008	Scholarship for outstanding master students of Vietnam National University of Hanoi funded by Toshiba Corporation
2007	Scholarship for outstanding master students of Vietnam National University of Hanoi funded by Toshiba Corporation

### **Publications**

6 international publications: [https://www.researchgate.net/profile/Bui\\_Duy\\_Anh](https://www.researchgate.net/profile/Bui_Duy_Anh)

## 5. List of publications and posters

### 5.1. Publications

1. **Duy Anh Bui**, Peter C. Hauser  
Absorbance measurements with light-emitting diodes as sources:  
Silicon diodes or light-emitting diodes as detectors?  
**Talanta, 116, (2013), 1073-1078**
2. **Duy Anh Bui**, Benjamin Bomastyk, Peter C. Hauser  
Absorbance detector based on a deep UV light-emitting diode  
for narrow-column HPLC  
**Journal of Separation Science, 36, (2013), 3152-3157**
3. **Duy Anh Bui**, Peter C. Hauser  
Absorbance detector for capillary electrophoresis based on  
light-emitting diodes and photodiodes for the deep-ultraviolet range  
**Journal of Chromatography A, 1421, (2015), 203-208**
4. **Duy Anh Bui**, Peter C. Hauser  
Analytical devices based on light-emitting diodes - a review of the  
state-of-the-art  
**Analytica Chimica Acta, 853, (2015), 46-58**
5. **Duy Anh Bui**, Peter C. Hauser  
Deep UV-LED based absorbance detectors for narrow-bore HPLC  
and capillary electrophoresis  
**Chimia, 69, (2015), 806**
6. **Duy Anh Bui**, Peter C. Hauser  
A deep-UV light-emitting diode-based absorption detector  
for the BTEX compounds  
**Sensors and Actuators B: Chemical (2016), manuscript in press**

## **5.2. Posters**

**Duy Anh Bui**, Benjamin Bomastyk, Peter C. Hauser

Absorbance detector based on a deep UV light-emitting diode for narrow-column HPLC

**CHanalysis 2015, Beatenberg, Switzerland, April 2015**